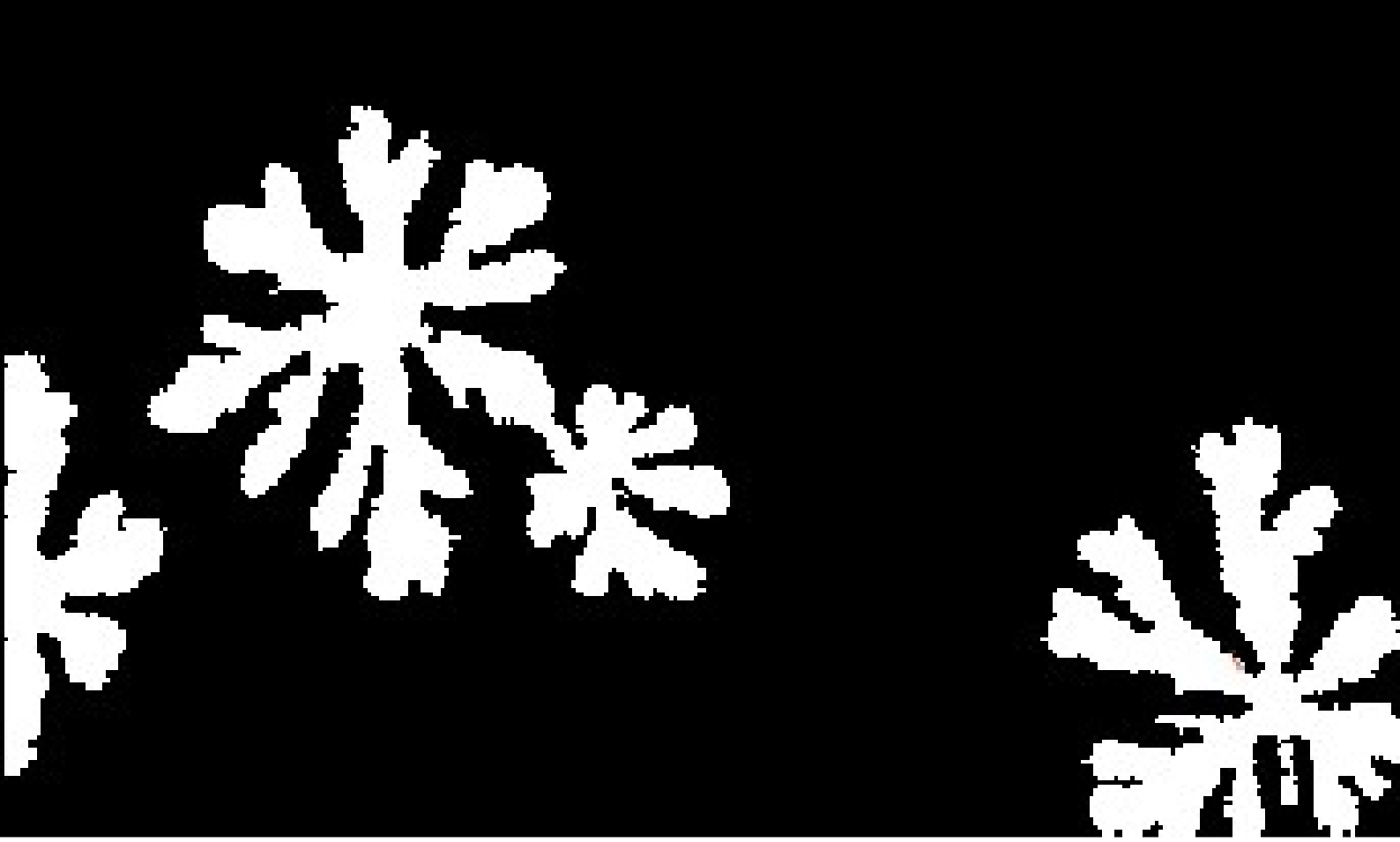

Phase Separation in Model Bilayer Membranes

Laura Scheidegger

DISS. ETH NO. 27498

DISS. ETH NO. 27498

Phase Separation in Model Bilayer Membranes

A thesis submitted to attain the degree of

DOCTOR OF SCIENCES of ETH ZURICH

(Dr. sc. ETH ZURICH)

presented by

LAURA SCHEIDEGGER

Master of Science ETH in Materials Science, ETH Zurich

born on 22.09.1991

citizen of Lucerne LU

Accepted on the recommendation of

Prof. Dr. Jan Vermant, examiner

Prof. Dr. Peter Fischer, co-examiner

Prof. Dr. Peter Walde, co-examiner

Prof. Dr. Peter Beltramo, co-examiner

2021

Acknowledgements

First and foremost, I would like to express my gratitude to Jan for giving me the opportunity to work in his group and for his supervision. His ability to never lose faith is greatly acknowledged.

I would like to thank Peter Beltramo for the great mentoring at the beginning of this project and for giving me valuable insights and sharing his experience.

This thesis would not have been possible without the help of numerous people. The Swiss National Science Foundation is acknowledged for funding this project. I want to thank Peter Walde and Peter Fischer for interesting discussions. Chris and Kirill, for their help on experimental designs. Vappu, for her invaluable help with all administrative issues. Stéphane, for his insights, and the interesting visit at PSI. Sandro, my first and only Master student, for his skill and patience. Hendrik, for his codes and help in understanding them. Rao and Claire, for their help in producing GUVs. Special thanks go to Dorothea Pinotsi and Justine Kusch of ScopeM, for helping me getting familiar with the CARS microscope. I am very grateful for the indispensable help of Prof. Elizabeth Mann and Huda Alwusaydi. Further I would like to thank Laura Stricker for her invaluable support with image analysis towards the end of this thesis.

I am grateful to all Softiez, past and present, for the great and tolerant working environment. I specially would like to thank my lab mates, Damian and the Büro babes, and Pierre in the last stage of the project, for the pleasant atmosphere.

Lastly, I want to thank my family, without whose continuous and unconditional support I would not be here.

Abstract

The plasma membrane separates the interior and exterior of the cells of all living organisms and is a highly complex structure. It is composed of hundreds of different lipid species, and contains additional constituents like proteins. It is therefore very complicated to investigate its properties. Several model membrane systems exist, all of which have their own particular shortcomings. In this thesis, we have employed a newly developed technique in order to study the heterogeneous nature of phospholipid membranes.

In the field of cell membrane research, it is believed that the lipids are not homogeneously distributed across the membrane, but that they form small, nanometer-sized structures, which are also called lipid domains or lipid rafts. These rafts are enriched with saturated lipids and cholesterol, and have a higher packing density than the surrounding membrane. They might play an essential role in certain cell membrane processes, such as signal transduction. For this reason, many resources have been dedicated to investigating how these domains are formed and how they behave. This has mainly been done by studying lipid phase transitions. Lipids can assemble into different phases. Their natural state in the cell membrane is the so-called liquid-disordered phase, where the packing density is low and the mobility high. When the temperature is reduced to below the main transition temperature of a lipid, it will form the solid-ordered phase. In this phase, the lipids are densely packed. A special case is reached when cholesterol is added to the system. Below the phase transition temperature, a liquid-ordered phase is formed, which has a high packing density, but at the same time a high mobility. Since this phase is only formed when cholesterol is present, it is assumed that this is the state that lipid rafts are in.

The focus of this thesis lies on studying specific properties of lipid domains, and how these properties are influenced by additives (like organic solvents) and other cell membrane components (like cholesterol).

In the first part, we have looked into the effects of three different organic solvents and of line-active molecules (linactants) on phase transition temperature and domain size. Organic solvents are present in several model membrane systems, and are also relevant for real cell membranes, which are in contact with oily lipid droplets. The influence of oil molecules on lipid membrane behaviour is generally underestimated. This is why they have not been investigated thoroughly to the present day. In our experiments, we have observed that the lipid domain size can be adjusted depending on the organic solvent that is chosen. Moreover, the phase transition temperature is increased or decreased (compared to the oil-free case) depending on the length of the alkane chains. Linactants additionally decrease domain size, thereby making it possible to adjust the domain size over a wide range.

The second part focused on the effects of cholesterol on lipid phase separation. Cholesterol is an essential cell membrane component. It has a pronounced effect on membrane permeability and fluidity, and it is believed that it is responsible for the formation of the liquid-ordered phase and therefore of paramount importance in lipid raft formation. First, we have found that cholesterol is not incorporated in sufficient amounts into bilayers containing *n*-hexadecane or squalene. This is important to know when working with oil-containing model membrane systems. Cholesterol can be incorporated into bilayers when using *n*-decane as the organic solvent, or when employing carrier molecules, such as cyclodextrins. Secondly, and very surprisingly, our experiments have shown that the liquid-ordered phase is formed even at very low cholesterol contents in the bilayer, suggesting that *n*-decane promotes the formation of this special phase. Lastly, and in contrast to literature values, increasing the amount of cholesterol in the bilayers led to higher phase transition temperatures. Cholesterol increases the packing of the lipids, thereby leaving less space for the *n*-decane, which usually decreases phase transition temperatures, and pushing it out.

The findings of this thesis provide novel insights into fundamental cell membrane properties. We believe that the results presented can be used to further improve current methods to produce model lipid membranes, and to correctly interpret the observations made in artificial cell membranes.

Zusammenfassung

Die Plasmamembran trennt das Innere und das Äussere der Zellen aller lebenden Organismen und besitzt eine sehr komplexe Struktur. Sie besteht aus hunderten von verschiedenen Lipiden, und enthält zusätzliche Komponenten, wie zum Beispiel Proteine. Darum ist es sehr kompliziert, ihre Eigenschaften zu untersuchen. Mehrere Modellsysteme für die Membran existieren. Alle haben ihre eigenen Nachteile. In dieser Arbeit haben wir eine neu entwickelte Technik angewendet, um die heterogene Natur von Phospholipidmembranen zu untersuchen.

In der Zellmembranforschung geht man davon aus, dass die Lipide nicht homogen über die Membran verteilt sind, sondern dass sie kleine, nanometergrosse Strukturen bilden, die auch Lipiddomänen oder Lipidflösse genannt werden. Diese Flösse sind mit saturierten Lipiden und Cholesterol angereichert, und haben eine höhere Packungsdichte als die umgebende Membran. Sie könnten eine wesentliche Rolle in bestimmten Prozessen der Zellmembran spielen, wie zum Beispiel in der Signalübertragung. Aus diesem Grund wurden viele Ressourcen darauf verwendet zu untersuchen, wie diese Domänen gebildet werden und wie sie sich verhalten. Dazu wurden hauptsächlich Phasenübergänge der Lipide untersucht. Lipide können sich in unterschiedliche Phasen anordnen. Ihr natürlicher Zustand in der Zellmembran ist die sogenannte flüssig-ungeordnete Phase, in der die Packungsdichte tief und die Mobilität hoch ist. Wenn die Temperatur unter die Hauptübergangstemperatur eines Lipids gesenkt wird, bildet es die fest-geordnete Phase. In dieser Phase sind die Lipide dicht gepackt. Ein spezieller Fall wird erreicht, wenn Cholesterol zum System hinzugegeben wird. Unterhalb der Phasenübergangstemperatur wird eine flüssig-geordnete Phase gebildet, die eine hohe Packungsdichte, aber gleichzeitig eine hohe Mobilität besitzt. Da diese Phase nur gebildet wird, wenn Cholesterol vorhanden ist, wird angenommen, dass Lipidflösse sich in diesem Zustand befinden.

Der Fokus dieser Arbeit liegt in der Untersuchung von spezifischen Eigenschaften von Lipiddomänen, und wie diese Eigenschaften von Zusatzstoffen (wie organischen

Lösungsmitteln) und anderen Komponenten der Zellmembran (wie Cholesterol) beeinflusst werden.

Im ersten Teil wurden die Effekte von drei verschiedenen organischen Lösungsmitteln und von linienaktiven Molekülen auf die Phasenübergangstemperatur und Domänengrösse untersucht. Mehrere Modellsysteme für Membrane enthalten organische Lösungsmittel. Zudem sind sie auch in realen Zellmembranen, die mit öligen Lipidtröpfchen in Kontakt kommen, relevant. Der Einfluss von Ölmolekülen auf das Verhalten von Lipidmembranen wird im Allgemeinen unterschätzt. Aus diesem Grund wurden sie bis heute nicht gründlich untersucht. In unseren Experimenten haben wir beobachtet, dass die Domänengrösse vom gewählten organischen Lösungsmittel abhängt. Zudem wird die Phasenübergangstemperatur abhängig von der Länge der Alkankette erhöht oder gesenkt (im Vergleich mit einer Membran ohne Öl). Linienaktive Moleküle senken die Domänengrösse zusätzlich. Dadurch kann die Domänengrösse über ein breites Spektrum eingestellt werden.

Im zweiten Teil liegt der Fokus auf den Effekten von Cholesterol auf die Phasentrennung von Lipiden. Cholesterol ist ein essentieller Bestandteil der Zellmembran. Es hat einen ausgeprägten Effekt auf die Durchlässigkeit und Flüssigkeit der Membran. Es wird angenommen, dass Cholesterol für die Bildung der flüssig-geordneten Phase verantwortlich und deshalb für die Bildung von Lipidflössen von grösster Bedeutung ist. Als Erstes haben wir herausgefunden, dass Cholesterol nicht in ausreichender Menge in Doppelschichten eingefügt wird, die Hexadekan oder Squalen enthalten. Das ist wichtig zu wissen, wenn mit Modellmembranen gearbeitet wird, die Öl enthalten. Cholesterol kann in Doppelschichten eingefügt werden, wenn Dekan als organisches Lösungsmittel verwendet wird, oder wenn Trägermoleküle, wie zum Beispiel Cyclodextrine, verwendet werden. Als Zweites haben unsere Experimente überraschenderweise gezeigt, dass die flüssig-geordnete Phase auch bei sehr tiefen Cholesterolgehalten in der Doppelschicht gebildet wird. Das legt den Schluss nahe, dass Dekan die Bildung dieser speziellen Phase fördert. Schliesslich führte eine Erhöhung der Cholesterolmenge zu höheren Phasenübergangstemperaturen. Cholesterol erhöht die Packungsdichte der Lipide, und verringert dadurch den Platz für Dekan, das normalerweise die Phasenübergangstemperatur senkt.

Die Erkenntnisse dieser Arbeit liefern neue Einblicke in fundamentale Eigenschaften der Zellmembran. Wir glauben, dass die präsentierten Resultate für weitere Verbesserungen von gegenwärtig verwendeten Methoden zur Herstellung von Modellmembranen und für die korrekte Interpretation von Beobachtungen in künstlichen Zellmembranen gebraucht werden können.

Contents

Chapter 1

Introduction

1.1. The cell membrane

The cells of all living organisms are enclosed by a membrane, the so-called cell or plasma membrane. Certain cell organelles, such as the Golgi apparatus, are also surrounded by membranes. In animal cells, the plasma membrane represents the only boundary between the cell interior (the cytoplasm) and the exterior environment (Figure 1.1). The cells of plants, fungi and most bacteria are additionally surrounded and protected by a cell wall, which mainly provides structural stabilization. In both cell types, the cell membrane plays a crucial role in many biological processes. It regulates transport into and out of the cell, is involved in cell-cell communication, cytokinesis and cell motility, and is therefore a vital part of the cell structure.

Despite its importance, two centuries lie between the discovery of cells in 1665 and the recognition that the cell membrane exists [1]. However, it was still considered an insignificant structure until the turn of the 20th century, when it slowly started to attract more interest. In 1925, Gorter and Grendel first proposed that cell membranes consist of a layer of lipid molecules [2]. This study was followed by the first measurements of membrane thickness [3, 4]. Robertson [4] determined it to be about 8 nm, which is in rough agreement with the thickness of a lipid bilayer. In 1972, the fluid mosaic model of cell membrane structure was presented by Singer and Nicolson [5]. This model is still widely accepted today. According to the fluid mosaic model (Figure 1.2), the cell membrane is essentially a two-dimensional material composed of a lipid bilayer with a hydrophilic and a hydrophobic part. Because of the predominantly fluidic nature of the membrane, the lipids and other membrane components such as proteins can freely diffuse within the structure. Proteins make up almost 50% of the membrane mass [6]. Depending on their chemical structure, they can interact with

both the hydrophilic (outer) and hydrophobic (inner) region of the membrane. The rest of the membrane mass comes from the lipids (up to 50%) and a small amount of carbohydrates (e.g. glycolipids).

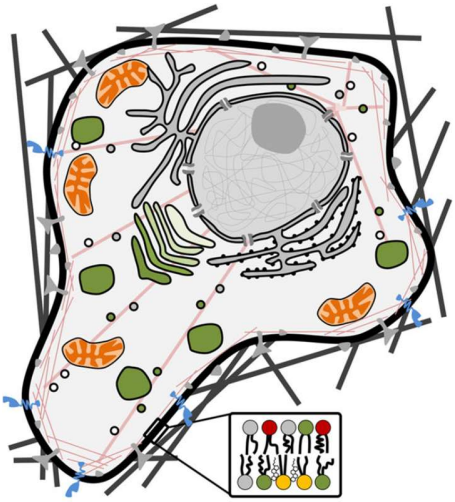

Figure 1.1: Representation of a cell. The curved black line represents the cell membrane, composed of a lipid bilayer and separating the cytoplasm from the exterior environment. Image taken from Ref. [7].

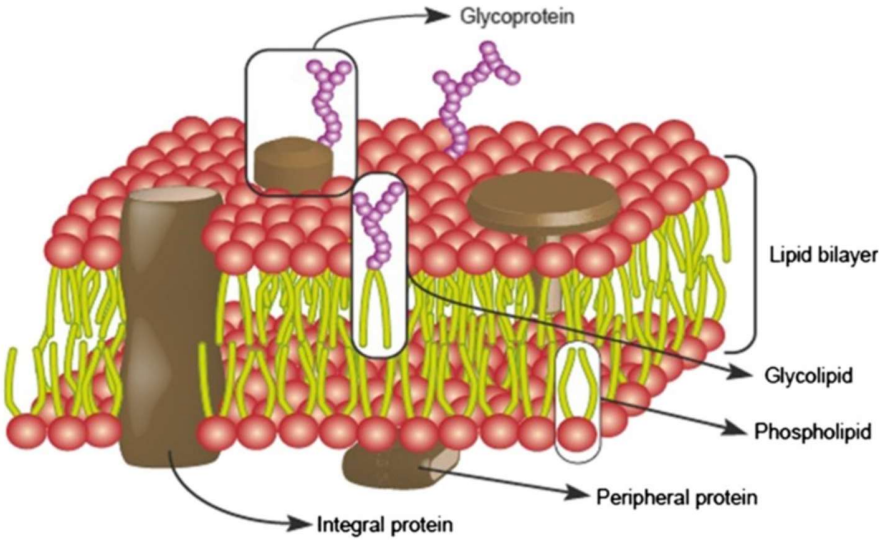

Figure 1.2: Representation of the fluid mosaic model. Image taken from Ref. [1].

The lipid bilayer is composed of a wide variety of lipid molecules [8]. They typically consist of a hydrophilic head group and a hydrophobic tail (fatty acid chain) (Figure 1.3a), and

thereby spontaneously form a bilayer in aqueous environments. The three main groups are phospholipids, sphingolipids and sterols (Figures 1.3 and 1.4). The exact lipid composition of the membrane depends on the cell type, but in most membranes, phospholipids are the major species [9]. A plethora of phospholipids exists, which differ from each other in the type of head group and fatty acid chain. The most common phospholipids are phosphatidylcholines [9, 10], where choline is the head group (Figure 1.3b). The fatty acid chains can differ from each other in length (i.e., the number of carbon atoms) and the degree of saturation (i.e., the number of double bonds).

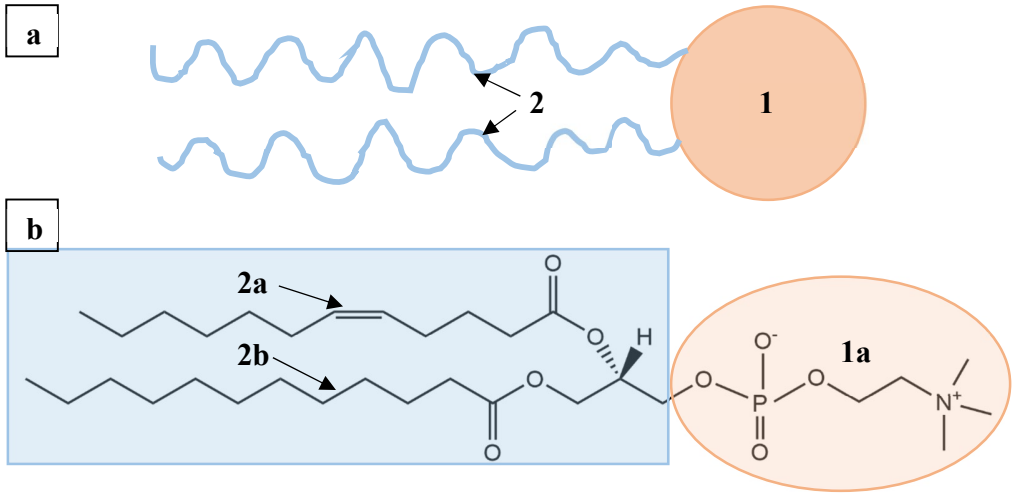

Figure 1.3: (a): Representation of a lipid, showing the hydrophilic head group (1) and two hydrophobic fatty acid chains (2). (b): Phosphatidylcholine, showing choline as the head group (1a) and an unsaturated (2a) and saturated (2b) fatty acid chain.

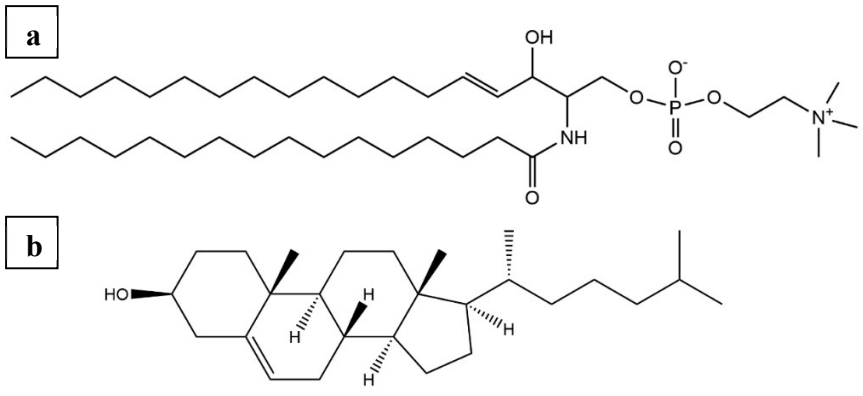

Figure 1.4: (a): Sphingomyelin, which is one type of sphingolipid, with choline as the head group. (b): Cholesterol.

Due to this variety, a cell membrane can easily contain hundreds of different lipid species [11]. Additionally, since the lipids can freely move within the membrane, they constantly reorganise and rearrange themselves, thereby making it a very dynamic and complex structure to model and investigate.

Despite this difficulty, and due to the importance of the cell membrane in various biological processes, many researchers have dedicated themselves to investigating the organization, properties and functions of cell membranes. However, many questions still remain unresolved, many of which relate to materials science questions. For example, the mechanical properties of the membrane, such as its bending rigidity [12], and the interactions between membranes and membrane proteins are ongoing topics of research [13-15]. Transport phenomena in and across the membrane, such as the exact mechanism of drug transport, are also an open question and are controversially discussed [16, 17]. Furthermore, the lipid phase behaviour and lipid organization within the membrane have received huge attention in the last two decades, especially since 1997, when lipid "rafts" were first mentioned in the literature [18].

1.1.1. Membrane heterogeneity

The heterogeneous nature of the lipid bilayer was already proposed almost 40 years ago [19]. Several authors later suggested that lipid domains are responsible for the sorting of certain membrane proteins [20, 21]. Simons and Ikonen then recognized the potentially important role of cholesterol for the formation of lipid rafts and the functional part that domains might play within the membrane [18]. It is believed that lipid domains, which are enriched with saturated lipids and therefore have a different composition than the surrounding membrane (Figure 1.5), play a key role in the binding of specific proteins to the cell membrane, and therefore play a major role in fundamental processes of the cell membrane, like signal transduction [18, 22, 23]. A widely accepted definition of "rafts" was coined in 2006 [24]: "Membrane rafts are small (10–200 nm), heterogeneous, highly dynamic, sterol- and sphingolipid-enriched domains that compartmentalize cellular processes. Small rafts can sometimes be stabilized to form larger platforms through protein-protein and protein-lipid interactions."

Because of their supposed prominent role in cell membrane functionality, the formation and properties of lipid domains have been increasingly studied within the past years. This has typically been done by investigating the **phase behaviour** of lipids and lipid mixtures. A

large number of studies exist where phase diagrams of various lipid mixtures have been probed [25-32] or where properties (nucleation and growth, diffusion coefficients, line tension, shape, interactions between domains) of lipid domains were investigated [33-41].

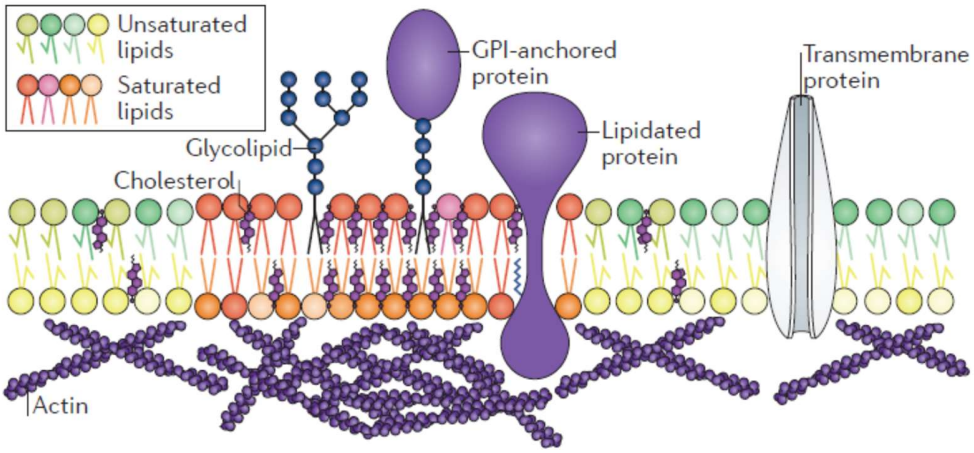

Figure 1.5: Lipid domains are enriched in saturated lipids and cholesterol. They can bind to specific proteins. Image taken from Ref. [42].

Lipids can form different structures, and depending on various external factors, such as temperature, they transition from one structure into another. A very important structure is the so-called liquid-disordered (L_d) phase, which represents the state that most lipids assume in the cell membrane. In accordance with the fluid mosaic model [5], the L_d phase has a low order and packing density, allowing the lipids and other membrane constituents to easily move around. When a bilayer is cooled below its main transition temperature, the so-called solid-ordered (S_o) or L_β phase is formed (also called the gel phase). In contrast to the L_d phase, this is a highly ordered phase.

The main transition or melting temperature T_m of lipids depends mainly on the length and number of double bonds of the fatty acid chains. The shorter they are and the more double bonds they have, the lower is the melting temperature. This is the reason why a saturated lipid like DPPC (1,2-dipalmitoyl-*sn*-glycero-3-phosphocholine, see Figure 1.6) has a much higher melting temperature (41 °C) than an unsaturated lipid like DOPC (1,2-dioleoyl-*sn*-glycero-3-phosphocholine, see Figure 1.6) (–18 °C) [43].

When the binary system DOPC/DPPC is cooled below its phase transition temperature, DPPC forms domains consisting of the S_o phase, while DOPC remains in the L_d phase [28,

44-47]. In order to decrease interactions between the head groups, the DPPC chains are tilted with respect to the bilayer plane [48]. If cholesterol is added to the system, the phase behaviour changes dramatically. Upon cooling, the system phase separates into two liquid phases, the liquid-disordered (L_d) and liquid-ordered (L_o) phase [31]. Due to its high concentration of saturated lipids and cholesterol, the latter phase is believed to be an excellent model for lipid rafts [42, 49], which is why this particular model system is one of the most investigated phase separating mixtures and has been extensively studied by Veatch et. al. [26, 27, 32] and others.

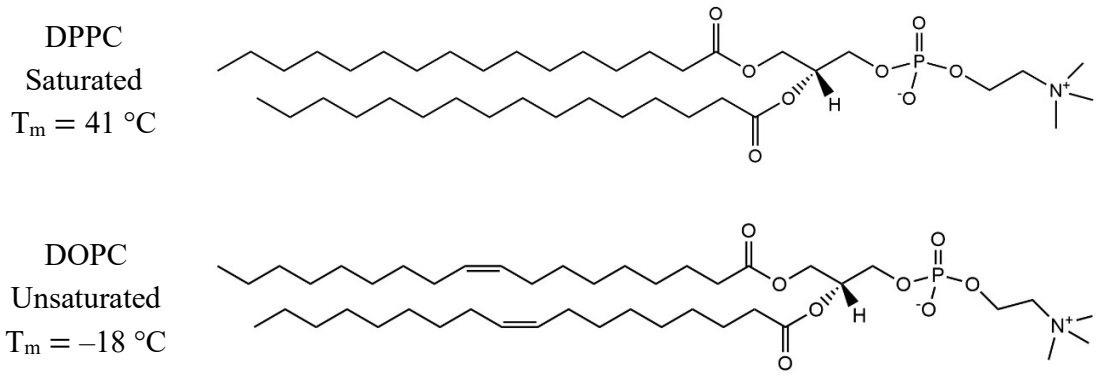

Figure 1.6: Chemical structures of the two phospholipids DPPC (saturated) and DOPC (unsaturated).

Considerable differences exist between these three phases (Figure 1.7). The S_o phase has a very high translational and conformational order [50], i.e., the lipids cannot diffuse easily within the bilayer, and the fatty acid chains are extended. This leads to a high packing density and an increased bilayer thickness. In the L_d phase, on the other hand, the order is drastically reduced. The lipid molecules have more translational as well as conformational freedom. The L_o phase is a special case, where the addition of cholesterol increases the conformational order of the fatty acid chains (compared to the L_d phase) [25], while at the same time the high lateral mobility of the lipids in the L_d phase is retained [50, 51].

While the biological relevance of the L_o phase is clear, the S_o phase has received less attention. However, based on the importance of specific lipid species (ceramides) in certain signaling processes such as apoptosis, several studies have recently looked at the formation of S_o domains in lipid membranes [52, 53]. Their results suggest that cells might be able to

adjust the packing density of domains according to their needs, which could partly explain why membranes contain such a high number of different lipids.

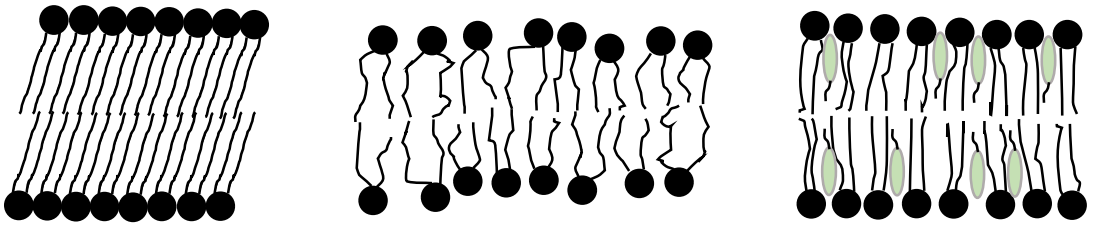

Solid-ordered (S_o) Liquid-disordered (L_d) Liquid-ordered (L_o)

Figure 1.7: Representations of the three phases mentioned in the main text. The liquid-ordered phase contains cholesterol molecules.

Despite extensive research, it has to be noted that there is still no definitive proof that lipid rafts exist [54, 55]. While macroscopic domains can be observed in model membranes, the postulated sizes of domains in live cell membranes are much smaller (10–200 nm), and therefore they cannot be resolved by light microscopy. Recently, cryogenic electron microscopy has been employed to image nanoscopic domains in model membranes and in membranes derived from cells [56, 57] by exploiting the thickness mismatch between the L_d and L_o phases. This was an important step towards proving that lipid rafts exist. However, although cell derived membranes have compositions which are comparable to the ones found in real cell membranes, they still lack many important characteristics, such as the interaction with the cytoskeleton.

Since cell membranes have such a complex structure, computer simulations, such as molecular dynamics (MD) studies, are a powerful tool to investigate lipid interactions and domain formation [58, 59]. Zhuang et. al. [60] have extensively studied the interactions between various lipid types, showing that results obtained from simulations and experiments agree reasonably well. The formation of lipid domains has been simulated in binary [61] as well as in ternary mixtures [62, 63] (Figure 1.8), confirming the increased order in the domain phases. Rosetti et. al. [63] showed that the mismatch between the saturated and the unsaturated lipid chains is an important factor for domain formation. Shahane et. al. [64] looked at lateral pressure profiles for different bilayer systems. The pressure within the bilayer is of particular importance, since it could play an important role in protein function

[65]. The lateral pressure profile for a pure POPC (1-palmitoyl-*sn*-2-oleoyl-glycero-3-phosphocholine) bilayer is shown in Figure 1.9. While positive pressures indicate repulsive forces, negative values indicate attractive ones. The most negative values are found between the hydrophilic heads and hydrophobic tails of the lipids. Here, the bilayer tries to reduce the contact points between the hydrophobic and hydrophilic regions. In the middle of the bilayer, repulsive forces act between the fatty acid chains to maximize entropy. Patra [66] has investigated the influence of cholesterol on the lateral pressure in DPPC bilayers. They showed that cholesterol increases the pressure within the bilayers, a result which is related to the increased rigidity when cholesterol is added.

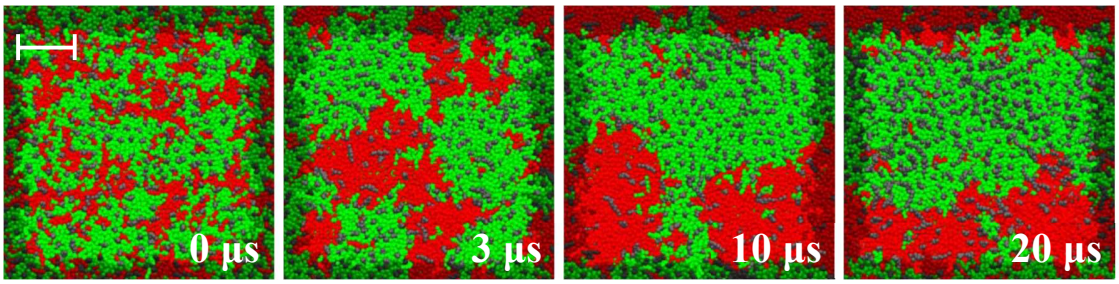

Figure 1.8: MD simulation of the formation of L_o domains in a ternary lipid mixture. The saturated lipids are depicted in green, the unsaturated lipids in red and cholesterol in gray. Scale bar is 5 nm. Image taken from Ref. [62].

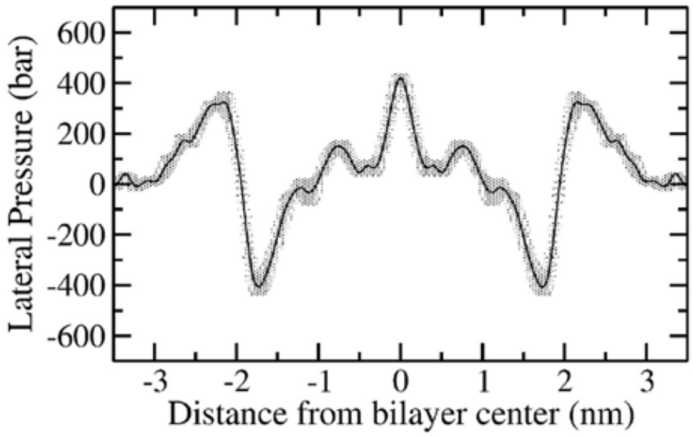

Figure 1.9: Lateral pressure profile for a pure POPC bilayer. Image taken from Ref. [64].

The complexity of the simulated systems is gradually increasing [67]. It will be possible to investigate interactions of cell membranes with the cytoskeleton in future computer simulations [68].

1.1.2. Membrane viscosity

Lipid domains were also used to probe membrane properties, such as membrane viscosity [33, 69]. The viscosity of a membrane has an effect on many processes (most of all, transport) and its quantification is highly sought after [70-72]. Many calculations rely on the Saffman-Delbrück (SD) approximation [73], which relates the diffusion coefficient D to the two-dimensional membrane viscosity η_{2D} and the coupling of the bulk fluid. D can be measured by tracing membrane inclusions, which can be particles or, as mentioned before, lipid domains. Unfortunately, the SD approximation was originally developed for proteins, and is only valid in a limited range, namely for $r < l$. Here, r is the inclusion size and $l = \eta_{2D}/(2\mu)$ is a length scale which characterizes the respective diffusion of momentum at the interface and into the bulk, as μ is the bulk viscosity of the surrounding medium. So, the SD approximation is valid for small inclusions or a large membrane viscosity. This problem was studied by Hughes et. al. [74], who developed a model (HPW model) that is valid for all inclusion sizes. In 2008, Petrov and Schwille [75] presented a simple expression based on Saffman's and Hughes' earlier works. All of these models assume that the interface is incompressible. Figure 1.10 illustrates the applicability ranges for all models.

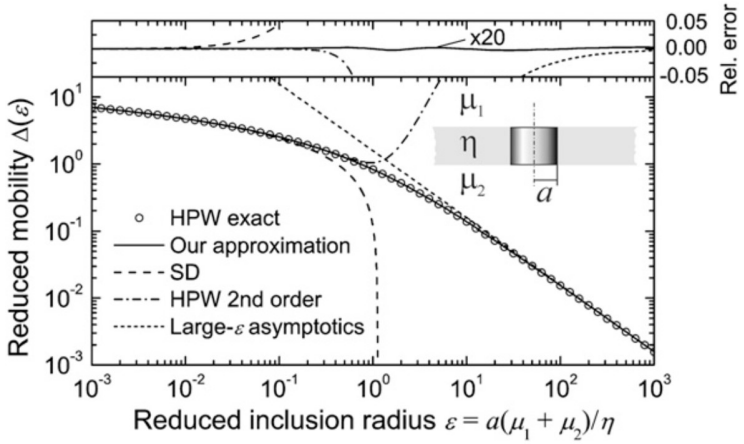

Figure 1.10: Applicability ranges of the models relating diffusion coefficients and membrane viscosity mentioned in the main text ("Our approximation" is Petrov's and Schwille's expression). Image taken from Ref. [75].

In Figure 1.10, $\varepsilon = \frac{2*r*\mu}{\eta_{2D}}$ stands for the reduced inclusion radius, a denotes the inclusion radius, μ_1 and μ_2 are the bulk viscosities of the surrounding fluids and η is the two-dimensional membrane viscosity. The HPW model calculates the exact values of the reduced mobility $\Delta(\varepsilon)$ (y-axis), shown with circles in Figure 1.10. Additionally, four different approximations for $\Delta(\varepsilon)$ are shown:

- Saffman-Delbrück (SD; only valid for $\varepsilon < 0.1$):

$$\Delta_{SD}(\varepsilon) = ln\left(\frac{2}{\varepsilon}\right) - \gamma$$

$\gamma = 0.5772$ stands for the Euler constant.

- HPW 2nd order (only valid for $\varepsilon < 0.6$):

$$\Delta_{HPW\ 2nd\ order}(\varepsilon) = ln\left(\frac{2}{\varepsilon}\right) - \gamma + \frac{4\varepsilon}{\pi} - \frac{\varepsilon^2}{2} ln\left(\frac{2}{\varepsilon}\right)$$

- Large-ε asymptotics (only valid for $\varepsilon > 30$):

$$\Delta_{\infty}(\varepsilon) = \frac{\pi}{2\varepsilon}$$

- Petrov and Schwille ("Our approximation"):

$$\Delta_{PS}(\varepsilon) = \left[ln\left(\frac{2}{\varepsilon}\right) - \gamma + \frac{4\varepsilon}{\pi} - \left(\frac{\varepsilon^2}{2}\right) ln\left(\frac{2}{\varepsilon}\right)\right] * \left[1 - \left(\frac{\varepsilon^3}{\pi}\right) ln\left(\frac{2}{\varepsilon}\right) + c_1\varepsilon^{b_1}/(1 + c_2\varepsilon^{b_2})\right]^{-1}$$

The values for the parameters are: $c_1 = 0.73761$, $b_1 = 2.74819$, $c_2 = 0.52119$ and $b_2 = 0.51465$.

As can be seen in Figure 1.10, Petrov's and Schwille's expression is valid for the whole range of ε, providing a simple and exact solution. Depending on the membrane composition, it can be used to measure the viscosity of the L_d as well as of the L_o phase. The viscosity of the L_o phase is particularly relevant for protein function.

1.2. Techniques for studying lipid membranes

Because of the intricate organisation of cell membranes, a widely used technique to study their properties is by investigating simplified model membranes. These can consist of different lipids and have varying complexity. Model membranes can be produced by several methods, two of which will be introduced here.

1.2.1. Black lipid membranes (BLMs)

BLMs (Figure 1.11) were first introduced over 50 years ago [76] and since then have been applied in several studies, such as membrane capacitance measurements [77-79]. Two preparation methods for BLMs exist. Both rely on the use of organic solvents, and although the bilayers produced with the second method are usually considered "solvent-free", it is very likely that small amounts of solvents remain within the bilayer. In the first method, the lipids are dissolved in an organic solvent (e.g. decane), and a small aperture surrounded by an aqueous phase is "painted" with this solution. In the second method, the so-called Montal-Mueller technique [80], a septum with an aperture is placed within and a monolayer of lipids is created on an aqueous phase. The level of the aqueous phase on one side of the aperture is then raised above the aperture, depositing the first monolayer. This is followed by raising the aqueous phase level on the other side of the aperture, resulting in a bilayer.

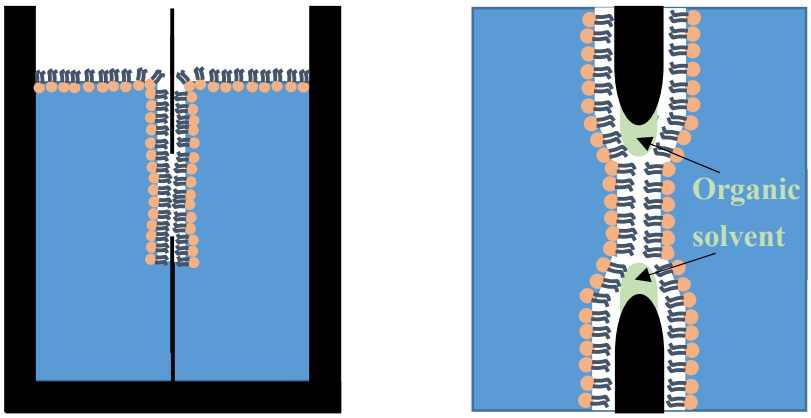

Figure 1.11: Black lipid membrane, produced by the Montal-Mueller technique. Small amounts of organic solvent remain within the bilayer.

BLMs are planar and free-standing, which is a huge advantage compared to e.g. supported lipid bilayers (SLBs), where the interactions between the support and the bilayer have to be taken into account. In spite of these advantages, BLMs are often only stable for less than an hour, which limits their application to a great extent.

1.2.2. Giant unilamellar vesicles (GUVs)

GUVs (Figure 1.12) are nowadays the most widely used technique to produce model membranes. They are circular structures filled with an aqueous phase and bounded by a single ("unilamellar") bilayer. They usually have a size of 1 – 100 µm [81], which is in the same range as most biological cells [82]. GUVs can be used for multiple applications [81], but have particularly often been used to study mechanical properties of membranes [28, 83] and for phase separation experiments [26-28, 33, 34]. Major findings include membrane shape changes upon the reduction of tension [83] and the observation of different liquid phases in various lipid compositions [26].

GUVs are often produced by electroformation [84], which is a highly reproducible approach. Another method involves assembling the lipids at an oil-water interface and then letting lipid-covered water droplets pass across this interface [85] (Figure 1.12). This principle is used in the cDICE (continuous droplet interface crossing encapsulation) method [86], which allows for efficient production of GUVs with tuneable size. However, it was recently shown that when using cDICE, cholesterol is not incorporated into the bilayer in sufficient amounts [87], probably because of the presence of residual oil in the vesicles. Recently, Dürre et. al. have overcome this obstacle by adding a second oil layer to the setup [88], thereby increasing the incorporation efficiency of cholesterol to 25 – 35%.

Giant plasma membrane vesicles (GPMVs) are vesicles formed directly from the plasma membrane of cultured cells and are therefore of much higher complexity than GUVs, which usually consist of only a few different lipid species. It has been shown in various studies that GPMVs also undergo phase transitions comparable to the ones observed in GUVs [89-91], not only proving that vesicles with complex compositions can indeed form heterogeneous structures, but also that simple bilayers like GUVs are adequate model systems to study phase separations.

Unfortunately, the composition of GPMVs highly depends on the growth conditions [92], which makes experimental results occasionally difficult to interpret [93]. Furthermore, and

although giant vesicles have the advantage of being very stable and allowing tension control, their curvature makes imaging more difficult and curvature effects cannot be isolated.

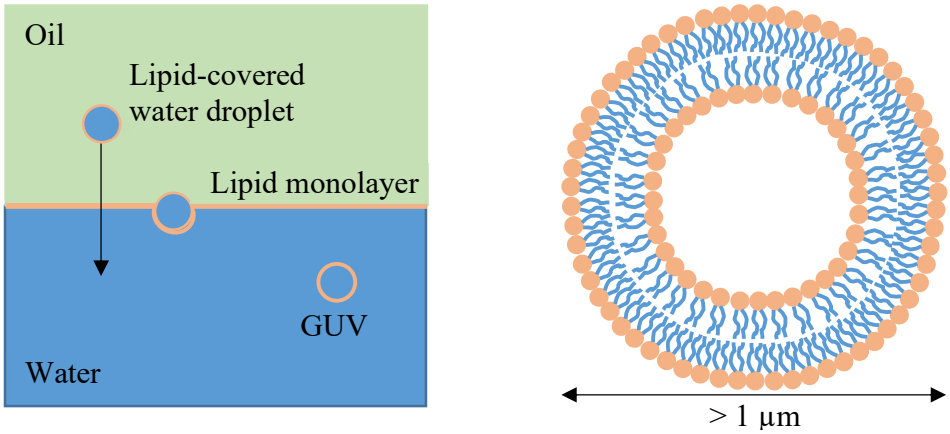

Figure 1.12: Giant unilamellar vesicle, produced by letting lipid-covered water droplets pass across a lipid-covered oil-water interface.

1.3. Outline

The goal of this work was to gain more insight into the organization of model phospholipid membranes. To this end, the phase separation of phospholipid bilayers was investigated by a novel experimental technique. Particular emphasis was put on questions related to materials science, i.e., the phase behaviour of phospholipid bilayers, lipid domain formation and growth and the effects of cholesterol on membrane properties.

Chapter 1 provided a general introduction into the complexity of cell membranes, lipid phase behaviour and model membrane studies, including their shortcomings. Many open questions remain in the field of membrane heterogeneity and lipid phase behaviour. Furthermore, the presence and influence of organic solvents in model lipid membrane studies is an unresolved issue.

In Chapter 2, a novel technique to produce model membranes will be introduced. Its advantages compared to other techniques will be presented.

Chapter 3 focuses on the formation of solid domains in a binary phospholipid system and the effects of various oil solvents on lipid phase behaviour. Additionally, the influence of so-called line-active molecules will be examined.

The complexity of the system is increased in Chapters 4 and 5, where the effects of cholesterol on phase separation are investigated. To achieve this, two different approaches were used. First, cholesterol was dissolved in the oil solvent together with the other lipids. In the second method, a cholesterol-free bilayer was first formed, and cholesterol was then added to the bilayer using a carrier molecule. This strategy revealed fundamental differences into how cholesterol is incorporated into model membranes.

Finally, Chapter 6 recapitulates the results of this thesis and outlines directions for possible future work.

Chapter 2

Large area model biomembranes

2.1. Introduction

As mentioned in section 1.2., the current methods to produce model membranes all suffer from individual disadvantages. Naturally, it is desired to have a platform that combines all of the best features of the aforementioned techniques. This has been achieved by large area model biomembranes (LAMBs) (Figure 2.1) [94]. This recently developed technique relies on an adapted thin-film balance setup with a bikewheel film holder (microchip; Figure 2.1b). The film holder has been adapted from the original design in [95] to allow for a more uniform drainage across the lipid film. The advantages of this platform include fine tension control, the possibility of creating free-standing, planar, and large area (up to 0.78 mm^2) membranes, and the ability of investigating transport properties across the membranes. Even the influence of curvature can be studied, despite the natural planarity of the membranes. This is made possible by independent access to both sides of the bilayer. Thereby, the initially planar membranes can be curved, e.g. by introducing an osmotic pressure gradient. In the next sections, the design of the setup and the experimental procedure to produce LAMBs will be described in detail.

2.2. Design of the thin-film balance setup

The bikewheel film holders are fabricated on demand by Micronit Microfluidics (Netherlands) using photolithography. They consist of two glass borosilicate slides. The channels are etched into one of the glass slides by HF. The hole in the centre of the bikewheel is drilled using a diamond drill. Its size can be varied, but in this work it was kept fixed at a

diameter of 1 mm. 24 channels are oriented radially from the hole and connected to larger entrance channels. The film holders are glued to titanium holders (Figure 2.2a).

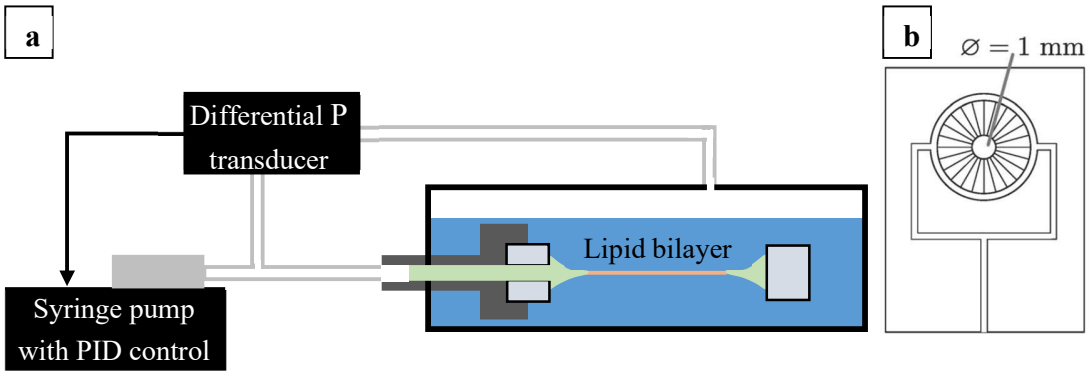

Figure 2.1: (a): LAMB setup. A differential pressure transducer is coupled with a syringe pump to precisely measure and control the pressure within the thin-film balance cell. The bilayer is formed within a 1 mm hole of the bikewheel film holder shown in (b). Image in (b) is taken from Ref. [94].

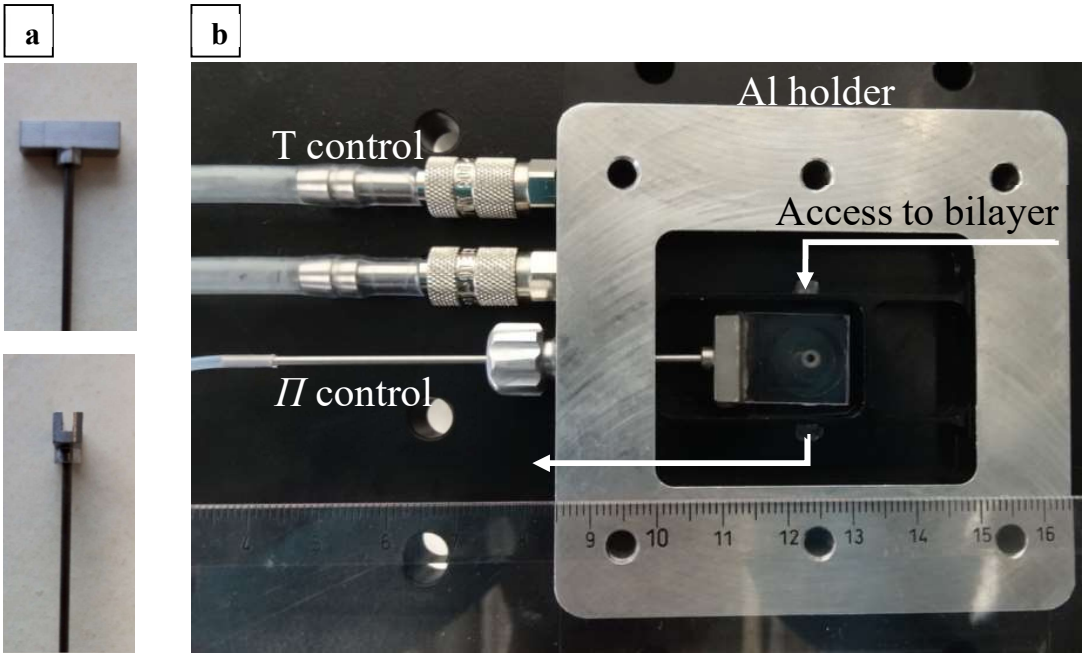

Figure 2.2: (a): The bikewheel film holders are glued to titanium holders. (b): The bikewheel film holder is placed in an aluminium pressure chamber with different compartments to ensure access to the bilayer. The chamber is connected to temperature and pressure controls. Image taken from Ref. [94].

To access both sides of the bilayer independently, the film holder is placed in a pressure chamber with different compartments (Figure 2.2b). The pressure chamber is made out of aluminium and allows for temperature control. Tubing connects the titanium holder to a syringe pump. The pump is connected to a Baratron pressure transducer, which controls the disjoining pressure Π in the film.

2.3. Experimental procedure

2.3.1. Materials

OTS (octadecyltrichlorosilane), *n*-hexadecane, *n*-decane and squalene are bought from Acros Organics (USA). Triolein is bought from Sigma-Aldrich. NaCl (99.99%, metals basis) and $NaHCO_3$ are obtained from Alfa Aesar, and $CaCl_2$ is purchased from Sigma-Aldrich. Deionized water (Milli-Q, Merck-Millipore, resistivity < 18.2 MΩcm) is used to prepare all buffers. Lipids are obtained from Avanti Polar Lipids.

2.3.2. Bikewheel and lipid preparation

First, the surface of the bikewheels has to be hydrophobized, in order to ensure stable lipid film formation. This is achieved by silanization in 1 mM OTS in *n*-hexadecane for a day, after having cleaned the bikewheels in a base bath (NaOH in ethanol).

The lipids in chloroform are mixed in the desired ratio and dried under nitrogen and vacuum. They are then dissolved in the desired oil solvent at a concentration of 2.5 – 5 mg/ml. Concentrations below 2.5 mg/ml result in unstable oil films. The lipid-oil mixture is sonicated for several hours before use to ensure that the lipids are fully dissolved in the organic solvent. For oil mixtures, better results were observed when the lipids were first dissolved in squalene, and *n*-hexadecane was added afterwards in the appropriate amount.

After filling the bikewheel film holders with the lipid-oil mixture, they are placed within the pressure chamber and connected to a syringe for pressure control. For temperature dependent experiments, the pressure chamber is pre-heated to the desired temperature. The physiological salt buffer (150 mM NaCl, 2mM $CaCl_2$, 0.2 mM $NaHCO_3$) (pH = 7.4) is filtered with 0.2 µm pore filters and then added into the pressure chamber. Before adding the buffer,

the pressure is slightly increased, to keep the buffer from entering the channels of the bikewheel.

2.3.3. LAMB formation

The steps for LAMB formation are shown in Figure 2.3. First, a thick oil film is formed within the small hole in the centre of the bikewheel (Figure 2.3b). This film is then slowly drained by decreasing the pressure. Interference patterns occur when the oil film is sufficiently thin (Figure 2.3c). Ultimately, a bilayer is formed (Figure 2.3d-e).

By measuring the thickness of the formed bilayers, it was shown that the composition of binary lipid bilayers is in accordance with the composition of the bulk lipid mixtures [96].

2.3.4. Influence of different organic solvents

During this thesis, it was observed that organic solvents (Figure 2.4) have a huge impact on the bilayer properties. A closer examination of the effects of organic solvents on bilayer phase behaviour will be undertaken in Chapter 3. Here, we focus on bilayer stability.

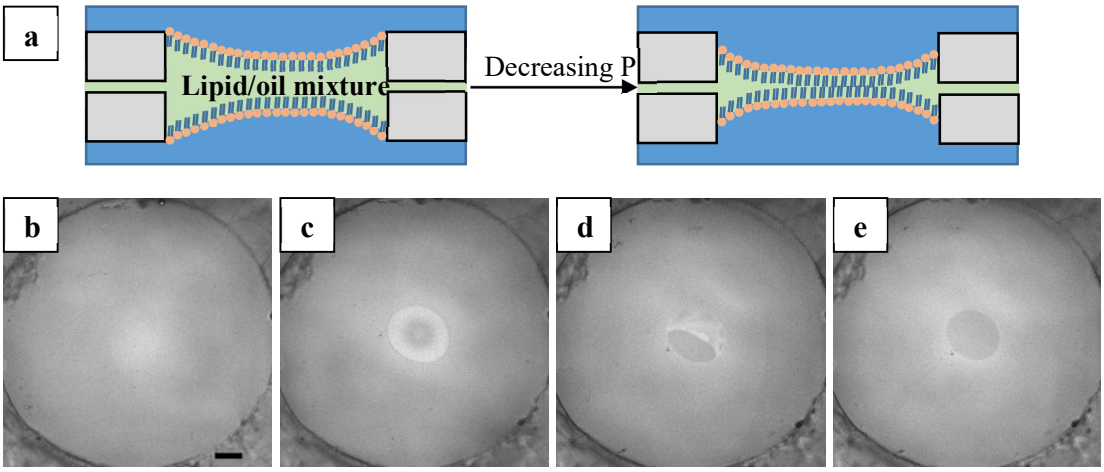

Figure 2.3: (a): Representation of the drainage process of a thick oil film upon decreasing the pressure. (b): Thick oil film. (c): Interference patterns occur when the oil film is sufficiently thin. (d)-(e): Bilayer formation. Scale bar is 100 µm.

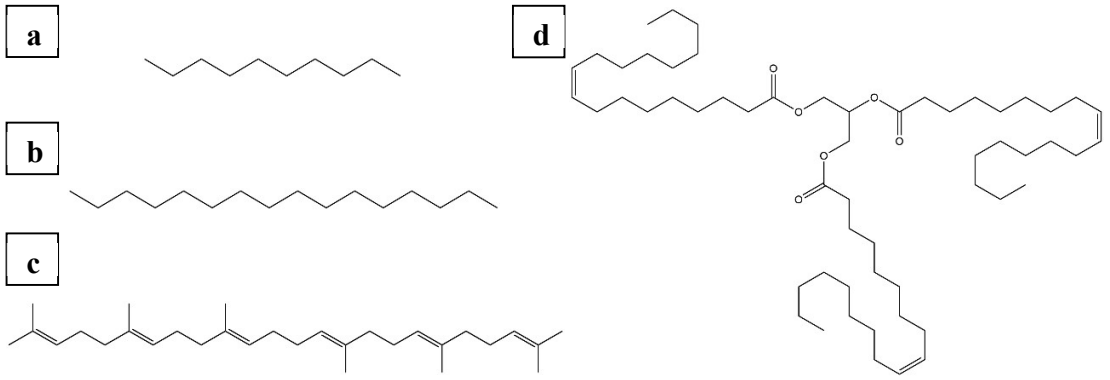

Figure 2.4: Different organic solvents. (a): *n*-Decane. (b): *n*-Hexadecane. (c): Squalene. (d): Triolein.

Different organic solvents require different hydrophobization procedures. It is not a trivial task to optimize the surface functionalization of the bikewheel to the requirements of the solvent. An iteration process is necessary, which can take several days, depending on the duration of the hydrophobization procedure. It was found that for simple alkanes like *n*-decane or *n*-hexadecane, hydrophobization in 1 mM OTS is sufficient. Bulkier molecules like squalene require a stronger hydrophobization (10 mM OTS). For solvents of even higher molecular mass (such as triolein), no appropriate surface functionalization could be found. Bilayers formed with these solvents were not stable.

Additionally, it was observed during the temperature dependent measurements that the long-term bilayer stability upon cooling is increased when using mixtures of *n*-hexadecane and squalene instead of pure *n*-hexadecane. This could be due to the higher heat capacity of squalene ($C_{p,gas} = 1321.66\, J * mol^{-1}K^{-1}$) compared to the one of *n*-hexadecane ($C_{p,gas} = 611.73\, J * mol^{-1}K^{-1}$).

2.3.5. Exchange of the surrounding phase

One of the advantages of the LAMB setup is that the environment on both sides of the bilayer can be changed easily and independently after its formation. This is not always possible in other systems. GUVs, for example, allow access only from one side.

The setup to exchange the surrounding phase is shown in Figure 2.5. A pump is used which enables simultaneous infusion of the new and withdrawal of the old phase. This is necessary to ensure a constant volume of the surrounding phase in the pressure chamber, so that a

constant pressure is acting on the bilayer. If only the phase on one side of the bilayer needs to be exchanged, the compartments in the pressure chamber need to be sealed from each other with high-viscosity vacuum grease.

It was shown previously that for the addition of Magainin II, an antimicrobial peptide, a ramp profile (0.01 ml/min to 0.1 ml/min in 10 min) was the most appropriate solution to ensure bilayer stability [97]. During the course of the present thesis, the exchange setup was used to add cholesterol to the bilayer (for further details see Chapter 5). No difference with respect to bilayer stability was observed when the new phase was added at 0.1 ml/min from the beginning. This faster infusion reduced the duration of the measurements, which was an advantage especially for the phase separation experiments, where the duration of light exposure is a critical factor due to the inevitable photobleaching of the fluorophores.

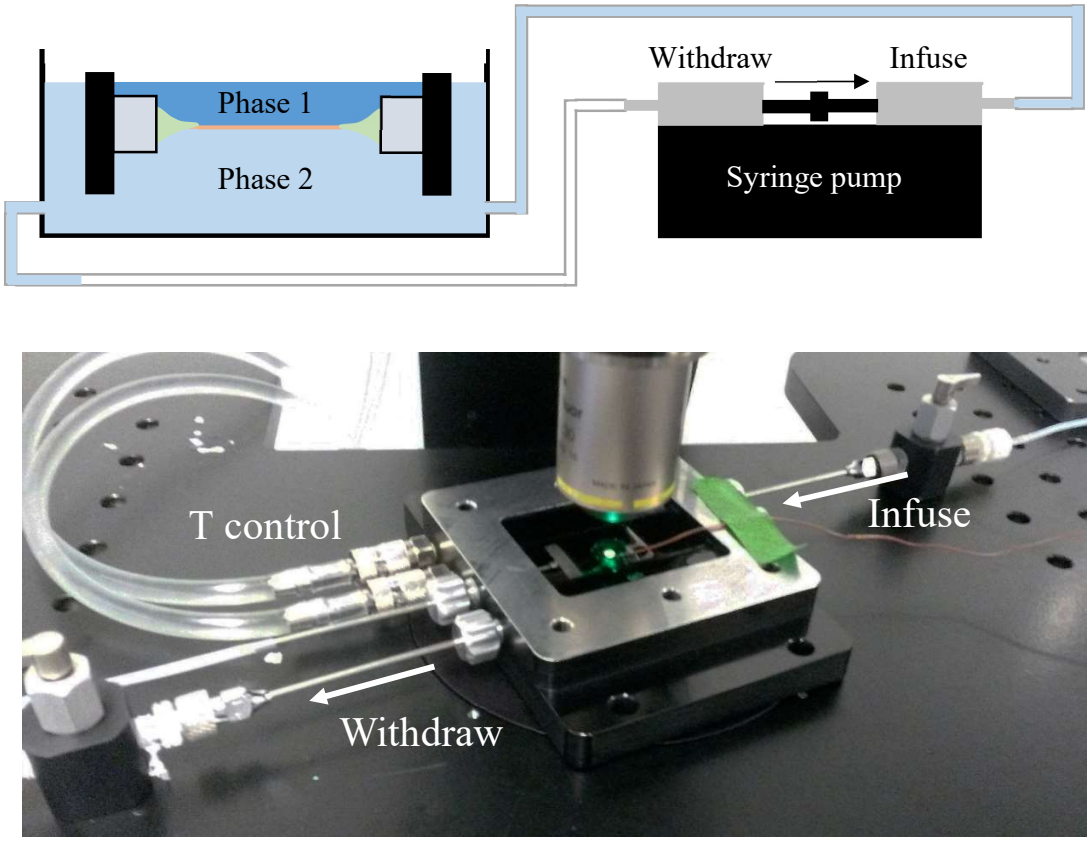

Figure 2.5: Setup to exchange the surrounding phase. A syringe pump is used which enables simultaneous infusion of the new and withdrawal of the old phase. The setup can be used to access only one (as shown in the top image) or both sides of the bilayer.

2.3.6. Asymmetric bilayers

Biological membranes are typically asymmetric, i.e. they have different compositions on the inner and outer leaflet. For example, the outer leaflet of erythrocytes contains more phosphatidylcholines than the inner leaflet [9, 98]. Therefore, and to increase the biological significance of the results, the production of asymmetric model membranes is a very dynamic field of research [99-101].

A promising approach to produce asymmetric LAMBs is to use the phase exchange setup described in the previous section. By sealing the top and bottom layer of the bilayer from each other, the bottom layer can be accessed independently by a new phase. This has been used in preliminary experiments, described below.

First, DPPC was dissolved in salt buffer, following the procedure described in [102]:

1. 0.006 g DPPC were weighed in a clear vial and pre-heated for 15 min at 56 °C.
2. 200 µL Milli-Q water were added (pre-heated at 56 °C).
3. This lipid paste was stirred at 200 rpm, while keeping it at 56 °C, until the lipids were dry to the naked eye.
4. This was repeated three times.
5. 1.6 mL salt buffer was added (pre-heated at 56 °C).

The bikewheel film holder was sealed with vacuum grease prior to bilayer formation to prevent fluid exchange between the top and bottom phase. The experiments were conducted at room temperature. A symmetric bilayer (pure DOPC, containing 1 mol% of a fluorescent lipid) was formed. Then, DPPC (in salt buffer at a concentration of 5 mM) was added by exchanging the bottom phase. After the addition of 1 mL DPPC, black domains form in the bilayer (Figure 2.6). Due to the high packing density in the solid-ordered DPPC phase, the fluorescent lipid is excluded from this phase and the domains appear black.

In another experiment, coalescence of two of these domains was observed (Figure 2.7), which is normally not seen for solid-ordered domains. A possible reason for this behaviour could be that the line tension of the domains, which depends on various factors, is increased if they only appear on one leaflet, thereby increasing the coalescing forces.

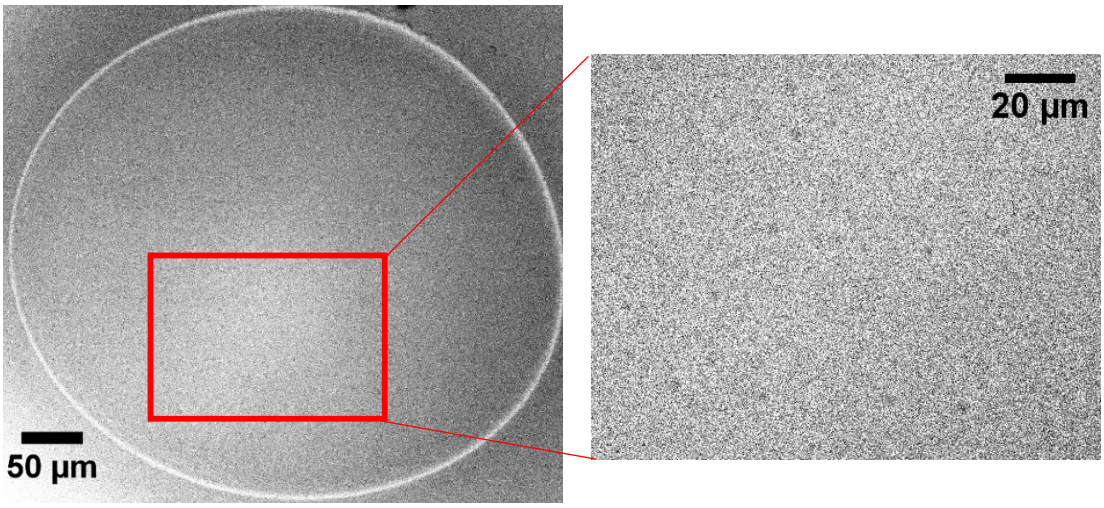

Figure 2.6: DOPC bilayer after the addition of 1 mL DPPC (in salt buffer, 5 mM) into the bottom phase. The image was taken at room temperature. Magnification: 20x.

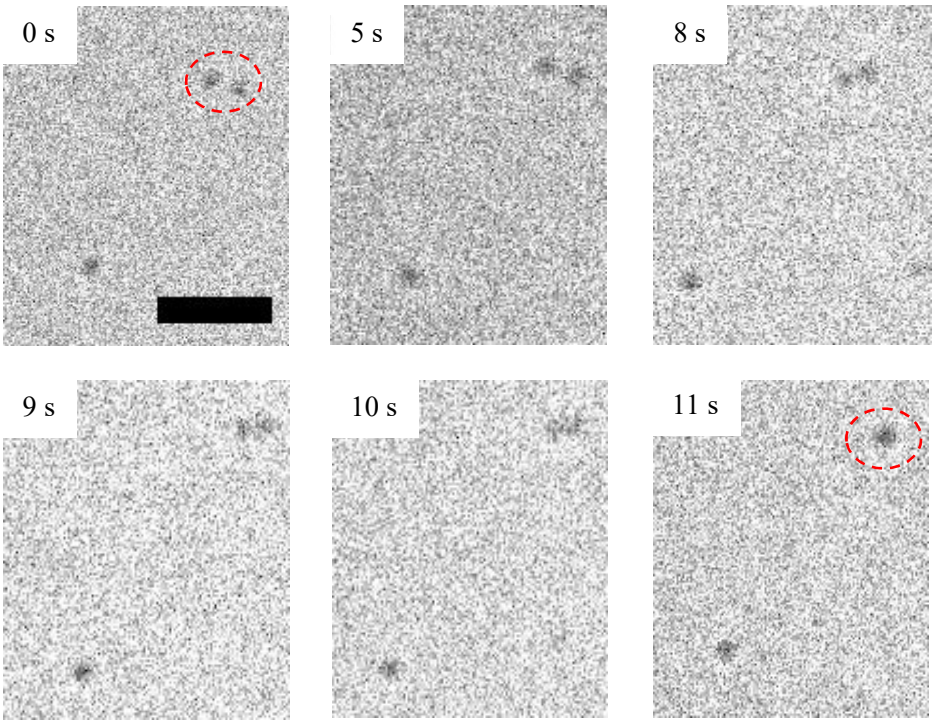

Figure 2.7: Coalescence of two black domains. Scale bar is 20 µm.

These preliminary experiments show that asymmetric, large area bilayers can be produced by a relatively simple approach.

Chapter 3

Domain size regulation in phospholipid model membranes using linactant and oil molecules

The formation of domains in multicomponent lipid mixtures has been suggested to play a role in moderating certain functions of cells. Understanding how domain size may be regulated by both hybrid lipid molecules and impurities is important, both for understanding real biological processes, and for developing model systems where domain size can be regulated to enable systematic studies of domain formation kinetics and thermodynamics. Here, we study how line-active hybrid phospholipids and oil molecules which swell the bilayer influence the phase separation in planar, free-standing lipid bilayers consisting of DOPC and DPPC. First, we find that *n*-hexadecane increases domain size by a factor of 5 compared to the smallest observed domains, while *n*-decane, a shorter alkane, leads to smaller domains. Secondly, POPC (1-palmitoyl-*sn*-2-oleoyl-glycero-3-phosphocholine), a line-active hybrid lipid, reduces the domain size when added in small amounts. Lastly, despite the regulation of domain size by both, we find that the phase transition temperature is influenced only by oil molecules, but not by linactants. This suggests that oil molecules have a greater effect on the phase separation in lipid bilayers than linactant molecules, a conclusion that is confirmed by the dependence of the area fraction of the fluid phase on oil composition and linactant content. The incorporation of linactant and oil molecules into this binary membrane model system makes domain size regulation over a wide range of length scales (several tens of microns) possible.

3.1. Introduction

Lipid organization within biological membranes has received huge attention in the last two decades, especially since 1997, when lipid "rafts" were first mentioned in the literature [18]. Because of their proposed importance in fundamental cell membrane processes, the formation and properties of lipid domains have been increasingly studied within the past years. Although lipid 'rafts' in real cells are nanometer scale and may be transient in nature [55, 103], the raft hypothesis was built upon model membrane studies related to understanding phase separation on the microscale. Similar to the domains in lipid monolayers [104, 105], a phase coexistence between a dense, liquid-ordered (L_o) and a liquid-disordered (L_d) lipid phase is believed to underpin raft assembly in living cells [55, 103]. The understanding of how to control phase behaviour of lipids and lipid mixtures can hence help rationalize the formation of these domains.

Experimentally observed domain sizes range from nano- to micrometers and depend on a complex interplay of various factors, with some analogy to the formation of nano- and microemulsions in bulk. Apart from composition and the distance from the binode and the critical point [34, 106], an important factor is the line tension between the different lipid phases [106-110]. It plays a role akin to interfacial tension in bulk systems, and is governed by the thickness (height) mismatch, hydrophobic interactions and the spontaneous curvature between the domain and the surrounding phase [111]. In particular, line tension increases quadratically with the thickness mismatch [112], and hence strongly depends on bilayer composition. It has been shown that the addition of line-active molecules (linactants), such as hybrid lipids composed of a saturated and an unsaturated tail, reduces both line tension and the average domain size [107, 108, 113-116]. Since lipid domains are enriched with saturated phospholipids, it is hypothesized that linactants concentrate at the interface between the domain and the surrounding membrane, decreasing the line tension and energy penalty for forming such an interface. Most prior experimental studies using linactants focus on liquid-liquid phase separations. The interaction of linactants with solid phases remains unclear. The most studied system for solid- liquid phase transitions is a mixture of a saturated lipid (e.g. DPPC) and an unsaturated lipid (e.g. DOPC). When cooling this system below its phase transition temperature, solid domains enriched with saturated lipid appear. Although solid-liquid phase transitions are commonly observed in model membranes [27, 32, 38, 52, 117], relatively less work has been done on domain size regulation in these systems. Solid domains can play significant roles in various cell processes, such as apoptosis [52], and it is paramount that their formation and growth mechanisms are thoroughly understood.

Apart from linactants, there are other molecules which influence bilayer structure and properties to a great extent. Cell membranes are in contact with a wide variety of molecules, such as oily lipid droplets [118, 119], and since some methods to form a model bilayer necessitate the use of a solvent for the lipids [94, 120, 121], oil molecules have been the subject of numerous studies [122-127]. The need for solubility makes it at the same time difficult to remove the oil from the lipid bilayer once formed. Attention has focused on how this residual oil affects bilayer structure and phase separation temperatures [122, 123, 126, 128]. An important result of these studies was that phase separation temperatures are increased when residual oil is present in the bilayer. However, its influence on domain size has not been examined thoroughly, especially for solid-liquid phase transitions. Likewise, membrane viscosity measurements in different oil solvents are scarce.

Results observed for different experimental techniques, both with respect to the size of the domains observed and whether or not equilibrium conditions are reached have been key to much of the discussions in literature [103, 106, 129-131]. The consensus seems to be that in cells mainly nanodomains are present, although micrometer domains have also been observed, depending on the technique. Stable micrometer sized domains have been observed for compositions closer to the binodes and using fluorescence microscopy [103]. Nanosized domains, stable or transient in nature, are more likely related to compositions close to a critical point [111]. Yet both the nano- and macroscopic domains are an emanation of the same underlying tendencies for phase separation. Phenomena such as coalescence and Ostwald ripening have been observed [103, 106, 110], but most studies in literature correspond to situations where the domains are kinetically trapped into non-equilibrium states as observation time of these domains are typically limited.

In the present work we investigate how linactants and selected oil molecules regulate macroscopic domain size in solid-liquid phase separations. By doing so, we turn the presence of oil, which is usually considered to be a disadvantage, into a possible advantage to create model bilayers which have domains as large as 50 micrometers making the effects readily studied by standard fluorescence microscopy. We use a thin film balance, which is a modification of the Montal-Mueller technique [80], where the pressure and tension in the film are controlled, to produce large-area model biomembranes (LAMBs) [94], which are stable in time. We then study the effects of a hybrid lipid (POPC) and of three different oils (*n*-hexadecane, squalene and *n*-decane) on bilayer phase separation of DOPC and DPPC, focusing on domain size and transition temperature, and also measuring membrane viscosity in three different oil conditions. It is well known that the oils used in the formation of bilayers remain present in the bilayer depending upon their water and lipid solubility and the size of

the solvent molecule relative to the length of the alkyl chain of the lipids [132]. Here, we use oils and mixtures thereof that are either about the same size as the alkyl chains in DOPC/DPPC (*n*-hexadecane) or that are significantly larger (squalene [133]) or smaller (*n*-decane). Squalene also has more saturated bonds and the lowest solubility in most lipids bilayers. However, for mixtures of lipids, less information is available onto how oils affect the bilayer structure and phase equilibria. LAMBs are planar, free-standing and have an area of up to 1 mm^2, thereby facilitating fluorescence imaging of microscale domains and decoupling effects from curvature. We adopt a stringent protocol where the phase separation is induced by a relatively slow temperature quench. Moreover, the planar interface of LAMBs facilitates tracking of domains over relatively long time scales to evaluate further changes of the domain size due to potential effects of coalescence or Ostwald ripening. We find that the nature and length of the oil chains has a strong influence on phase separation and domain size, while the inclusion of linactant molecules regulates domain size over a narrow concentration window without modifying the transition temperature.

3.2. Experimental

3.2.1. Materials

The phospholipids 1,2-dioleoyl-*sn*-glycero-3-phosphocholine (DOPC), 1,2-dipalmitoyl-*sn*-glycero-3-phosphocholine (DPPC), 1-palmitoyl-*sn*-2-oleoyl-glycero-3-phosphocholine (POPC), and 1,2-dioleoyl-*sn*-glycero-3-phosphoethanolamine-N-(lissamine rhodamine B sulfonyl) (ammonium salt) (Rh-DOPE) were obtained from Avanti Polar Lipids. Squalene, *n*-hexadecane, *n*-decane, and octadecyltrichlorosilane (OTS) were purchased from Acros Organics (USA). NaCl (99.99%, metals basis) and $NaHCO_3$ were obtained from Alfa Aesar. $CaCl_2$ was purchased from Sigma-Aldrich. Deionized water (Milli-Q, Merck-Millipore, resistivity < 18.2 MΩcm) was used to prepare all buffers.

3.2.2. Sample preparation

Phospholipids, initially stored in chloroform, are dried under nitrogen before being placed under vacuum, and resuspended in either *n*-hexadecane, squalene or *n*-decane following the same procedure as in previous work [94] and as described in Chapter 2. The fraction of DPPC

in the solvent mixture was kept constant at 40 mol%. The fraction of the fluorescent lipid added to the lipid mixture was between 0.5 and 1.5 mol%.

3.2.3. Experimental setup

The creation of large-area model biomembranes (LAMBs), including the fabrication and functionalization of the microfluidic chips and the setup of the pressure control system, follows the same protocol as explained previously (Chapter 2). Membrane tensions of the resulting bilayers are kept high, and are in the range of 1-5 mN/m. First, we determined the phase transition temperature of each bilayer composition. We define the phase transition temperature T_m as the temperature when the first domain appeared. At least three measurements were conducted per lipid mixture to determine T_m. Bilayers were formed above the expected melting point of the lipid mixture, and then cooled at a constant cooling rate of 0.8 °C/min. This is a relatively slow cooling rate compared to the time scales of lipid diffusion (1-80 $\mu m^2/s$ in free-standing membranes [106]).

To observe the long-time domain formation kinetics, bilayers were formed 3-4 °C above the previously determined phase transition temperature T_m of the lipid mixture, and then cooled at a cooling rate of 0.8 °C/min to about 1 °C below T_m. Bilayers were kept at this temperature to observe domain growth. We define a domain diameter, D, as the average of the major and minor axis length, measured at about 1 °C below the phase transition temperature. For the system under investigation we observe that 20-25 minutes after nucleation the domains stop growing and a stable diameter is reached. The average domain diameter was then calculated by taking the average of the diameters of at least three domains. The growth of domains formed at the edge of the bilayer or too close to other domains was influenced by the boundary effects and therefore these domains were excluded.

3.2.4. Image analysis

In order to analyse the domain dynamics, a MATLAB (Mathworks Inc., Boston, Massachusetts) code was written. Fluorescence images were cropped, inverted, bandpass filtered and thresholded. The domains were tracked with an adaptation of the famous IDL particle tracking software written by David Grier, John Crocker, and Eric Weeks. The MATLAB adaptation was written by Daniel Blair and Eric Dufresne and is freely available

[134]. Examples of processed images for the tracking algorithm are shown in Figures 3.1 and 3.2.

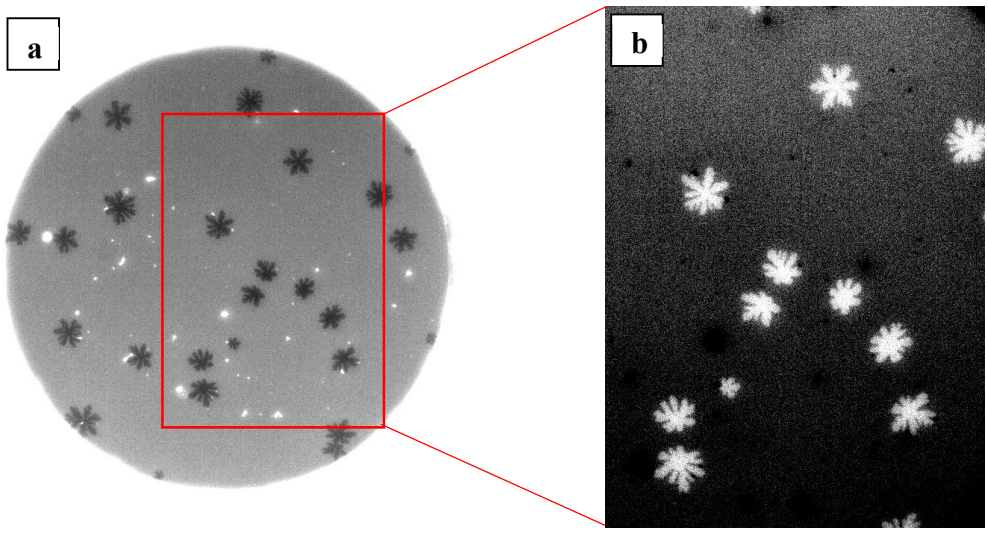

Figure 3.1: (a): Original fluorescence microscopy image of a bilayer formed from a 3:2 DOPC:DPPC lipid mixture in *n*-hexadecane. (b): Cropped and inverted image with enhanced contrast.

To derive the ratio between the area occupied by the solid DPPC domains (black areas) and the total area of the bilayer (light grey + black areas), the images are analysed according to the following procedure. We first extract the total area of the bilayer and we use it to define the region of interest (ROI) for the detection of the solid domains. For the extraction of the total area, each image is preprocessed by applying cropping, brightness adjustment, smoothing (namely a filter replacing each pixel with the average value of the surrounding 3x3 square) and using a "rolling ball" background subtraction [135]. The image is then binarized via thresholding, to obtain a mask of the total area of the lipid bilayer. We visually inspect the result, to verify correspondence between the sharp edge of the bilayer and the detected mask. When required, we remove spurious detections and we fill occasional undetected pixels inside the bilayer. The total area of the bilayer is then used to define the ROI for the detection of the solid domains, on the original images. The preprocessing steps are repeated, on such a region, with the addition of contrast limited adaptive histogram equalization (CLAHE [136]). Each image is binarized by means of thresholding and visually inspected to correct for spurious detections. Finally, the black pixels are counted and the ratio between darker solid domains and total area of the lipid bilayer is derived.

The analysis is performed using an in-house code written in ImageJ macro language, based on the native Fiji plugins Brightness/Contrast Adjustment, Smooth, Subtract Background, Analyze Particles, as well as Stephan Saalfeld's CLAHE plugin [137].

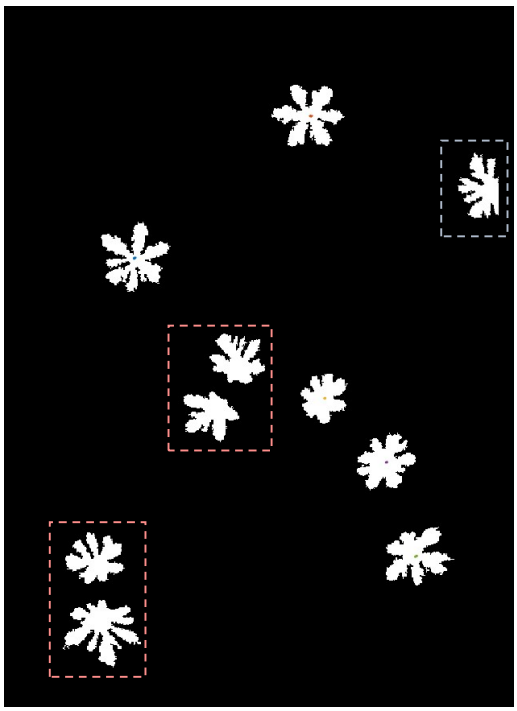

Figure 3.2: Example of a processed image with domain tracks (coloured points in the domain centres). The corresponding original fluorescence microscopy image is shown in Figure 3.1a. Domains close to the image edges (light blue square) or domains that are too close to neighbouring domains (light red squares) are not tracked.

3.2.5. Membrane viscosity

The translational diffusion coefficient D_T was determined by first calculating the mean-squared displacement (MSD) from the domain tracks and then fitting it to the following equation:

$$MSD = \langle r^2(\tau) \rangle = 4 * D_T * \tau$$

Here, τ denotes the delay. Prior to the fitting, the MSD was corrected for drift. Domains close to the image edges and domains that were very close to neighbouring domains were not tracked, since their movement was hindered by each other.

To determine the membrane viscosity η_m, domain diffusion coefficients were binned every 0.5 µm in radius and fitted to the Petrov-Schwille equation:

$$D_T(\varepsilon) = \frac{k_B T}{4\pi\eta_m} * \left[ln\left(\frac{2}{\varepsilon}\right) - \gamma + \frac{4\varepsilon}{\pi} - \left(\frac{\varepsilon^2}{2}\right) ln\left(\frac{2}{\varepsilon}\right) \right] * \left[1 - \left(\frac{\varepsilon^3}{\pi}\right) ln\left(\frac{2}{\varepsilon}\right) + c_1 \varepsilon^{b_1} / (1 + c_2 \varepsilon^{b_2}) \right]^{-1}$$

with the parameters $c_1 = 0.73761$, $b_1 = 2.74819$, $c_2 = 0.52119$ and $b_2 = 0.51465$. $\gamma = 0.5772$ is the Euler constant and $\varepsilon = \frac{2*r*\mu}{\eta_m}$ is the reduced inclusion size.

3.3. Results and discussion

3.3.1. Effects of oil solvents

We first focus on the effects of three different oils (*n*-hexadecane, squalene and *n*-decane) on lipid phase separation in a 3:2 DOPC:DPPC lipid mixture. The molecular structures of all the lipids and oils used in this work are shown in Figures 1.6 and 2.4. Figure 3.3a shows typical fluorescence microscopy images of the phase separation experiment at constant temperature after decreasing the temperature from 32 to 27 °C at a cooling rate of 0.8 °C/min (the contrast was enhanced for better visability using the software ImageJ). Upon the formation of solid domains enriched with DPPC, the fluorophore gets excluded from the structured domains and hence the solid phase appears dark. The domains grow in size congruent with a nucleation and growth mechanism. The domains reach a stable size 20-25 minutes after nucleation, as can be seen in Figure 3.3b. In order to compare the extent of phase separation and the evolution of the domain size, experiments were carried out at equal degree of undercooling. The temperature was set at 1 °C below the phase transition temperature. Shortly after nucleation, the temperature was not constant yet, therefore no data points are reported. The dashed line is a fit to the equation $d = \beta * t^{\alpha}$. The best fit was obtained at $\alpha = 0.33$, $\beta = 13.06$. The growth exponent [138] $\alpha = 1/3$ as well as the dendritic shape of the domains [27, 38, 139] have been observed in other studies on domain growth in these systems, both indicating a diffusion-controlled growth process rather than a reaction-controlled growth, which generally results in more compact structures [140].

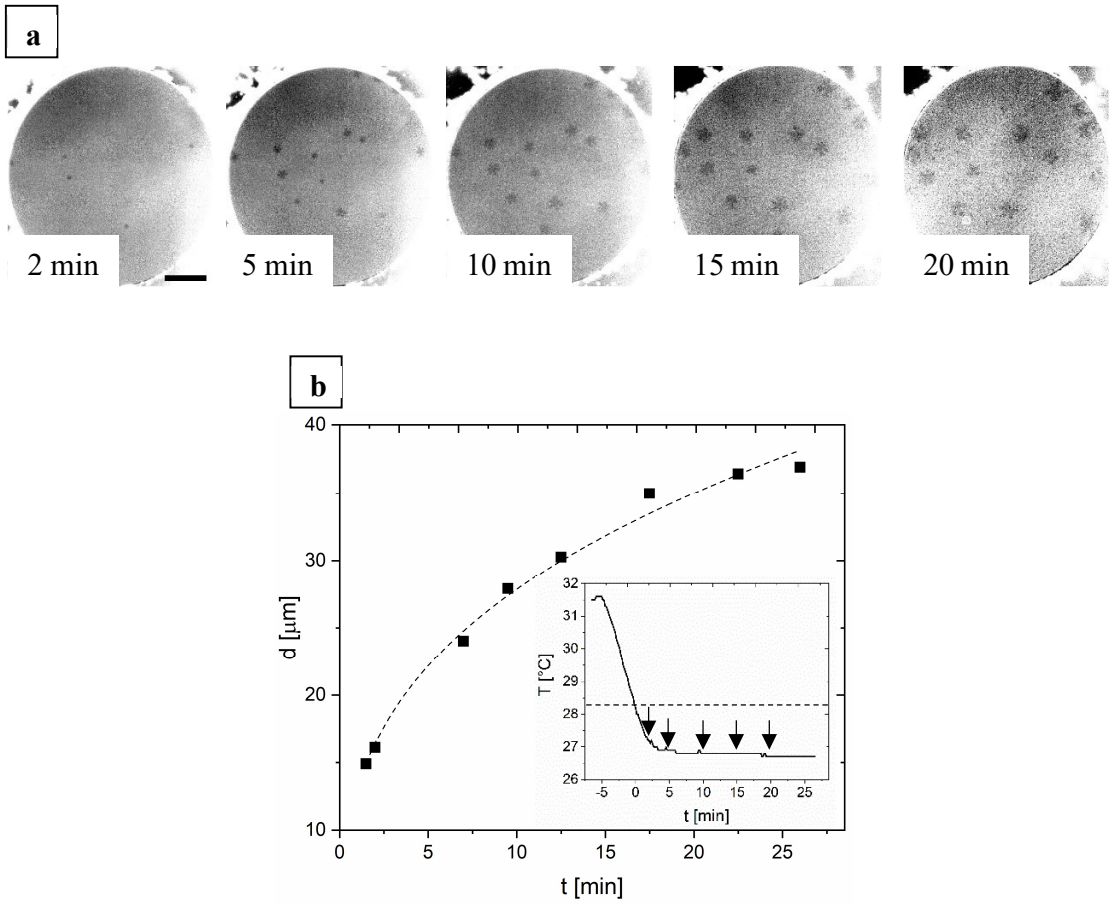

Figure 3.3: (a): Fluorescence microscopy images of a typical temperature quench phase separation experiment. A liquid-disordered bilayer was formed from a 3:2 DOPC:DPPC lipid mixture in a 50:50 *n*-hexadecane:squalene oil mixture. Solid domains first appeared as dark spots at 28.2 °C. The images were taken at 27 °C and between 2 and 20 min after phase separation. The fluorescent lipid Rh-DOPE preferentially partitions into the more fluid phase, making the solid domains appear dark. The scale bar represents 100 µm. (b): Time evolution of the average diameter, d, of the domains in (a). Domains reach a stable size 20-25 minutes after nucleation. The dashed line is a fit to $d = \beta * t^{\alpha}$, with $\alpha = 0.33$, $\beta = 13.06$. The inset shows the temperature profile of the experiment. The dashed line in the inset marks the phase transition temperature (28.2 °C). The arrows mark the points where the images in (a) were taken.

The stable domain diameter *D*, measured after the steady state is reached, for four different oil conditions is shown in Figure 3.4a. *D* was calculated by taking the average of at least three domains per experiment, and at least three experiments per composition were conducted. The largest sized domains are formed in mixtures of 75% *n*-hexadecane and 25%

squalene. Domain size decreases the more squalene is added. The smallest domains are formed in 100% *n*-decane. We have not observed any changes in the nucleation density when changing the composition of the system, suggesting a heterogeneous nucleation due to unavoidable impurities. In 100% *n*-hexadecane, no data could be acquired because the bilayers were not stable for a sufficient amount of time (> 25 min) to measure domain size. In the case of 100% squalene, the domains were too small to be resolved and the contrast too weak to measure domain size and T_m in a reliable matter (resolution limit: 1 μm). However, the trends in the data are clear. T_m decreases the more squalene is used in the solution from which the bilayers are formed, suggesting that the oil partitions into the bilayer proportional to their bulk concentrations. Congruent with other measurements, the phase transition temperature approaches the one found in solvent-free giant unilamellar vesicles [28] (Figure 3.4b).

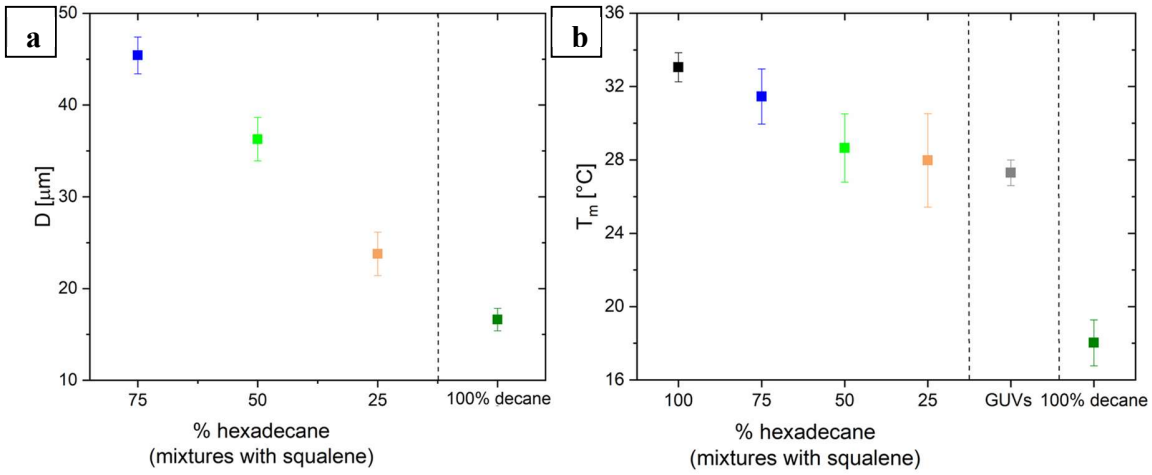

Figure 3.4: (a): Dependence of stable domain size, *D*, on oil composition in 3:2 DOPC:DPPC lipid mixtures. (b): Phase transition temperatures for 3:2 DOPC:DPPC lipid mixtures with different oil compositions. At least three measurements per point were conducted. For comparison, a literature value obtained for oil free GUVs is shown [28].

While *n*-hexadecane increases T_m, *n*-decane, on the other hand, decreases it by almost 10 °C. For squalene, results tend to be the same as for solvent-free methods. The effects of long and short alkanes on phase transition temperature in single lipid bilayers were already measured and rationalized decades ago [122, 128]. The phase transition temperature is determined by the change in the Gibbs free energy, ΔG:

$$\Delta G = \Delta H - T\Delta S$$

If ΔG is negative, the system undergoes a phase transition. Longer alkanes, such as *n*-hexadecane, tend to align themselves predominantly parallel to the lipid chains, as evidenced from MD simulations and neutron scattering data [141], thereby increasing lipid packing and chain interaction and decreasing the entropic contribution, S. This leads to an increased T_m. The results in Figure 3.4 suggest that the same trends are confirmed for mixed lipid bilayers. On the other hand, the incorporation of shorter alkanes like *n*-decane in single lipid bilayers has been understood to result in decreased chain interaction and T_m [142]. Capacitance measurements have shown that squalene, a high molecular weight, branched, and unsaturated molecule, is predominantly excluded from bilayers formed using oil solvents [96, 133], forming thinner membranes. However, recent measurements using second-harmonic microscopy have shown that traces of squalene stay within the bilayer [143]. The fact that using squalene as oil solvent results in phase transition temperatures close to the ones found in GUVs leads to the conclusion that, if there is some squalene still present in the bilayer, it is orientated parallel to the membrane plane and between the two leaflets, thereby not influencing the interaction between the chains (in contrast to *n*-hexadecane and *n*-decane) or the structural packings in the outer membrane. Figure 3.4 shows how the phase transition temperature and domain size for oil mixtures seems to follow, to first order, simple mixing rules even in mixed DPPC/DOPC bilayers.

To further investigate the effect of oil on the phase behaviour, we have measured the area fraction of the fluid phase A_{fluid}. This is shown in Figure 3.5 for mixtures of *n*-hexadecane and squalene. It can be seen that the relative amount of fluid phase changes dramatically when 50% squalene is added to the system, indicating a shift of the phase boundaries in the phase diagram towards a higher miscibility of the components. The relative quantities and compositions of each phase in an equilibrated system is determined by the location in the phase diagram and the lever rule. The equilibrium between two phases and therefore the phase boundaries are determined by the Gibbs free energy G, which in turn depends on the chemical potentials μ_i of the components:

$$\mu_i = \frac{\partial G}{\partial N_i}$$

N_i denotes the particle number of component i. Adding oil to the lipid system affects the chemical potentials of the lipid components greatly by influencing the enthalpy H (i.e., the interaction between the chains) and the entropy S (i.e., the degree of order) of the system. As mentioned before, *n*-hexadecane increases the chain interaction and reduces the entropy by

reaching far into the bilayer and orienting itself parallel to the lipid chains [122, 141]. This increases the order of the system. Squalene, on the other hand, is too bulky to fit in between the lipid chains and is probably oriented parallel to the membrane plane. It increases membrane disorder slightly by reaching into the hydrophobic region of the bilayer with its branches and by reducing interdigitation of the lipid chains. In mixtures of *n*-hexadecane and squalene, adding more squalene increases the miscibility of the different lipid components by decreasing the lipid chain interactions due to squalene's branched molecular structure. Figure 3.5 reflects how at equal degrees of undercooling, *n*-hexadecane decreases the propensity to form solid domains, as it is a good solvent for both DOPC and DPPC. When the *n*-hexadecane content falls below 50% in the bulk mixture, this changes and the solid domain fraction increases.

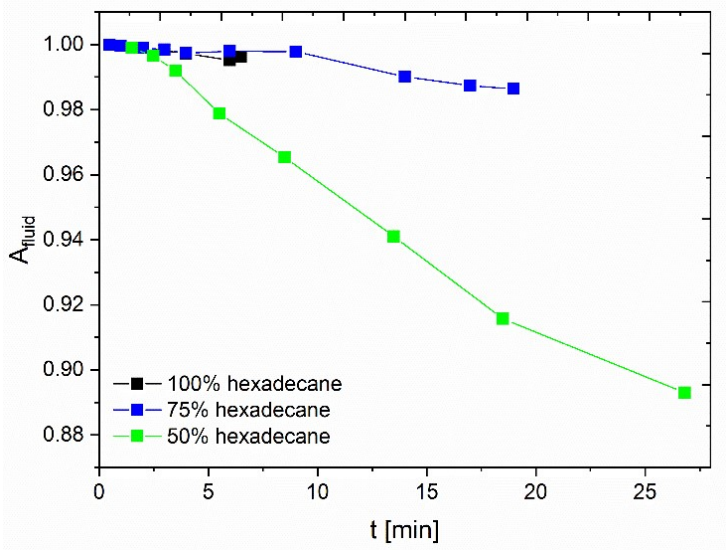

Figure 3.5: Dependence of area fraction of the fluid phase versus time for different oil compositions in 3:2 DOPC:DPPC lipid mixtures.

n-Decane has a similar, yet stronger, effect as squalene. Compared to the chain lengths of DOPC and DPPC, it is a short molecule that does not fit well into the space between the fatty acid chains and is located predominantly in the midplane of the bilayer. This is confirmed by bilayer thickness measurements [144]. *n*-Decane remains more present within the bilayer, and hence, despite being a smaller molecule, it disrupts the lipid chain order even more than squalene (which is expelled more), leading to a strongly decreased phase transition

temperature. Apart from the size of the solvent molecule and the interactions (methyl groups versus methylene groups), the degree of incorporation matters.

Another contribution to the chemical potential comes from the line tension. Increasing line tension generally results in bigger domains. A major contributor to line tension is the height mismatch between the solid DPPC and the fluid phase, where DOPC is the dominant lipid [110, 112]. This mismatch is influenced by the amount of oil that stays in the bilayer. Results from earlier studies show that *n*-hexadecane remains between the DPPC chains in the solid phase [122, 123, 128], in contrast to *n*-decane [145]. McIntosh et. al. [122] moreover stated that long alkanes (with 12 or more C-atoms) remove the chain tilt in DPPC bilayers in the gel state, thereby increasing bilayer height (from 4.2 to 4.8 nm). A pure DOPC bilayer containing *n*-hexadecane has an approximate thickness of 3.3 nm [96]. In a phase-separated bilayer consisting of solid DPPC domains and fluid DOPC and containing *n*-hexadecane, this results in a thickness mismatch at the edge of the domains of 1.5 nm. In the case of *n*-decane, the thickness of the gel phase is reduced by 0.6 nm. Since the thickness of the fluid DOPC phase increases when *n*-hexadecane is replaced by *n*-decane [144], the thickness mismatch is reduced to a great extent. Therefore, the line tension between DPPC and DOPC regions is significantly increased when *n*-hexadecane is used. Increasing squalene concentrations reduces the amount of *n*-hexadecane retained in the bilayer, leading to a reduced height mismatch and line tension.

Figure 3.6 shows the membrane viscosities η_m for three different oil conditions. In 100% *n*-decane, there was too much drift to measure the diffusion coefficient in a reliable matter. No significant trend for η_m can be observed when changing the composition of the oil solvent. It was expected that η_m would decrease when more squalene was added, since this oil is pushed out from the bilayer. These results indicate that even for mixtures of 50% *n*-hexadecane and 50% squalene, there is still a considerable amount of oil left in the bilayer. The temperature at which the viscosity measurements were carried out decreases the more squalene is added, since T_m also decreases.

3.3.2. Effects of linactants

POPC is a so called hybrid lipid composed of a saturated and an unsaturated tail, which can be expected to preferentially accumulate to the interline between the coexisting phases, acting as a linactant [115]. We define $\rho \equiv$ [DOPC]/([DOPC]+[POPC]) [146]. The higher ρ, the more DOPC is present in the bilayer. The amount of DPPC in the mixture is kept constant at

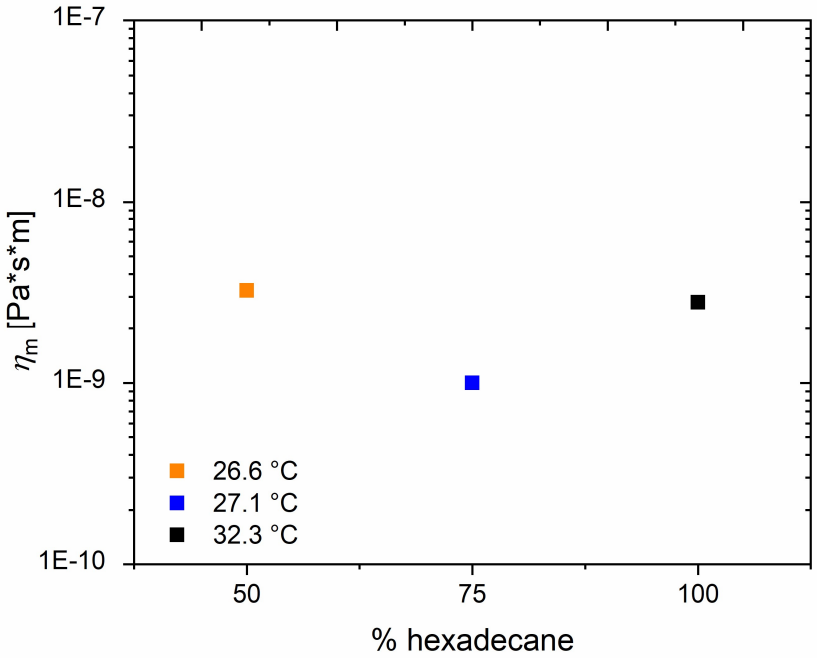

Figure 3.6: Membrane viscosities η_m for 3:2 DOPC:DPPC lipid mixtures with different oil compositions.

40 mol%. Different oil compositions (mixtures of *n*-hexadecane and squalene) are also used, since the degree of bilayer swelling of the fluid phase in the bilayer influences the line tension. Figure 3.7a shows the domain diameter D vs. ρ for three different oil compositions (mixtures of *n*-hexadecane and squalene). Adding POPC decreases the domain size for all oil compositions, as observed earlier [146, 147]. The linactant molecules accumulate at the interface between solid and liquid domains [115], which reduces the height mismatch and therefore the line tension, leading to smaller domains. Only small concentrations of linactant are necessary to saturate this effect. Adding more linactant after ρ = 0.9 (5.4 mol% POPC) has no effect on the domain size. This effect is similar to the one seen in surfactants in bulk, which reduce surface tension only up to the point, known as the critical micelle concentration (CMC) [148]. Once sufficient linactant is at the interface between the two phases, the differences between bilayers formed from different oils is reduced, as seen in the agreement between the 75% and 50% *n*-hexadecane data. In contrast, there are still differences with majority squalene bilayers, likely due to the packing differences explained earlier. Since line tension is to a large extent dictated by the height difference between the domains, addition of linactant to bilayers with significant amounts of *n*-hexadecane may serve to "smooth out" the otherwise step-like difference in thickness between solid and liquid domains.

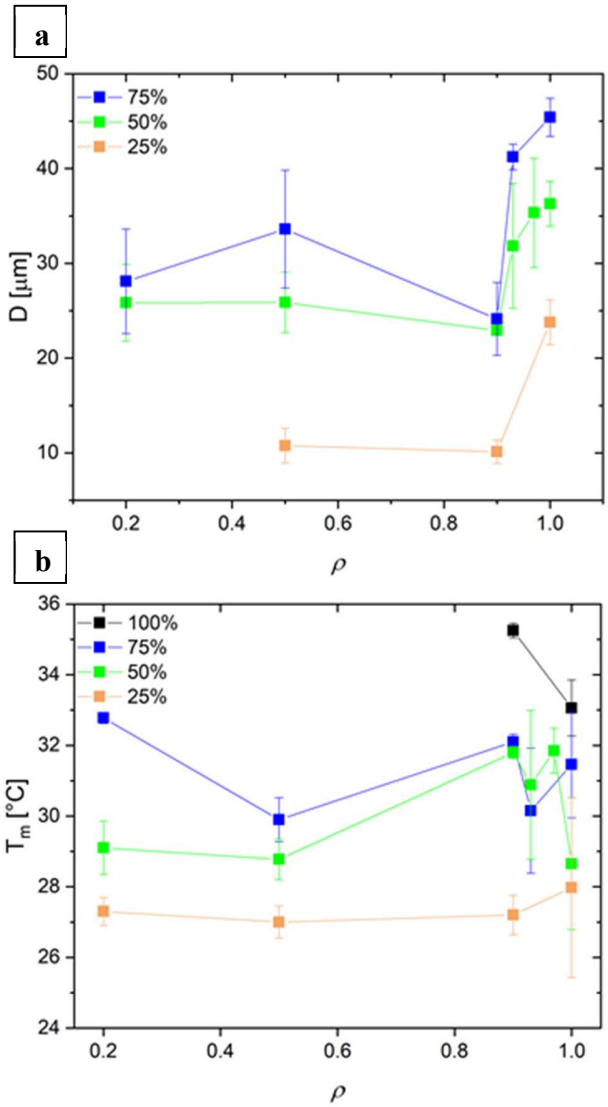

Figure 3.7: (a): Stable domain size, D, vs. ρ for 3:2 (DOPC+POPC):DPPC mixtures with different oil compositions (*n*-hexadecane/squalene). Domain size decreases once linactant is added. (b): Phase transition temperature vs. ρ for 3:2 (DOPC+POPC):DPPC mixtures with different oil compositions (*n*-hexadecane/squalene). The effect of linactant on T_m depends on oil composition. At least three measurements per point were conducted.

Figure 3.7b shows that the effect of POPC on the phase transition temperature depends on oil composition (mixtures of *n*-hexadecane and squalene). At low *n*-hexadecane content in bulk (25%), T_m remains unchanged within experimental accuracy. When more *n*-hexadecane is added (50-100%), T_m seems to increase for $\rho = 0.9$, but then again decreases to the original value. This indicates that there is a small window where "linactant" effects on phase

separation are measurable. At large POPC concentrations, the molecule behaves as a bulk constituent and the phase separation is dictated by the ternary POPC/DOPC/DPPC phase diagram. At small amounts of POPC, the molecule is able to preferentially accumulate at the interface between the two phases, causing the phase transition temperature to increase. However, in contrast to the oil molecules, POPC does not have as large an effect on phase transition temperature.

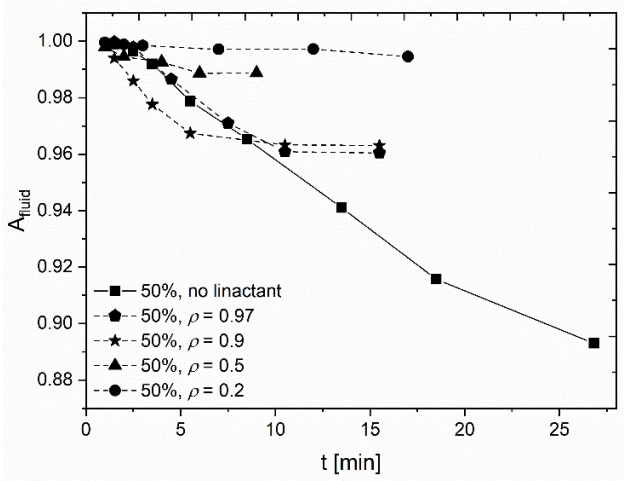

Figure 3.8: Dependence of area fraction of the fluid phase on ρ in 3:2 DOPC:DPPC lipid mixtures containing 50% *n*-hexadecane and 50% squalene.

The area fraction of the fluid phase A_{fluid} decreases when linactant is added to the system (Figure 3.8). This is in accordance with the reduced domain size when adding linactant. It can be noted that a stable area fraction is reached faster when linactant is present in the system. Furthermore, there is a large initial effect when adding linactant (from no linactant to ρ = 0.97), but the effect of adding more linactant is quite small. While oil molecules influence both phase transition temperatures and domain sizes, linactants change only the latter by reducing the line tension. In total, by combining the effects of oils and linactants, systematic control of equilibrium domain sizes ranging from 10 µm to 50 µm are achieved.

3.4. Conclusion

The effects of linactants and different oils on the phase separation have been studied systematically for planar, free-standing lipid bilayers containing DOPC and DPPC, focusing

on phase transition temperatures and evolution of solid domains. Long alkanes like *n*-hexadecane swell the bilayer and increase phase transition temperature and domain size, while short alkanes like *n*-decane significantly decrease them. Linactants, like POPC, decrease the domain sizes, but only at low concentrations. When adding more linactant, the domain size remained constant, suggesting effects strikingly similar to the existence of a critical micelle or crucial aggregation concentration of surfactants in bulk systems. This is an important result, showing that domain size can only be influenced by linactants up to this critical concentration. The phase transition temperature was not highly influenced by the presence of linactant. The effect of both oil and linactant molecules can be explained by changes in the chemical potentials of the lipid molecules. Oil molecules highly influence the chemical potentials by changing enthalpic and entropic terms, while linactants only act on the line tension, which is confirmed by the dependence of the area fraction of the fluid phase. From these results, it is apparent that oil molecules are not passive bystanders to lipid membrane formation, but rather alter the entire phase behaviour of a lipid system. Overall, we have shown that solid phase domain size can be regulated not only by line-active agents, but also by structurally simple molecules. This may need to be considered when using model bilayer systems containing oil and comparing results with non-model membrane systems.

Chapter 4

Effect of cholesterol on phase transition temperature and domain line tension

Cholesterol is one of the most important components of animal cell membranes. However, its effects on cell membrane structure and especially the formation and regulation of lipid rafts are still not completely understood. Here, we study how cholesterol affects the phase behaviour of 1:1 DOPC:DPPC lipid bilayer containing *n*-decane, an oil selected here since the lipids are well soluble in the oil, and we observed that direct cholesterol incorporation from the bulk lipid mixture into the bilayer is possible here. We find, contrary to what is reported in literature for solvent-free bilayers, that the addition of cholesterol increases the phase transition temperature. This can be rationalized by the expulsion of *n*-decane from the bilayer upon adding cholesterol. Furthermore, low and high amounts of cholesterol in the bilayer have different effects on the domain line tension, depending on whether cholesterol is mainly incorporated in the L_o or the L_d phase. Lastly, we find that *n*-decane reduces the amount of cholesterol necessary to form the L_o phase, a result which may be very important for understanding the role of fat molecules and cholesterol in lipid raft formation.

4.1. Introduction

Sterols, or steroid alcohols, are a major class of lipids found in all cell membranes. They assume very important functions in animal cells as well as in cells of plants and fungi. Most importantly, they are responsible for regulating cell membrane properties such as fluidity,

permeability and stability, and act as precursor molecules for several vitamins and hormones [149-151].

All sterols consist of a four-ring structure (Figure 4.1). This structure is responsible for the rather rigid and flat nature of the molecule. The hydroxyl group renders the compounds amphiphilic. Without this small entity, sterols would be hydrophobic in nature.

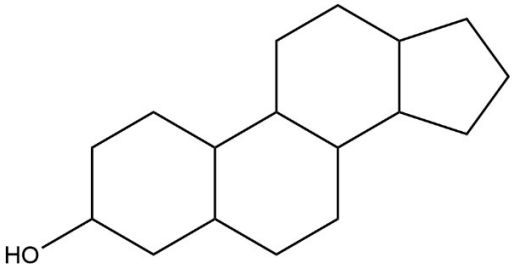

Figure 4.1: Typical four-ring structure of sterols. The hydroxyl group renders the compounds amphiphilic.

Sterols are usually divided into three classes: animal sterols, plant sterols (phytosterols) and fungisterols. While in animals cholesterol is the major species, fungi mostly contain ergosterol (Figure 4.2) [149]. Plant membranes embody several different sterols. Among them are stigmasterol and sitosterol (Figure 4.2) [149, 152].

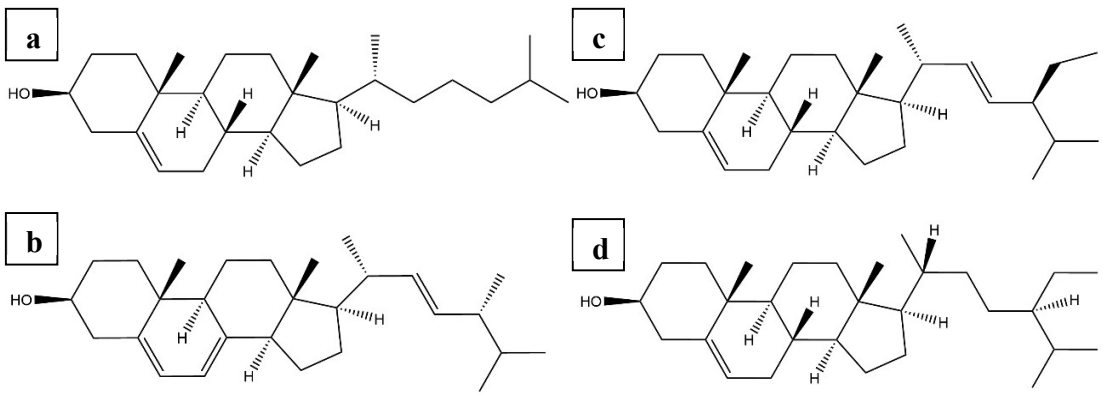

Figure 4.2: (a): Cholesterol. (b): Ergosterol. (c): Stigmasterol. (d): Sitosterol.

While ergosterol has received particular attention as a precursor for vitamin D2 and other vital hormones [153, 154], phytosterols are responsible for several processes in plants. For example, stigmasterol and sitosterol control membrane fluidity, while others are essential for growth [155, 156]. However, the role of several phytosterols in plant membranes is not yet clear and multiple mechanisms that might involve these molecules are still under investigation [155, 157].

Despite its somewhat bad reputation, cholesterol is an essential component of the lipid bilayers in animal cells, but is also present in plant membranes [152, 158]. Due to its large significance for cell functioning and health, the focus of this Chapter lies on the effects of cholesterol on phospholipid bilayer properties. In particular, its influence on phase separation will be investigated.

4.1.1. The role of cholesterol in cell membranes

Discovered in 1769 [159], cholesterol has received huge attention over the last half century because of its supposed negative role in health issues. Animal cells produce cholesterol, but it is also taken up with food. Despite major efforts, the exact effects of dietary cholesterol uptake are still not entirely clear [160, 161].

Similarly, the role of cholesterol and its arrangement in cell membranes is not yet fully elucidated. For example, very different reports exist on cholesterol's effects on the phase behaviour and the phase transition temperature between the liquid and ordered phases, and in particular for multicomponent systems effects are not fully clear. De Meyer and Smit [162] have used a coarse-grained model to calculate cholesterol's impact on a DMPC (1,2-dimyristoyl-*sn*-glycero-3-phosphocholine) bilayer and found increasing phase transition temperatures with increasing cholesterol content. On the other hand, Veatch and Keller [27] have observed experimentally using fluorescence microscopy studies that the phase transition temperature decreases upon the addition of cholesterol in GUVs consisting of a 1:1 mixture of DOPC and DMPC. They also tested other mixtures and found similar results [26, 27]. Contradicting results can even come from the same group. Levental et. al. [91] reported decreasing phase transition temperatures when increasing cholesterol levels in GPMVs. In a later publication [93], the same group observed the opposite. They argued that they derived the GPMVs from different cell types with different lipid compositions, and that these differences were probably the reason for the mismatching results. Gunderson and Honerkamp-Smith [163] have analyzed the differences between phase transition

temperatures measured in GUVs and on SLBs. They used a mixture of 1:1 DOPC:DPPC and varying amounts of cholesterol. They found that for all cholesterol concentrations, higher phase transition temperatures are measured in SLBs, and that phase transition temperatures in both systems decrease when adding cholesterol. However, the differences between phase transition temperatures measured in GUVs and SLBs increase with increasing cholesterol content. The authors did not give an explanation for these differences. All of these studies show that the effects of cholesterol on phase transition temperature in phospholipid bilayers vary over a wide range and experiments are occasionally difficult to interpret. Many mismatching results can be attributed to varying experimental conditions and lipid compositions. As shown by Veatch and Keller [32], even the growth temperature used during the electroformation of GUVs can change their composition and subsequently their phase transition temperature. Furthermore, the amount of cholesterol incorporation into bilayers depends on the lipid composition and preparation methods [164, 165].

For other bilayer properties, reported results from different research groups are more congruent. There is general agreement obtained from simulation studies as well as X-ray scattering experiments that the area per lipid decreases (i.e., the lipid packing increases) for small cholesterol fractions (< 10 mol%) and that bilayer thickness increases upon cholesterol incorporation, because the lipid fatty acid chains become more ordered [162, 166-168]. Additionally, consensus has been reached on cholesterol's impact on bilayer fluidity and permeability, both of which decrease upon adding cholesterol [169, 170]. Boughter et. al. [171] have conducted a broad MD simulation study on the effects of cholesterol on different lipid species, and found that lipid order and packing in the L_d phase increase for various types of headgroups and degrees of saturation. As a consequence of the increased lipid packing and order, diffusion coefficients decrease while membrane viscosities generally increase with increasing cholesterol content [172, 173].

However, it has to be noted that these results are generally valid for bilayers in the fluid, disordered state (i.e., above their phase transition temperature). In DPPC vesicles in the gel phase, cholesterol leads to a decrease in lipid order and an increase in fluidity [25, 174], results which are consistent with the ones found in DMPC vesicles [175]. Finally, the effects of cholesterol on some membrane properties, such as bending rigidity [176], highly depend on the specific lipids that constitute the membrane. Unsaturated lipids like DOPC are affected differently than saturated lipids like DMPC [177, 178].

All in all, these results suggest that cholesterol's actions on lipid bilayers are very complex and not easy to understand or predict. In addition, several research groups have reported that

the actions of cholesterol on real cells differ from the ones found in model membranes [169, 179, 180], which further complicates the problem. While in model membranes in the liquid-disordered state an increased cholesterol content usually leads to a decreased fluidity, this is not the case in real cell membranes. Byfield et. al. [179] have measured an increased cell stiffness upon cholesterol depletion, and attributed this effect to the interactions of the membrane with the cytoskeleton. Similar results were published by Hissa et. al. [180], who observed that the cell stiffness and bending modulus increase when removing cholesterol. This is in sharp contrast to the results reported by Needham and Nunn [181], who investigated vesicles with varying compositions, and found an increasing membrane cohesion and toughness when adding cholesterol. Of course, simplified model membranes never contain the complex lipid composition that real cell membranes do. Additionally, real cell membranes contain small nonpolar molecules that can freely diffuse within them and which might influence the effects of cholesterol. However, the main difference between the two systems is the absence of the cytoskeleton, and it is plausible that the contradicting results measured in model bilayers are mainly attributed to the missing membrane-cytoskeleton interactions. This has to be kept in mind when investigating the effects of cholesterol on membrane properties. Especially for protein functioning, the mechanical properties of cell membranes are of paramount importance.

4.1.2. The role of cholesterol in lipid raft formation

The significance of cholesterol for the formation of lipid rafts has already been mentioned earlier. Cholesterol is responsible for the formation of the L_o phase, which has a huge impact on protein functionality and mobility [50, 182, 183]. However, it is nowadays still unclear why the presence of cholesterol leads to these major changes in the cell membrane organization. Especially two questions remain unanswered:

1. **The interaction of cholesterol with saturated and unsaturated lipids**: For many years, it was assumed that the L_o phase forms because of the preferential interaction of cholesterol with saturated lipids, which can accommodate its rigid structure more easily. This is why a lot of studies focused on cholesterol-saturated lipid interactions [184]. However, recent results suggest that repulsive forces between cholesterol and unsaturated lipids could be at least equally important for lipid raft formation [185-188]. Additionally, Engberg et. al. [185] found that the number of double bonds in the unsaturated lipid

influences the order in the L_o as well as the L_d phase. This could be another explanation for why cell membranes contain so many different lipid species, namely to finely tune lipid organization and physical properties according to their current needs.

2. **The role of the molecular structure of cholesterol**: One of the most intriguing questions in cell membrane research, which remains unanswered, is why nature requires this huge library of different lipids. On a similar note, it is still unclear why cholesterol in particular has evolved to one of the most important components in the membrane. The synthesis of cholesterol is not easy and requires a large amount of reactions and energy [189, 190]. This raises the question why cholesterol was chosen in the evolutionary pathway to play such an important role in cell membranes and not, for example, its direct precursor lanosterol. The main difference between lano- and cholesterol are three methyl groups (marked in red in Figure 4.3). An even smaller difference in molecular structure can be identified between desmo- and cholesterol (namely, a double bond, marked in red in Figure 4.3). Desmosterol is another cholesterol precursor and present in animal cells. Vainio et. al. [191] have found that this small difference is responsible for cholesterol's ability to highly order the fatty acid chains in lipid bilayers, an ability which is critical for the formation of lipid rafts. All sterols can order fatty acid chains to some degree due to their rigid ring structure, but not all are so efficient as cholesterol. This is shown in Figure 4.4, which depicts results from MD simulations [191]. The molecular order parameter $-S_{CD}$ of the DPPC chain is shown for pure DPPC (black), DPPC-cholesterol (gray) and DPPC-desmosterol (dashed) systems. It can be seen that cholesterol leads to a higher order than desmosterol. Moreover, ergosterol, the main sterol in fungi, has a lower ordering efficiency, especially for unsaturated lipids [192, 193]. However, it is unclear whether this high ordering ability is the reason for the evolution of the distinct molecular structure of cholesterol. Yeagle [194] has hypothesized that the reason for this specificity is that sterols bind to enzymes, and since different cell types contain different enzymes, they have different requirements to the sterol structure. Furthermore, Beck et. al. [195] have shown that stigma- and sitosterol are also capable of forming the L_o phase.

To summarize, the effects of sterols, and of cholesterol in particular, highly depend on the lipid environment in the cell membrane. Certain sterols interact favourably with specific lipid species. This shows that the distinct molecular structure of cholesterol is of particular importance for a flawless functioning of animal cell membranes.

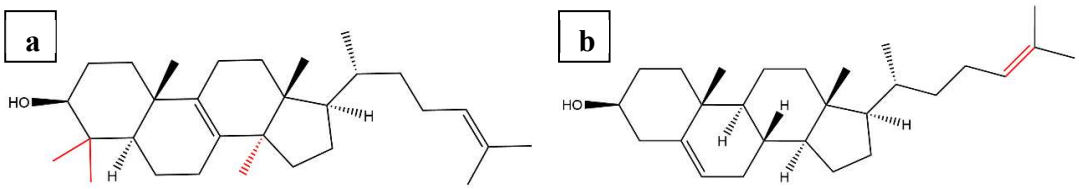

Figure 4.3: (a): Lanosterol. (b): Desmosterol. The main differences to the structure of cholesterol are marked in red.

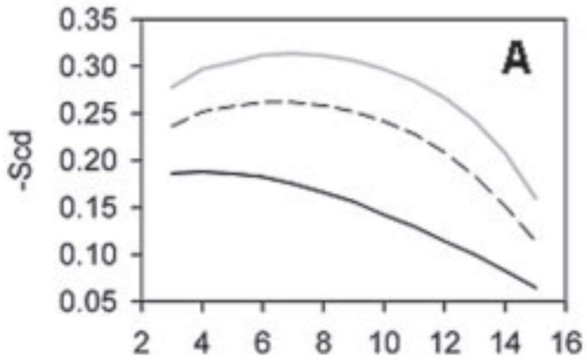

Figure 4.4: Molecular order parameter $-S_{CD}$ for the DPPC chain, obtained from MD simulations, for three different systems. Black: pure DPPC. Gray: DPPC-cholesterol. Dashed: DPPC-desmosterol. Carbon atoms close to the DPPC head group have the smallest segment number on the x-axis. Image taken from Ref. [191].

4.1.3. The arrangement of cholesterol in cell membranes

Cholesterol is usually depicted as lying parallel to the lipid fatty acid chains, with its hydrophilic head group located at the water interface (Figure 4.5a). However, this is not al-

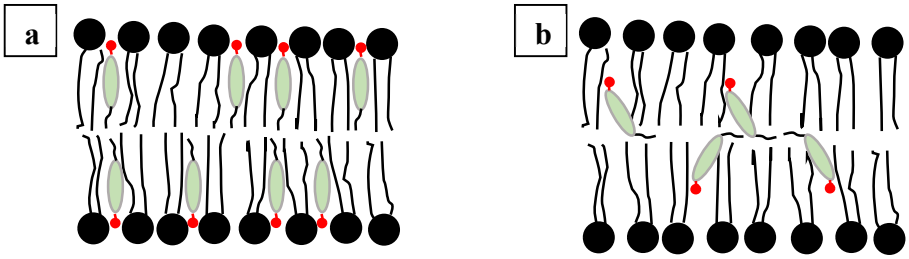

Figure 4.5: (a): Cholesterol is usually arranged horizontally to the lipid fatty acid chains. The hydrophilic head group (marked in red) is located at the water interface. (b): In bilayers consisting of polyunsaturated lipids, cholesterol is located in deeper, hydrophobic parts of the bilayer.

ways the case. For example, in thin bilayers or in bilayers consisting of polyunsaturated lipids, cholesterol seems to prefer a location deep within the hydrophobic part of the bilayer (Figure 4.5b) [196-198]. These results, obtained from neutron scattering experiments and MD simulations, show that the interactions of cholesterol with other lipids are to a high degree responsible for its organization within the cell membrane.

The exact mechanism for cholesterol arrangement has not yet been fully elucidated, but several models have been proposed:

1. **Condensed-complexes model**: This model (Figure 4.6) suggests that cholesterol forms close-packed structures with other lipids in the membrane, preferentially with saturated lipids. These complexes have a short-range order and a short lifetime [199].

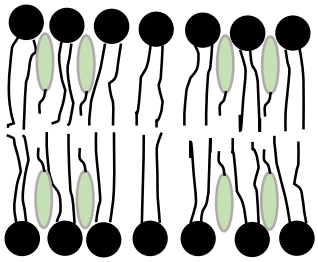

Figure 4.6: Representation of the condensed-complexes model.

2. **Superlattice model**: This model (Figure 4.7) states that cholesterol is regularly distributed within the lipid bilayer, forming a well-ordered lattice. Hexagonal and rectangular distributions have been proposed [200].

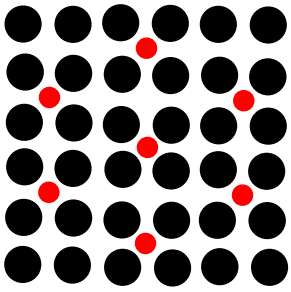

Figure 4.7: Representation of the superlattice model. Lipids are shown in black, cholesterol in red.

3. **Umbrella model**: The small hydroxyl group of cholesterol is not large enough to shield its hydrophobic body from aqueous environments. Therefore, the surrounding lipids have to provide this protection. This is the basis of the umbrella model (Figure 4.8). It hypothesizes that only hydrophobic interactions are responsible for the arrangement of cholesterol within membranes [201, 202].

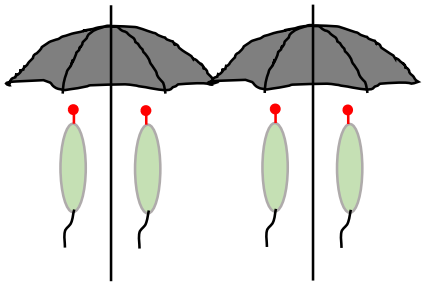

Figure 4.8: Representation of the umbrella model. Cholesterol is protected from the aqueous environment by the other lipids (shown as umbrellas).

Although several studies have been published in favour of one model or the other [202-204], no conclusive evidence has been found so far to unequivocally support one of these models. It is likely that, as evidenced by Giri et. al. in monolayers of DMPC and cholesterol [205], all models are applicable, but at different cholesterol molar fractions in the bilayer.

4.1.4. Methods to measure domain line tension

The size of domains and lipid rafts is an important quantity, as already mentioned in the previous Chapter 3, and depends to a large degree on the line tension between the L_o and the L_d phase. Two particularly often used methods to determine the domain line tension will be introduced below.

1. **Boundary fluctuations**: This method is based on tracing the boundaries of the domains and using the Fourier transform to get the fluctuation modes. Esposito et. al. [206] have used this method in GUVs of the composition 1:1:1 DOPC:DPPC:Cholesterol and obtained domain line tensions < 0.1 pN, which is a small value. Analysing boundary fluctuations is only suitable for these small line

tensions, since at higher values the fluctuation modes cannot be traced reliably (Figure 4.9).

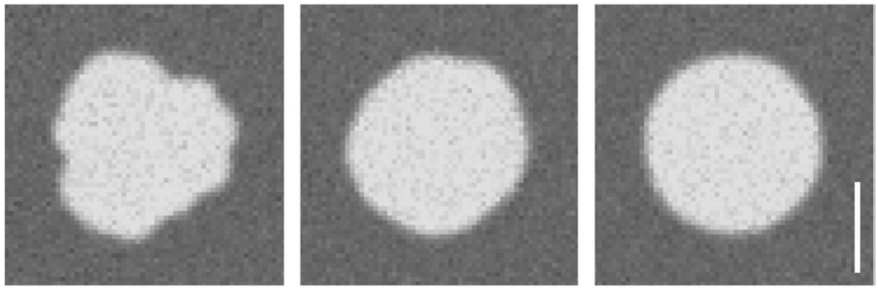

Figure 4.9: Fluctuating domains with line tension of 0.01, 0.1 and 1 pN (from left to right), obtained from computations. Fluctuations at a line tension above 0.1 pN are difficult to trace in a reliable manner. Image taken from Ref. [206].

2. **Domain relaxation** This method has often been applied to measure the line tension in Langmuir monolayers [104, 207]. The lipid domains are distorted by using a shear stress, and relax after removing the stress. By tracing the boundary of the relaxing domains and fitting it to a simulated relaxation, one can determine a characteristic relaxation time t_* [207]:

$$t_* = \frac{2 * \eta_{3D} * A}{\lambda}$$

Here, A is the area of the relaxing domain, η_{3D} is the bulk viscosity of the surrounding phase (in this case, water), and λ is the domain line tension. The factor 2 takes into account that the surrounding phase is present on both sides of the membrane.

In bilayers with fluid-fluid coexistence, this method can be used by monitoring the shape relaxation following the merging or coalescence of two domains (Figure 4.10).

It is important to note that this model can only be applied for isolated domains (i.e., the minimum distance between relaxing domains and any other domain should be at least one diameter of the bigger relaxing domain) and a stress free relaxation. This means that no external stresses (such as subphase flow or electric stresses) should act on the domain, otherwise the relaxation is not only driven by the line tension.

In this work, the second method was chosen to measure domain line tension, because the boundary fluctuation method requires a very high optical resolution to accurately trace the boundaries of domains with high line tensions.

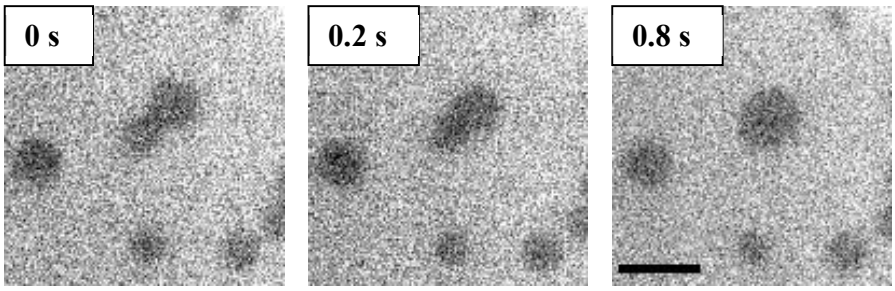

Figure 4.10: Merging of two domains in a 1:1 DOPC:DPPC bilayer, containing 25 mol% cholesterol in the bulk lipid mixture. Images were taken at 10 frames/s. Scale bar is 20 μm.

4.2. Experimental

4.2.1. Sample preparation and experimental setup

The lipid sample preparation and the production of LAMBs follows the same protocol as outlined in section 3.2. Here, only the differences compared to the previous experiments are described.

Cholesterol powder was received from Avanti Polar Lipids and dissolved in chloroform to produce a stock solution at a concentration of 2 mg/ml. It was then added to the lipid mixture in the appropriate amount. After drying the lipids, they were redissolved in *n*-decane at a concentration of 5 mg/ml.

4.2.2. Image analysis

To determine the bilayer viscosity, images were processed and analysed as explained in section 3.2. To calculate the domain line tension, images of two merging domains were again pre-processed as previously described. Then, the MATLAB code developed by Jacob Wintersmith [207] was used.

Starting from the initial condition (i.e., the first image of domain merger), the code simulates the relaxation using a boundary-integral method to capture the underlying hydrodynamics. The experimental images are then compared to the simulated domain shapes, to confirm that the simple model of line tension, membrane viscosity and bulk hydrodynamics captures the observed phenomena. Each experimental image is compared to all the simulated ones and the time scale of the simulations is then matched to the experiments by finding the time step in the simulation when the shape of the simulated domain most closely matches the domain shape in the experimental image, using a symmetric difference metric (Figure 4.11). The relaxation time t_* is then calculated using the following equation (Figure 4.12):

$$t_* = \frac{t_i - t_0}{T_{best}}$$

Here, t_i and t_0 are the experimental times of image i and the initial condition, respectively. T_{best} denotes the time in the simulation where the best-fitting domain shape is found.

4.3. Results and discussion

4.3.1. Phase separation

A typical phase separation experiment for a 1:1:1 DOPC:DPPC:Cholesterol mixture is shown in Figure 4.13. As expected for bilayers containing cholesterol, the formed domains are in the L_o phase, which is evidenced by their circular shape and the coalescence events.

Figure 4.14 shows the phase transition temperature T_m as a function of the cholesterol content of the bulk lipid mixture. As a comparison, literature values for 1:1 DOPC:DPPC mixtures measured in GUVs (oil-free) are shown [26].

Strikingly, and in contrast to the experiments conducted with GUVs, T_m increases when adding cholesterol to LAMBs. At 70 mol% cholesterol in the bulk lipid mixture, T_m reaches values (around 32.5 °C) comparable to the ones measured in GUVs at low cholesterol contents (between 10 and 25 mol%). When the cholesterol content is further increased to 90 mol%, T_m remains unchanged within experimental accuracy.

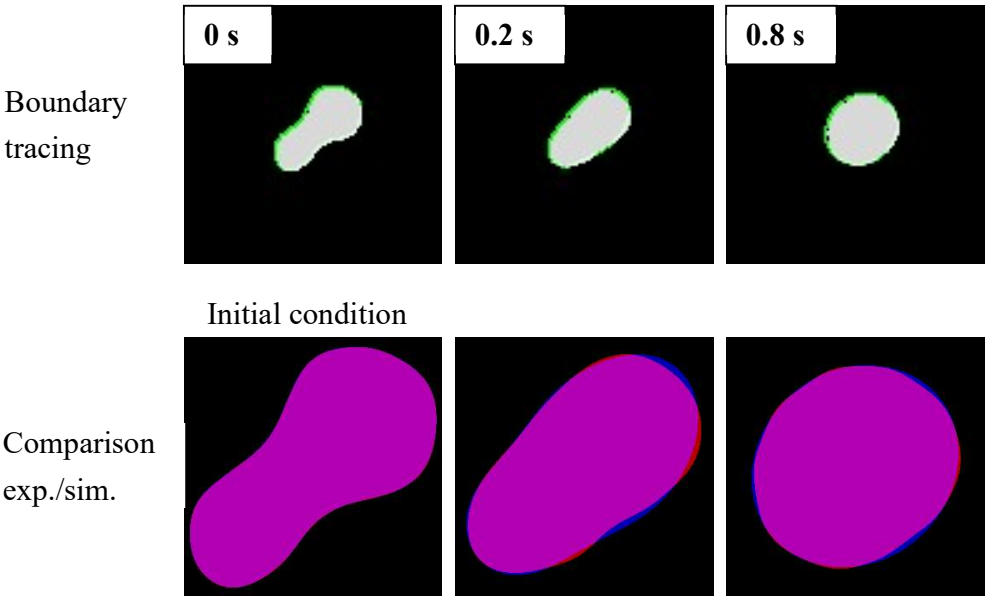

Figure 4.11: Top row: Tracing the boundary of the merging domains shown in Figure 4.9. Bottom row: Comparison between the experimental images (violet) and the best simulated shape. The difference is shown in red and blue.

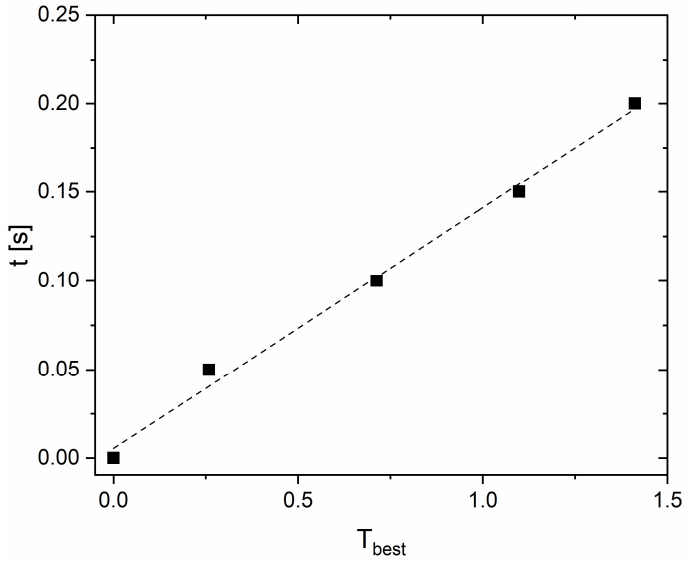

Figure 4.12: Mapping of the time steps in the boundary-integral simulations to the experiments of shape relaxation in bilayers. Plot of the experimental times t vs. T_{best} (time step in the simulation where the best-fitting domain shape is found). The dashed line is a fit to the equation $y = m * x + q$. The slope m determines the characteristic relaxation time t_* and is in this specific example equal to 0.13563.

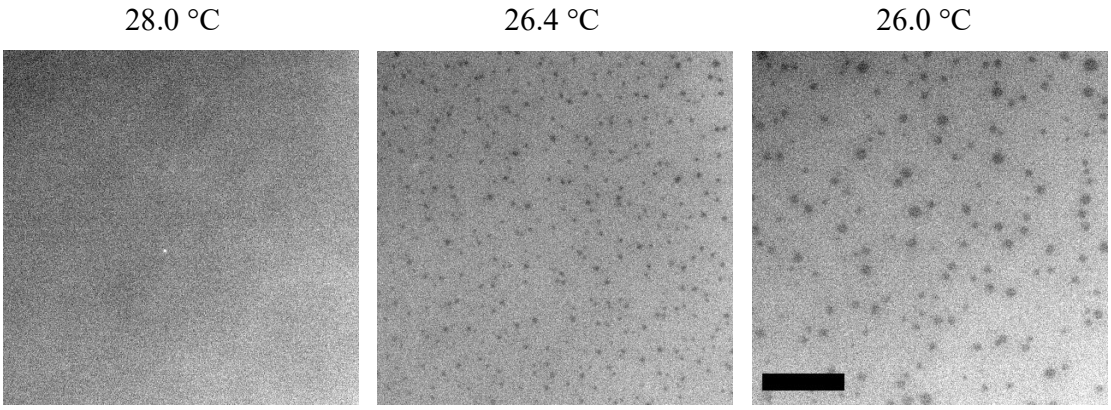

Figure 4.13: Fluorescence microscopy image of the phase separation of a 1:1:1 DOPC:DPPC:Cholesterol mixture. Scale bar is 50 µm.

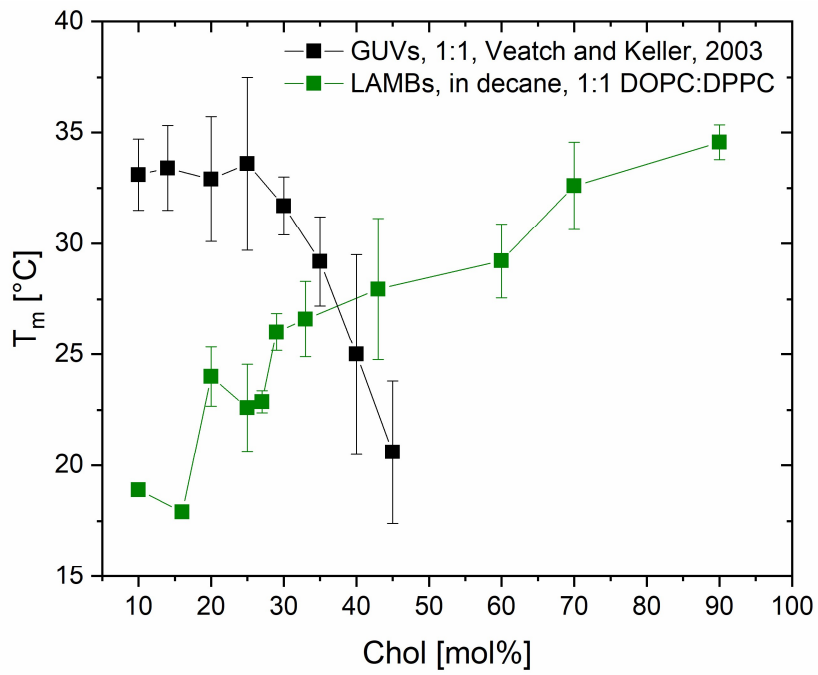

Figure 4.14: Phase transition temperatures for 1:1 DOPC:DPPC lipid mixtures with different bulk cholesterol concentrations. Except for the two lowest cholesterol concentrations, at least three measurements per point were conducted. For comparison, literature values obtained for oil-free GUVs are shown [26].

To explain this, one has to keep in mind that *n*-decane by itself *decreases* the phase transition temperature in bilayers significantly [122, 128]. It was shown in Chapter 3 that *n*-decane

decreases T_m in bilayers consisting of a mixture of 3:2 DOPC:DPPC by almost 10 °C. Therefore, a lower T_m in *n*-decane-containing bilayers is to be expected. Since the addition of cholesterol should decrease T_m, the increasing trend can only be explained by a decreasing amount of *n*-decane in the bilayer. Cholesterol increases the packing of the lipids, thereby leaving less space for the oil molecules and pushing them out of the bilayer.

Additionally, the amount of cholesterol in the bilayer is most probably much lower than it is in the bulk mixture. The difficulty of incorporating large amounts of cholesterol is a common problem, which is not only observed in other oil-based systems [87, 88, 208], where the efficiency of cholesterol incorporation tends to be below 50%, but also in GUVs [165]. If we assume a reasonable incorporation efficiency of 30% in the LAMB experiments, we arrive at cholesterol contents in the bilayer between 20 and 30 mol% if more than 70 mol% cholesterol was present in the bulk mixture. These results agree very well with the phase transition temperatures measured in GUVs at these cholesterol values. One can assume that most of the *n*-decane is pushed out at these high cholesterol contents.

4.3.2. Membrane viscosity and domain line tension

The membrane viscosity η_m of the fluid-disordered phase for different cholesterol contents in the bulk lipid mixture is depicted in Figure 4.15, at equal degrees of undercooling, essentially just below the phase transition temperature. The results show that η_m seems to decrease slightly with increasing cholesterol content, contrary to results found in the literature [172, 173]. However, it has to be noted that the temperature at which the membrane viscosity was measured increases with increasing cholesterol content in order to ensure equal degrees of undercooling and to have domains of a well resolvable size, since the phase transition temperature also increases. This could be a reason for the slightly decreasing membrane viscosity.

Figure 4.16 shows the second important parameter to characterize domain dynamics, i.e. the line tension λ as a function of the cholesterol content. Values around 0.4 pN are found for low cholesterol contents. The line tension then increases to around 2.5 pN, only to decrease again to around 0.5 pN. This behaviour is not known in literature. Usually, it has been found that cholesterol only reduces the line tension [209, 210]. Tsai and Feigenson [209] explained this behaviour with the increased partitioning of cholesterol into the L_d phase. This reduces

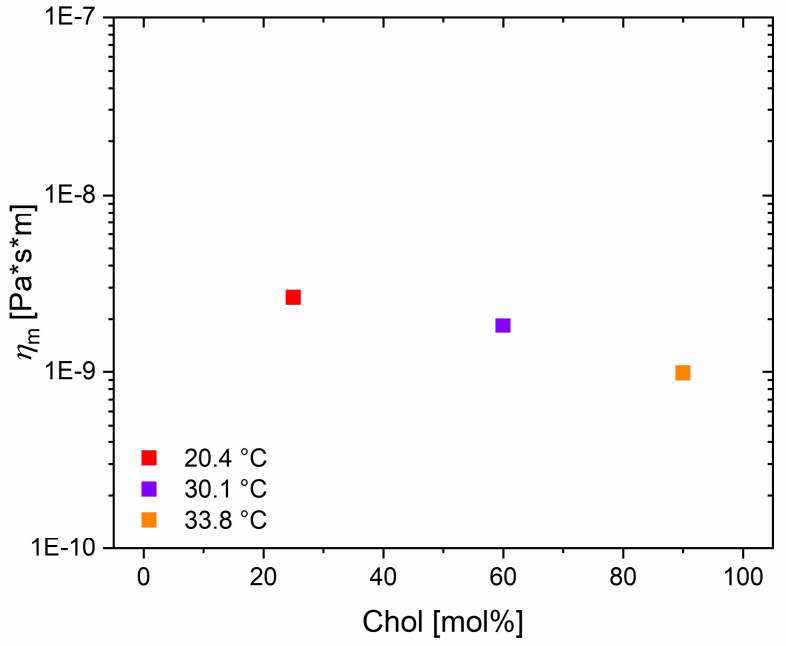

Figure 4.15: Membrane viscosities η_m for 1:1 DOPC:DPPC lipid mixtures with different bulk cholesterol concentrations.

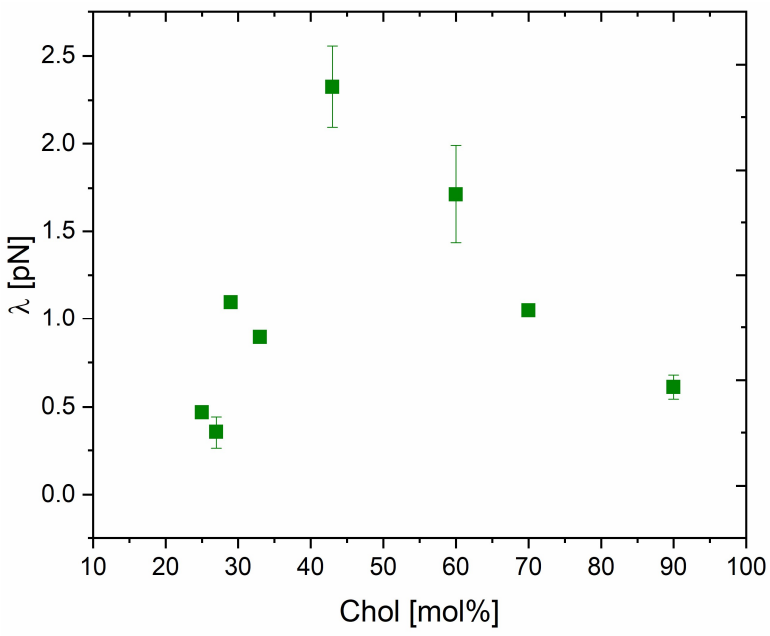

Figure 4.16: Line tension λ for 1:1 DOPC:DPPC lipid mixtures with different bulk cholesterol concentrations.

the thickness mismatch between the two phases (L_d and L_o), and thereby the line tension. It has to be pointed out that both Tian et. al. [210] and Tsai and Feigenson [209] only looked at cholesterol contents above 15 mol%. For an incorporation efficiency of 30% in the LAMB system, the lowest line tension values were measured below 10 mol% cholesterol. One can expect that Tsai's and Feigenson's argument is also valid in the LAMB system. At low cholesterol contents in the lipid mixture, it is mainly incorporated into the L_o phase due to its preference for saturated lipids. This leads to a higher thickness mismatch between the two phases and a higher line tension. At higher cholesterol contents, and when the L_o phase is saturated with cholesterol, it is mostly incorporated into the L_d phase.

4.3.3. Oil effects

Surprisingly, it was observed during these experiments that fluid, circular domains were formed even at bulk cholesterol concentrations < 10 mol% (Figure 4.17). This was not expected, since literature reports that *at least* 10 mol% cholesterol is required in the bilayer to form the L_o phase . Since it is very unlikely that all of the cholesterol present in the lipid-cholesterol-oil mixture is incorporated in the bilayer, the amount of cholesterol in a bilayer formed from a bulk lipid mixture containing 8 mol% cholesterol must be quite low.

A similar result was observed very recently by Suryabrahmam et. al. [211], who investigated the effects of 1-decanol on DMPC membranes and found that fluid-fluid coexistence occurred. This is a very interesting result, since usually it is expected that cholesterol is required to observe fluid-fluid coexistence. In contrast to 1-decanol, *n*-decane itself does not induce fluid-fluid coexistence (see Chapter 3). However, if both cholesterol and *n*-decane are present in the system, it seems that the threshold for L_o phase formation is lowered significantly, suggesting that *n*-decane leads to a disordering of the DPPC fatty acid chains in the otherwise formed gel phase. This is a very important result, showing that not only cholesterol, or sterols in general, can induce fluidity in solid domains.

4.4. Conclusion

The effects of cholesterol on lipid bilayer behaviour and structure are complex and clearly non-universal. We studied how cholesterol changes the phase behaviour of phospholipid bilayers consisting of DOPC and DPPC, swollen by *n*-decane. We found that the addition of cholesterol increases the phase transition temperature T_m, in contrast to what is to be expected

from literature values. This can be explained by cholesterol pushing the *n*-decane molecules out of the bilayer, thereby increasing the interactions between the lipid chains. The domain line tension is highly influenced by the cholesterol content in the membrane. At low concentrations, cholesterol is mainly incorporated in the L_o phase, which increases the line tension, while at high concentrations, cholesterol goes into the L_d phase. Remarkably, we also observed that *n*-decane influences the phase behaviour of the lipid bilayer, indicating that fluid-fluid coexistence is not only dependent on the presence of sterols in cell membranes. The investigation of the effects of additives (such as *n*-alkanes and *n*-alcohols) on lipid phase behaviour and the structure of membrane heterogeneities is a very promising research area, and further work will be necessary to elucidate the interactions between phospholipids, cholesterol and other molecules. Simulation studies provide valuable insights into the interactions of lipid bilayers with various molecules, but especially for cholesterol-containing membranes, results remain scarce due to the complexity of the system [212] and it is difficult to study large enough systems to understand domain dynamics. Recently, Centi et. al. [213] have shown using MD simulations that small molecules can change the phase separation behaviour in ternary lipid mixtures. Depending on which lipid species the molecules prefer, they either contribute to mixing or demixing of the membrane. Further studies, experimental as well as computational, will need to be made to investigate the effects of more complex solutes.

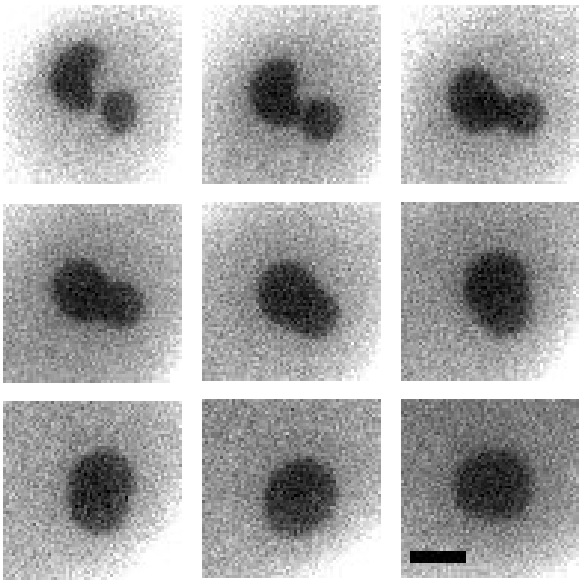

Figure 4.17: Coalescing domains in a 1:1 DOPC:DPPC bilayer. The bulk lipid mixture contained 8 mol% cholesterol. The time between each image is 10 s. Scale bar is 10 μm.

Chapter 5

Cholesterol incorporation using carrier molecules

The controlled introduction of cholesterol to model lipid bilayer membranes is not a trivial task. Several approaches commonly used to create model lipid bilayers fail to incorporate cholesterol into bilayers, and even more so in a controlled manner. This is usually circumvented by using a carrier molecule, namely cyclodextrin, to carry cholesterol to a previously formed bilayer. Here, we have used this method to add cholesterol to a 1:1 DOPC:DPPC bilayer formed from a 1:1 mixture of *n*-hexadecane and squalene, which forms a very stable bilayer enabling detailed studies of domain melting kinetics. We first compare this method to methods where the cholesterol is incorporated by mixing it into the bulk lipid-in-oil solutions from which the bilayers are prepared. We have found that when using these combination of oils, cholesterol is not incorporated directly in the bilayer (contrary to the results of Chapter 4 for *n*-decane), which makes the use of a carrier molecule necessary. First, we show that empty (i.e., cholesterol-free) cyclodextrins do not change the composition of the bilayer. Second, we report significant differences in the domain formation between direct and indirect cholesterol incorporation. When cholesterol is added to the bilayer from the bulk lipid mixture, domains form preferentially at the bilayer edges, while in the other case, they form in the middle of the bilayer. A possible explanation for this behaviour is that the bilayer composition is heterogeneous. Third, the addition of cholesterol is found to decrease the membrane viscosity, which disagrees with certain literature reports. However, the way in which the cholesterol is added here tends to give a clear-cut answer that cholesterol seems to act similar to a plasticizer, at least for the hydrophobic part of the lipid domains. Lastly, we conducted a preliminary scaling analysis of the growth behaviour of liquid domains, and found that the growth kinetics appear to follow universal scaling laws.

5.1. Introduction

In Chapter 1, it was mentioned that residual oil in the lipid bilayer can reduce the incorporation efficiency of cholesterol. Blosser et. al. [87], who used mineral oil in their system, give two possible explanations for this behaviour: either cholesterol's solubility in mineral oil is not sufficient, or cholesterol is too hydrophobic to go to the water interface. This resulted in an incorporation efficiency of less than 1% for their system. In Chapter 4, we showed that small alkanes can show different behaviour. Here, we will investigate a 1:1 DOPC:DPPC bilayer formed from a 1:1 mixture of *n*-hexadecane and squalene. This oil mixture forms a very stable bilayer, enabling detailed studies of domain melting kinetics. However, this specific combination of oils suffers from the aforementioned problems of low cholesterol incorporation efficiency. A common way to solve this problem is by using a carrier molecule, such as cyclodextrins, to bring cholesterol to the previously formed bilayer.

5.1.1. Cyclodextrins (CDs)

Cyclodextrins are cyclic supramolecular structures consisting of several glucose units (Figure 5.1). The glucose units are arranged in a way so that the inner part of the structure has hydrophobic properties, while the outer part is hydrophilic. This makes CDs soluble in water. Three different CDs exist: α-, β- and γ-cyclodextrins. Each of them contain a different amount of glucose units (α: 6, β: 7, γ: 8), which leads to a different size of the hydrophobic cavity (between 5 and 8 Å) [214].

CD can form inclusion complexes with hydrophobic compounds, thereby making these compounds water-soluble. This is why CDs have been extensively studied in the last century [214, 215]. Additionally, since the 1980s, they have been used in various applications (e.g. as drug carriers). Due to their differently sized hydrophobic cavity, each type of CD has a preference for specific molecules and applications. For example, large molecules can only be completely solubilized by γ-CD, which is particularly useful in the food industry [216]. On the other hand, β-CDs have shown a very high affinity towards cholesterol [217, 218].

5.1.2. Methyl-β-cyclodextrin (mβCD)

In 1989, Ohtani et. al. [217] investigated the removal of cholesterol from cells, and found that β-CD by far showed the best results. α- and γ-CDs removed much less cholesterol. A few years later, Christian et. al. [218] studied the effects of two types of β-CDs, namely 2-

hydroxylpropyl-β-CD (2OHpβCD) and methyl-β-CD (mβCD) (Figure 5.2) on cholesterol donation to cells. They found that when using mβCD, the increase in cell cholesterol concentration was much higher, making this compound also much more effective for choles-

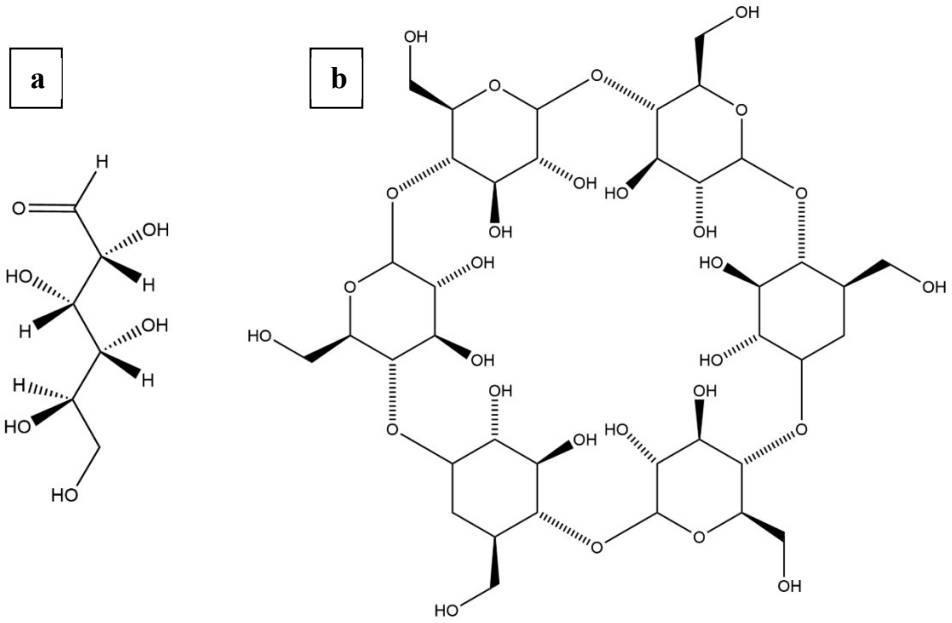

Figure 5.1: (a): Glucose unit. (b): α-cyclodextrin. The size of the hydrophobic cavity in the middle of the molecule is about 5 Å.

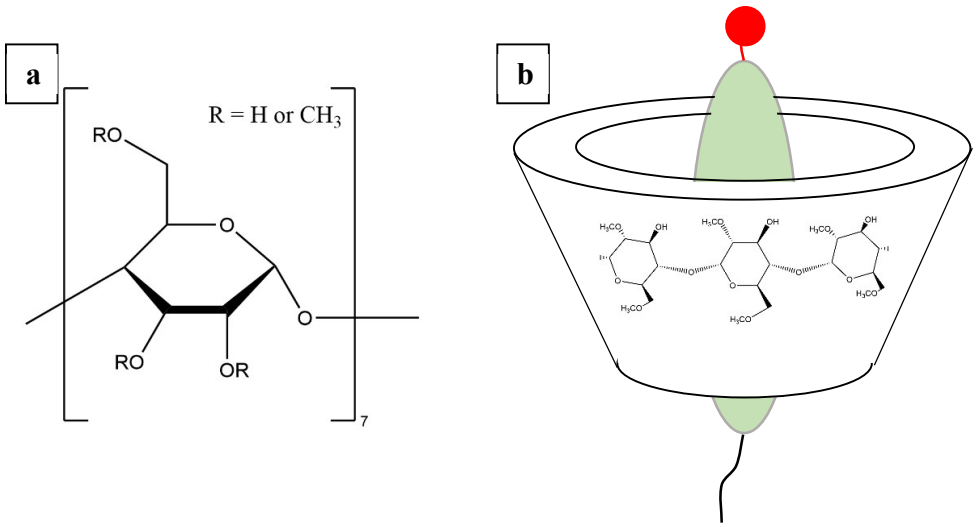

Figure 5.2: (a): methyl- β-CD. (b): Representation of a mβCD-cholesterol complex.

terol enrichment of cholesterol-free bilayers, as we will explore here. Due to these findings, β-CDs, and mβCD in particular, have widely been used in cholesterol depletion studies [219-222] and have also been applied to carry cholesterol to the bilayer [87, 218, 220, 223]. For example, Blosser et. al. [87] have circumvented the problem of low cholesterol incorporation efficiency by adding cholesterol-loaded mβCD to previously formed, phase separated GUVs. Before the cholesterol was added, domains of the solid-ordered phase were formed. After cholesterol incorporation, the domains transformed into the liquid phase, evidenced by their circular shape and coalescence events.

Although β-CDs are very efficient in cholesterol removal and enrichment and are frequently used in cell studies, one has to keep in mind that they can also influence the other lipid species in the bilayer. Puglisi et. al. [224] have shown that the presence of β-CDs can lead to an increase of the phase transition temperature in DPPC vesicles. Other authors report that mβCD is capable of removing lipids from the membrane [225, 226]. The degree of solubilization depends on the type of lipid and concentration of mβCD. For example, it seems that DPPC vesicles are more resistant to lipid removal than other lipids. Generally, the effects of β-CDs on lipid bilayers depend on the type of lipid and β-CD, and also on the concentration of β-CD. One has to consider this important fact when using β-CDs in cholesterol studies.

5.1.3. Kinetics of the 2D domain growth process

The formation and growth of 2D colloidal aggregates at interfaces [227], or the growth of sessile droplets on substrates have applications in many different fields, for example in the growth of films with regularly arranged pores [228] or the production of ordered microarrays [229]. The process of the growth by aggregation and/or coalescence with the development of a specific size distribution can be understood by using scaling arguments [230, 231]. The droplet size distribution (and its moments) at late times of the growth process can be described by simple power law scaling relations with exponents which depend only on the dimensionality of the system (2D) and the nature of the coalescence process (reaction- or diffusion-controlled) [230, 231]. Moreover, the time dependence of the number of droplets per unit area $N(t)$ and the porosity, i.e. the area not covered by droplets $p(t)$ even follow the same power law behaviour at late times of the growth process [230, 231], i.e.

$$N(t) \sim p(t) \sim t^{-k}.$$

Here, we want to investigate the potential of such a universal scaling approach to describe the growth of liquid domains in cholesterol-containing lipid bilayers. The time evolution of

the size distribution can be used as a dynamic fingerprint of the aggregation and coalescence mechanism, and vice versa understanding the mechanism would provide insights into the kinetics of coarsening in other conditions.

5.2. Experimental

The lipid sample preparation and the production of LAMBs follows the same protocol as outlined in section 3.2. Here, only the differences compared to the previous experiments are described.

A lipid mixture of 1:1 DOPC:DPPC was prepared. The lipids were dissolved in an oil mixture of 50% *n*-hexadecane and 50% squalene. Cholesterol powder was received from Avanti Polar Lipids. Methyl-β-cyclodextrin powder (1 g) was obtained from Sigma-Aldrich. The mβCD-cholesterol complex was produced by the following protocol: 10 mg of cholesterol were dissolved in 1.35 ml chloroform. 111.2 mg of mβCD were dissolved in a stirring solution of 3.58 ml chloroform on a water bath at 80 °C. Then, the cholesterol mixture was slowly added to the mβCD mixture. This solution was subsequently dried under N_2 for ~ 1 h and then under vacuum for 30 min. The resulting crystals were rehydrated at a concentration of 1 mg/ml cholesterol. The solution was kept stirring at 45 °C until it was used.

In a first experiment, the cholesterol complex was pipetted into the buffer. Later, the mixture was brought into the holder by exchanging the solvent (see section 2.3.5). Cholesterol was added at constant temperature after the bilayer had phase separated, and until the first domains started to become circular.

5.2.1. Image analysis

The image analysis follows the same steps as previously described in section 3.2.4 to derive the ratio between the area occupied by the solid DPPC domains and the total area of the bilayer. The only difference here is that the position, shape, size and number of domains are detected from the black and white images (Figure 5.3b), with an in-house code written in MATLAB, which is based on the regionprops command (from the Image Processing Toolbox).

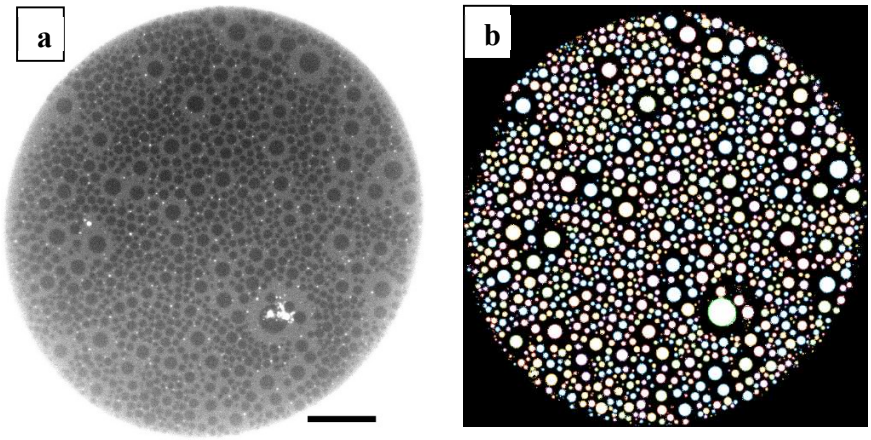

Figure 5.3: (a): Original fluorescence microscopy image of a bilayer formed from a 1:1 DOPC:DPPC lipid mixture in 50% *n*-hexadecane and 50% squalene. The cholesterol complex was added after the formation of the bilayer. Scale bar is 100 µm. (b): Domain detection from the black and white image corresponding to the image in (a).

5.3. Results and discussion

5.3.1. Effect of different organic solvents on cholesterol incorporation

First, to examine whether a sufficient amount of cholesterol is incorporated into LAMBs formed from *n*-hexadecane, a control experiment was conducted. For this, a 1:1:1 DOPC:DPPC:Cholesterol (containing 1 mol% of Rh-DOPE as a fluorescent lipid) was prepared. A lipid membrane was formed and cooled down to initiate the phase separation. The formed domains were star-shaped reflecting a highly ordered DPPC crystal solid phase (Figure 5.4a). However, according to the DOPC:DPPC:Cholesterol phase diagram [26], the domains in this composition range should be liquid. This raises the suspicion that cholesterol was not efficiently incorporated. To verify this, about 200 µL of the mβCD-cholesterol complex was pipetted into the buffer using the carrier molecule approach to bring cholesterol to the bilayer. Upon addition of the mβCD-cholesterol complex, domains became circular and also started to coalesce (Figure 5.4b), proving that a liquid phase was formed. The same was observed for LAMBs formed from 100% squalene or from *n*-hexadecane:squalene mixtures. On the contrary, as shown in Chapter 4, cholesterol is easily incorporated into the bilayer when using *n*-decane as the solvent, making the carrier molecule approach obsolete.

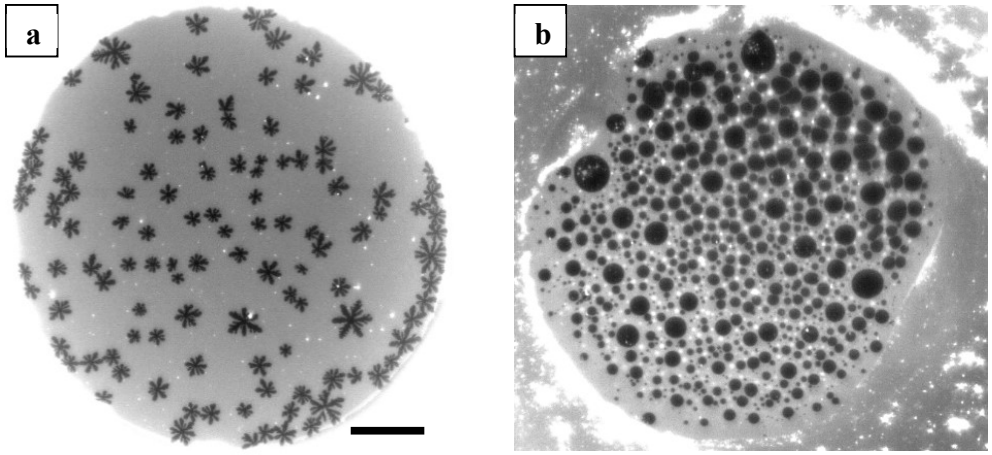

Figure 5.4: Phase separation without cholesterol in the bilayer leads to star-shaped domains. (b): After adding the mβCD-cholesterol complex, the domains became circular and started to coalesce, proving the incorporation of cholesterol into the bilayer. Scale bar is 100 μm.

Of course, the insufficient incorporation of cholesterol into the bilayer when using certain oil solvents is a disadvantage of LAMBs. A possible explanation for this observation is that *n*-hexadecane displaces cholesterol from the bilayer. As already pointed out in Chapter 3, long alkanes like *n*-hexadecane most likely align themselves parallel to the lipid chains. This reduces the available space. On the other hand, *n*-decane, a shorter alkane, is predominantly located in the middle of the bilayer, leaving still enough space for cholesterol between the fatty acid chains.

5.3.2. Effect of mβCDs

The effect of empty (i.e., not loaded with cholesterol) mβCDs on the bilayer was first studied by measuring the phase transition temperature T_m of a 3:2 DOPC:DPPC bilayer before and after adding 800 μL of mβCD dissolved in water (11 mg/ml). T_m was constant within experimental accuracy (Figure 5.5), proving that empty mβCDs had no significant effect on the composition of the bilayer. This shows that the observed differences after adding the mβCD-cholesterol complex (which will be significant) can be attributed to cholesterol only.

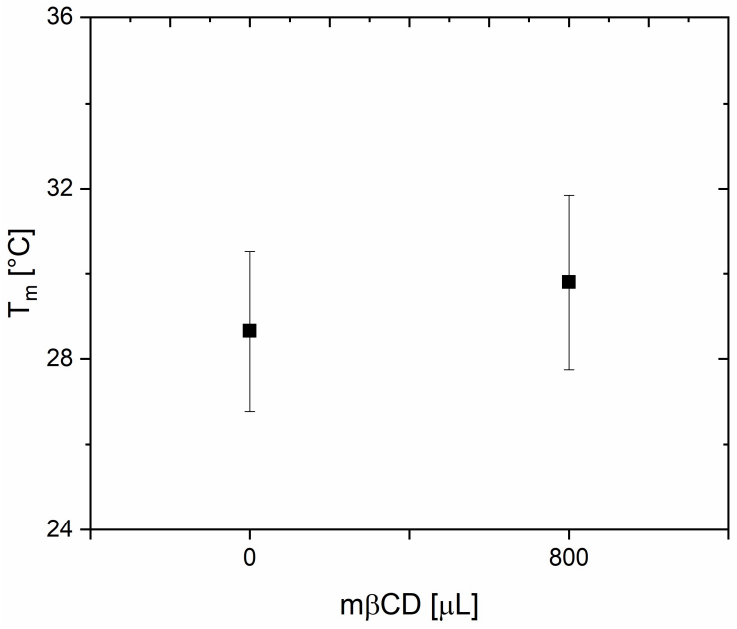

Figure 5.5: Phase transition temperatures of a 3:2 DOPC:DPPC bilayer before and after adding 800 μL of mβCD dissolved in water.

5.3.3. Differences between direct and indirect cholesterol incorporation

In Chapter 4, we reported the results for the case when cholesterol is added directly to the bulk lipid mixture. Here, cholesterol is added through the aqueous phase after forming the bilayer. Figure 5.6 shows a phase separated 1:1 DOPC:DPPC bilayer before (a) and after (b-d) the addition of 1 mL of the mβCD-cholesterol complex. One can see that upon the addition of cholesterol, the initially solid, star-shaped domains transform into liquid, circular domains.

A striking difference between direct and indirect (i.e., by using mβCD) cholesterol incorporation is the location of the formation of the first domains. This is illustrated in Figures 5.7 and 5.8. When cholesterol is incorporated directly into the lipid-oil mixture used to make the bilayer, the domains preferentially form at the edges (Figure 5.7b), while in the indirect case, they form in the middle (Figure 5.7a). Likewise, solid domains located in the middle of the bilayer transform into circular domains slightly before the ones at the edges (Figure 5.8).

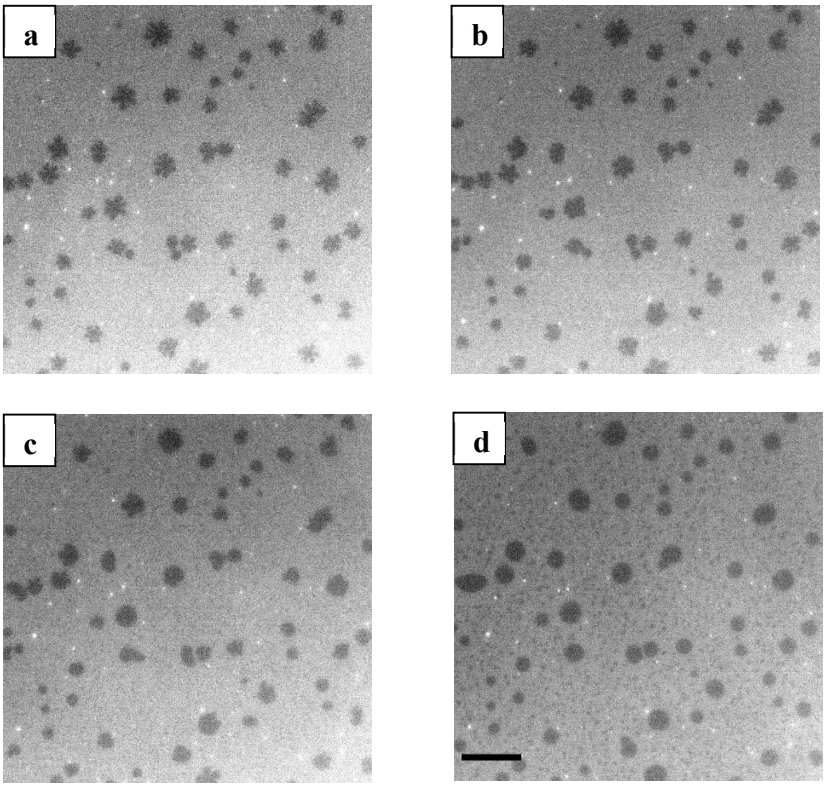

Figure 5.6: Transformation of solid, star-shaped (a) into liquid, circular domains (b-d) after the addition 1 mL of the mβCD-cholesterol complex to a 1:1 DOPC:DPPC bilayer. Scale bar is 50 μm.

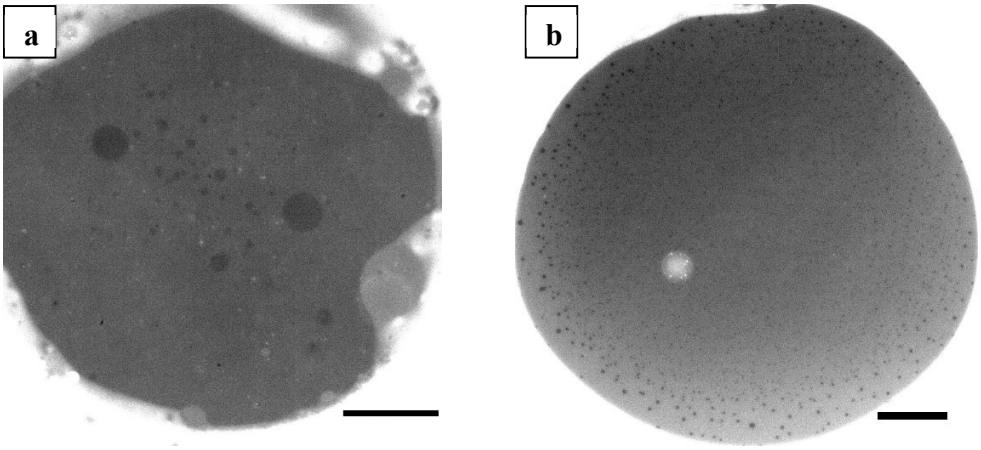

Figure 5.7: (a): Indirect incorporation of cholesterol (i.e., using mβCD): Domains preferentially form in the middle of the bilayer. (b): Direct incorporation of cholesterol (i.e., from the bulk lipid mixture): Domains preferentially form at the edge of the bilayer. Scale bars are 100 μm.

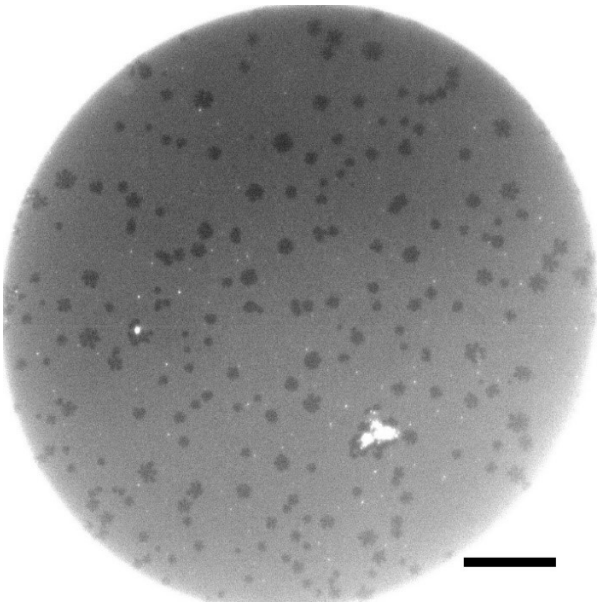

Figure 5.8: Solid domains located in the middle of the bilayer transform into circular domains before the ones at the edges. Scale bar is 100 μm.

Different reasons can be given for this behaviour. First, it could be that the lipid composition of the bilayer is not homogeneous, with in particular lateral variations in composition, leading to a different phase behaviour at different locations. Second, the oil distribution within the bilayer is not known. It was already shown in the previous Chapters that the amount and type of oil has a tremendous effect on the lipid chain packing and the phase separation. It is possible that the oil is not equally distributed across the whole bilayer. Additionally, in the indirect case, the ratio between *n*-hexadecane and squalene can have a large effect on the cholesterol incorporation.

5.3.4. Membrane viscosity

The use of a carrier molecule, which was shown not to change bilayer composition, enables a direct analysis of the effect of cholesterol on membrane viscosity, as all other factors can be kept constant. Figure 5.9 shows the membrane viscosity η_m before and after the addition of 1 mL of the mβCD-cholesterol complex to a swollen 1:1 DOPC:DPPC bilayer containing *n*-hexadecane (and possibly squalene) molecules. The measurements were made at 32.4 °C. η_m decreases when adding cholesterol, which is in contrast to results found in the literature

for oil-free systems [172, 173]. It is widely acknowledged that cholesterol increases the packing in the L_d phase, which should lead to a higher η_m. It is not entirely clear why this cannot be observed here, however, the *n*-hexadecane and squalene molecules present in the bilayer could interact with cholesterol in a previously unknown manner. Cholesterol can be thought of as a better plasticizer for the hydrophobic core of the swollen lipid bilayer.

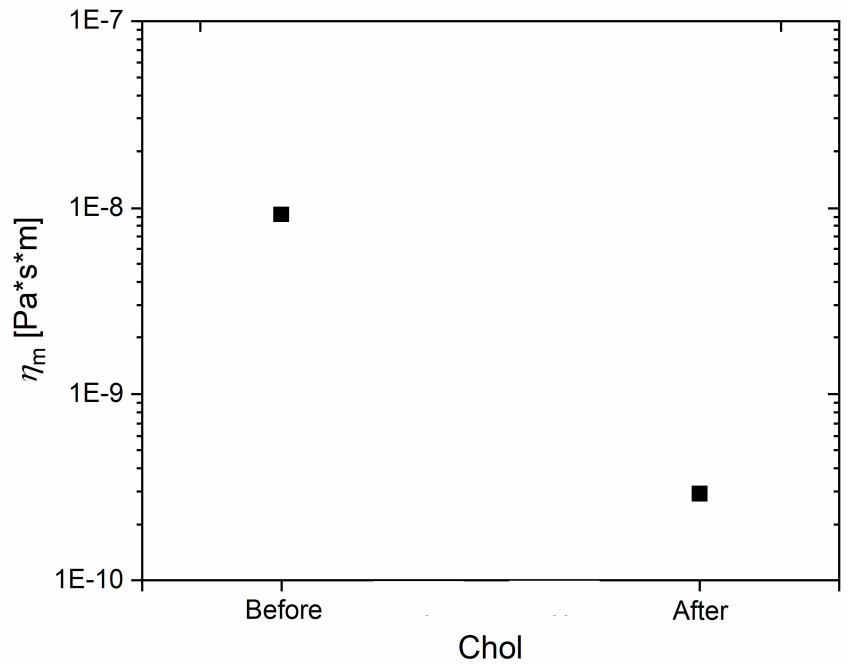

Figure 5.9: Membrane viscosities η_m for 1:1 DOPC:DPPC lipid mixtures before and after the addition of 1 mL of the mβCD-cholesterol complex.

5.3.5. Kinetics of the growth process of liquid domains after domain melting

To investigate the potential of dynamic scaling theory for the kinetics and structures during domain coarsening, prospective analysis was carried out. In Figure 5.10, the number of liquid domains per unit area $N(t)$ (orange, right vertical axis) and the percentage of the liquid-disordered phase $p(t)$ (blue, left vertical axis) are shown after the addition of 1 mL of the mβCD-cholesterol complex to a 1:1 DOPC:DPPC bilayer. In the late stages of the domain growth, both $N(t)$ and $p(t)$ follow the same power law behaviour. However, these are only preliminary results. The analysed range is too small to make a strong statement. More data has to be acquired and longer experiments are necessary for a full quantitative analysis. Still, these preliminary results show that even such complicated systems as multicomponent

phospholipid bilayers can be described by well-understood theoretical predictions, which would give new ways to think about domain formation kinetics in these systems.

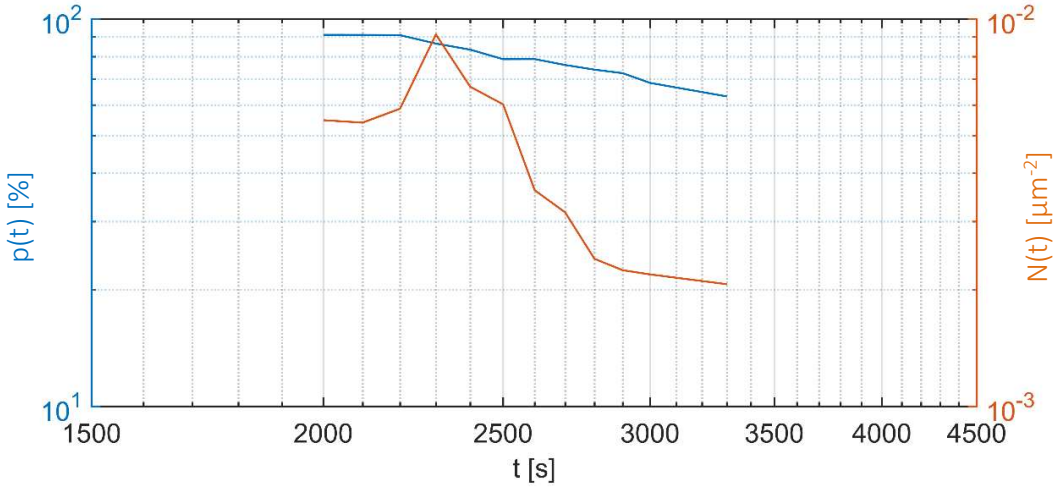

Figure 5.10: Time dependence of the number of liquid domains per unit area (orange, right vertical axis) and of the percentage of the liquid-disordered phase (blue, left vertical axis).

5.4. Conclusion

The incorporation of cholesterol into lipid bilayers is challenging. Here, we have identified commonly used oil molecules (*n*-hexadecane and squalene) as major obstacles for direct cholesterol incorporation in 1:1 DOPC:DPPC bilayers. To overcome this limitation, we have used cholesterol-loaded cyclodextrins as transporters to bring cholesterol to the bilayers. The uptake of cholesterol by the bilayer was proven by the transformation of solid domains to fluid domains. Furthermore, we have observed significant differences between domain formation mechanisms for direct and indirect cholesterol incorporation, showing that results obtained from different experimental protocols cannot be easily compared. The distribution of lipid and oil molecules and of cholesterol within the bilayer might not be homogeneous and might also differ when using different methods to incorporate cholesterol. Additionally, we have found that the membrane viscosity η_m decreases after adding cholesterol to these swollen bilayers, which once again puts emphasis on the need to investigate interactions between lipids and membrane additives. Finally, in a preliminary analysis, we have found that the domain growth kinetics seem to follow universal scaling laws.

Chapter 6
Conclusions and Outlook

In this thesis, the effects of various additives on phase separation in model lipid membranes were studied by using a novel experimental technique called LAMB. In the first part of the thesis, the focus laid on the influence of commonly used preparatory organic solvents and linactants on phase transition temperature and domain size. In the second part, we looked into the effects of cholesterol.

We have shown for the first time that the size of lipid domains can be systematically controlled by a judicious choice of the organic solvents. This result has implications not only for the understanding of how cell membranes can control domain size and domain morphology in presence of small organic molecules, but also for model membrane studies that use organic solvents to produce lipid bilayers. Oil molecules have fundamental effects on lipid bilayer properties, a fact that seems to have been underestimated so far. In addition, linactants, so far predominantly investigated in liquid domain systems, have been shown here to also impact solid domain formation and morphology.

Cholesterol is an intriguing membrane component. Its effects are diverse, depend on various factors, and are at times hard to predict and understand. However, cholesterol's supposed prominent role in the formation of lipid rafts makes it important to unravel the exact nature of cholesterol-membrane interactions. We have investigated how cholesterol impacts phase transition temperature, domain line tension and membrane viscosity in *n*-decane-containing bilayers. We have seen that, once more, the presence of oil is of paramount importance and changes the phase behaviour of the system dramatically and that there is a subtle interplay between the different components inside the lipid bilayer, with the interplay with the oils used to create the bilayers playing a major role. Effects on the degree of swelling and subsequently on the height mismatch, as well as effects on local ordering are key

determinants in controlling the domain size and shape. Unexpectedly, domains of the liquid-ordered phase were observed even at cholesterol concentrations below 10 mol%. While the prevailing opinion in the field is that this is the minimum amount of cholesterol necessary to induce liquid-liquid coexistence, our experiments have shown that this threshold can be lowered if other molecules are present in the bilayer. This surprising result has a bearing on the importance of cholesterol in cell membranes. Generally, the ability of cholesterol to reduce membrane permeability and fluidity is viewed as its most important roles. However, its ability to induce fluid-fluid coexistence has received increased attention in the last decade, since it was the predominant belief that cholesterol is necessary for liquid-ordered domains to form. This idea now has to be reconsidered. Other molecules might also be responsible for the formation of liquid phases in cell membranes. This shows that studying cholesterol's effects and distribution in lipid bilayers is a promising and rewarding field of research. Many open questions remain yet to be answered.

We have observed that it is not possible to incorporate cholesterol into bilayers containing *n*-hexadecane or squalene due to packing problems. Carrier molecules have to be employed to solve this problem. However, this is not the ideal solution. The amount of cholesterol that is brought to the bilayer in this manner cannot be controlled and therefore it is difficult to study cholesterol's effects in a systematic way. This makes it necessary to search for more organic solvents that allow the direct incorporation of cholesterol into LAMBs (apart from *n*-decane). One could also try to let the thick oil-lipid layer equilibrate over a very long time at a high temperature before draining it. This could allow the cholesterol molecules to partition to the oil-water interface.

Outlook for future research

The advantages of the LAMB technique are manifold. The long lifetime of the bilayers and their planarity make LAMBs particularly useful for phase separation studies. In this area, many more questions remain to be answered. The effects of linactants on bilayers containing cholesterol can be investigated further. Moreover, the influence of proteins on lipid domain formation is a heavily discussed topic in the field. One could also make use of the independent access to both sides of the bilayer and induce an osmotic pressure gradient. By that, even curvature effects on phase separation could be studied.

The effects of oil solvents on lipid bilayer properties are not yet completely understood and remain an area where intensive research is still necessary. Various organic solvents, not just

alkanes, are used in model membranes, each of which have different effects. In order to interpret results obtained from synthetic bilayers correctly, one has to understand how every component affects their behaviour.

The LAMB technique provides a versatile platform that can easily be adapted to different needs. For example, we have used a slightly modified chip and pressure chamber to conduct preliminary experiments with coherent anti-Stokes Raman spectroscopy (CARS). This technique can be used to determine the composition of the bilayer. Knowing the exact lipid composition is a problem in several model lipid systems, and it would be a great step forward in lipid membrane research if it was possible to measure it with sufficient sensitivity. Our preliminary experiments have shown that phase separated LAMBs can be produced within the CARS setup. However, the sensitivity has to be improved in order to distinguish between different lipid species.

Bibliography

1. Lombard, J., Once upon a time the cell membranes: 175 years of cell boundary research. Biology Direct, 2014. **9**(1): p. 32.
2. Gorter, E. and F. Grendel, On bimolecular layers of lipoids on the chromocytes of the blood. The Journal of Experimental Medicine, 1925. **41**(4): p. 439-443.
3. Fricke, H., The electric capacity of suspensions with special reference to blood. The Journal of General Physiology, 1925. **9**(2): p. 137-152.
4. Robertson, J.D., New observations on the ultrastructure of the membranes of frog peripheral nerve fibers. The Journal of Biophysical and Biochemical Cytology, 1957. **3**(6): p. 1043-1048.
5. Singer, S.J. and G.L. Nicolson, The fluid mosaic model of the structure of cell membranes. Science, 1972. **175**(4023): p. 720-31.
6. Alberts, B., Johnson, A., Lewis, J., et. al., Molecular Biology of the Cell. 4th ed. 2002: New York: Garland Science.
7. Lagny, T.J. and P. Bassereau, Bioinspired membrane-based systems for a physical approach of cell organization and dynamics: usefulness and limitations. Interface Focus, 2015. **5**(4): 20150038.
8. van Meer, G., Cellular lipidomics. The EMBO Journal, 2005. **24**(18): p. 3159-3165.
9. van Meer, G., D.R. Voelker, and G.W. Feigenson, Membrane lipids: where they are and how they behave. Nature Reviews Molecular Cell Biology, 2008. **9**(2): p. 112-124.
10. Ohvo-Rekilä, H., et al., Cholesterol interactions with phospholipids in membranes. Progress in Lipid Research, 2002. **41**(1): p. 66-97.

11. Coskun, Ü. and K. Simons, Cell Membranes: The Lipid Perspective. Structure, 2011. **19**(11): p. 1543-1548.

12. Dimova, R., Recent developments in the field of bending rigidity measurements on membranes. Advances in Colloid and Interface Science, 2014. **208**: p. 225-234.

13. Li, N., et al., Curvature-Driven Migration of Colloids on Tense Lipid Bilayers. Langmuir, 2017. **33**(2): p. 600-610.

14. van der Wel, C., et al., Lipid membrane-mediated attraction between curvature inducing objects. Scientific Reports, 2016. **6**: p. 32825.

15. Starling, A.P., et al., Effects of phosphatidylethanolamines on the activity of the Ca^{2+}-ATPase of sarcoplasmic reticulum. Biochemical Journal, 1996. **320**(1): p. 309-314.

16. Kell, D.B., P.D. Dobson, and S.G. Oliver, Pharmaceutical drug transport: the issues and the implications that it is essentially carrier-mediated only. Drug Discovery Today, 2011. **16**(15–16): p. 704-714.

17. Sugano, K., et al., Coexistence of passive and carrier-mediated processes in drug transport. Nat Rev Drug Discov, 2010. **9**(8): p. 597-614.

18. Simons, K. and E. Ikonen, Functional rafts in cell membranes. Nature, 1997. **387**(6633): p. 569-572.

19. Karnovsky, M.J., et al., The concept of lipid domains in membranes. The Journal of Cell Biology, 1982. **94**(1): p. 1-6.

20. Simons, K. and G. Van Meer, Lipid sorting in epithelial cells. Biochemistry, 1988. **27**(17): p. 6197-6202.

21. Brown, D.A. and J.K. Rose, Sorting of GPI-anchored proteins to glycolipid-enriched membrane subdomains during transport to the apical cell surface. Cell, 1992. **68**(3): p. 533-44.

22. Simons, K. and D. Toomre, Lipid rafts and signal transduction. Nat Rev Mol Cell Biol, 2000. **1**(1): p. 31-39.

23. Brown, D.A. and E. London, Functions of lipid rafts in biological membranes. Annual Review of Cell and Developmental Biology, 1998. **14**(1): p. 111-136.

24. Pike, L.J., Rafts defined: a report on the Keystone symposium on lipid rafts and cell function. Journal of Lipid Research, 2006. **47**(7): p. 1597-1598.

25. Vist, M.R. and J.H. Davis, Phase equilibria of cholesterol/dipalmitoylphosphatidylcholine mixtures: deuterium nuclear magnetic resonance and differential scanning calorimetry. Biochemistry, 1990. **29**(2): p. 451-464.

26. Veatch, S.L. and S.L. Keller, Separation of Liquid Phases in Giant Vesicles of Ternary Mixtures of Phospholipids and Cholesterol. Biophysical Journal, 2003. **85**(5): p. 3074-3083.

27. Veatch, S.L. and S.L. Keller, Organization in Lipid Membranes Containing Cholesterol. Physical Review Letters, 2002. **89**(26): p. 268101.

28. Chen, D. and M.M. Santore, Three dimensional (temperature–tension–composition) phase map of mixed DOPC–DPPC vesicles: Two solid phases and a fluid phase coexist on three intersecting planes. Biochimica et Biophysica Acta (BBA) - Biomembranes, 2014. **1838**(11): p. 2788-2797.

29. de Almeida, R.F.M., A. Fedorov, and M. Prieto, Sphingomyelin/Phosphatidylcholine/Cholesterol Phase Diagram: Boundaries and Composition of Lipid Rafts. Biophysical Journal, 2003. **85**(4): p. 2406-2416.

30. Feigenson, G.W. and J.T. Buboltz, Ternary Phase Diagram of Dipalmitoyl-PC/Dilauroyl-PC/Cholesterol: Nanoscopic Domain Formation Driven by Cholesterol. Biophysical Journal, 2001. **80**(6): p. 2775-2788.

31. Hjort Ipsen, J., et al., Phase equilibria in the phosphatidylcholine-cholesterol system. Biochimica et Biophysica Acta (BBA) - Biomembranes, 1987. **905**(1): p. 162-172.

32. Veatch, S.L. and S.L. Keller, Seeing spots: Complex phase behavior in simple membranes. Biochimica et Biophysica Acta (BBA) - Molecular Cell Research, 2005. **1746**(3): p. 172-185.

33. Cicuta, P., S.L. Keller, and S.L. Veatch, Diffusion of Liquid Domains in Lipid Bilayer Membranes. The Journal of Physical Chemistry B, 2007. **111**(13): p. 3328-3331.

34. Stanich, Cynthia A., et al., Coarsening Dynamics of Domains in Lipid Membranes. Biophysical Journal, 2013. **105**(2): p. 444-454.

35. Moran-Mirabal, J.M., Aubrecht, D. M., and Craighead, H. G., Phase Separation and Fractal Domain Formation in Phospholipid/Diacetylene-Supported Lipid Bilayers. Langmuir, 2007. **23**(21): p. 10661-10671.

36. Miller, A., W. Knoll, and H. Möhwald, Fractal Growth of Crystalline Phospholipid Domains in Monomolecular Layers. Physical Review Letters, 1986. **56**(24): p. 2633-2636.

37. Fogedby, H.C., E.S. So/rensen, and O.G. Mouritsen, Fractal growth in impurity-controlled solidification in lipid monolayers. The Journal of Chemical Physics, 1987. **87**(11): p. 6706-6709.

38. Bernchou, U., Ipsen, J. H., and Simonsen, A. C., Growth of Solid Domains in Model Membranes: Quantitative Image Analysis Reveals a Strong Correlation between Domain Shape and Spatial Position. The Journal of Physical Chemistry B 2009. **113**(20): p. 7170-7177.

39. Laradji, M. and P.B. Sunil Kumar, Dynamics of Domain Growth in Self-Assembled Fluid Vesicles. Physical Review Letters, 2004. **93**(19): p. 198105.

40. Min, Y., Phase dynamics and domain interactions in biological membranes. Current Opinion in Chemical Engineering, 2017. **15**: p. 76-83.

41. Mangiarotti, A. and N. Wilke, Electrostatic interactions at the microscale modulate dynamics and distribution of lipids in bilayers. Soft Matter, 2017. **13**(3): p. 686-694.

42. Sezgin, E., et al., The mystery of membrane organization: composition, regulation and roles of lipid rafts. Nat Rev Mol Cell Biol, 2017. **18**: p. 361-374.

43. Koynova, R. and B. Tenchov, Phase Transitions and Phase Behavior of Lipids, in Encyclopedia of Biophysics, G.C.K. Roberts, Editor. 2013, Springer Berlin Heidelberg: Berlin, Heidelberg. p. 1841-1854.

44. Chen, D. and M.M. Santore, Large effect of membrane tension on the fluid–solid phase transitions of two-component phosphatidylcholine vesicles. Proceedings of the National Academy of Sciences, 2014. **111**(1): p. 179-184.

45. Attwood, S.J., Y. Choi, and Z. Leonenko, Preparation of DOPC and DPPC Supported Planar Lipid Bilayers for Atomic Force Microscopy and Atomic Force Spectroscopy. International Journal of Molecular Sciences, 2013. **14**(2): p. 3514-3539.

46. Chen, D. and M.M. Santore, 1,2-Dipalmitoyl-sn-glycero-3-phosphocholine (DPPC)-Rich Domain Formation in Binary Phospholipid Vesicle Membranes: Two-Dimensional Nucleation and Growth. Langmuir, 2014. **30**(31): p. 9484-9493.

47. Parasassi, T., et al., Two-photon fluorescence microscopy of laurdan generalized polarization domains in model and natural membranes. Biophysical Journal, 1997. **72**(6): p. 2413-2429.

48. Kranenburg, M. and B. Smit, Phase Behavior of Model Lipid Bilayers. The Journal of Physical Chemistry B, 2005. **109**(14): p. 6553-6563.

49. Dietrich, C., et al., Lipid rafts reconstituted in model membranes. Biophys J, 2001. **80**(3): p. 1417-28.

50. Simons, K. and W.L. Vaz, Model systems, lipid rafts, and cell membranes. Annu Rev Biophys Biomol Struct, 2004. **33**: p. 269-95.

51. Mills, T.T., et al., Effects of cholesterol and unsaturated DOPC lipid on chain packing of saturated gel-phase DPPC bilayers. General Physiology and Biophysics, 2009. **28**(2): p. 126-139.

52. Siavashi, R., et al., Lamellar Phases Composed of Phospholipid, Cholesterol, and Ceramide, as Studied by 2H NMR. Biophysical Journal, 2019. **117**(2): p. 296-306.

53. Busto, J.V., et al., Lamellar gel (lβ) phases of ternary lipid composition containing ceramide and cholesterol. Biophysical Journal, 2014. **106**(3): p. 621-630.

54. Munro, S., Lipid rafts: elusive or illusive? Cell, 2003. **115**(4): p. 377-88.

55. Levental, I., K.R. Levental, and F.A. Heberle, Lipid Rafts: Controversies Resolved, Mysteries Remain. Trends in Cell Biology, 2020. **30**(5): p. 341-353.

56. Heberle, F.A., et al., Direct label-free imaging of nanodomains in biomimetic and biological membranes by cryogenic electron microscopy. Proceedings of the National Academy of Sciences of the United States of America, 2020. **117**(33): p. 19943-19952.

57. Cornell, C.E., et al., Direct imaging of liquid domains in membranes by cryo-electron tomography. Proceedings of the National Academy of Sciences of the United States of America, 2020. **117**(33): p. 19713-19719.

58. Marrink, S.J., A.H. de Vries, and D.P. Tieleman, Lipids on the move: Simulations of membrane pores, domains, stalks and curves. Biochimica et Biophysica Acta (BBA) - Biomembranes, 2009. **1788**(1): p. 149-168.

59. Bennett, W.F.D. and D.P. Tieleman, Computer simulations of lipid membrane domains. Biochimica et Biophysica Acta (BBA) - Biomembranes, 2013. **1828**(8): p. 1765-1776.

60. Zhuang, X., et al., An extensive simulation study of lipid bilayer properties with different head groups, acyl chain lengths, and chain saturations. Biochimica et Biophysica Acta (BBA) - Biomembranes, 2016. **1858**(12): p. 3093-3104.

61. Faller, R. and S.-J. Marrink, Simulation of Domain Formation in DLPC−DSPC Mixed Bilayers. Langmuir, 2004. **20**(18): p. 7686-7693.

62. Risselada, H.J. and S.J. Marrink, The molecular face of lipid rafts in model membranes. Proceedings of the National Academy of Sciences, 2008. **105**(45): p. 17367-17372.

63. Rosetti, C. and C. Pastorino, Comparison of Ternary Bilayer Mixtures with Asymmetric or Symmetric Unsaturated Phosphatidylcholine Lipids by Coarse Grained Molecular Dynamics Simulations. The Journal of Physical Chemistry B, 2012. **116**(11): p. 3525-3537.

64. Shahane, G., et al., Physical properties of model biological lipid bilayers: insights from all-atom molecular dynamics simulations. Journal of Molecular Modeling, 2019. **25**(3): p. 76.

65. Sukharev, S.I., et al., A large-conductance mechanosensitive channel in E. coli encoded by mscL alone. Nature, 1994. **368**(6468): p. 265-268.

66. Patra, M., Lateral pressure profiles in cholesterol–DPPC bilayers. European Biophysics Journal, 2005. **35**(1): p. 79-88.

67. Chavent, M., A.L. Duncan, and M.S. Sansom, Molecular dynamics simulations of membrane proteins and their interactions: from nanoscale to mesoscale. Curr Opin Struct Biol, 2016. **40**: p. 8-16.

68. Marrink, S.J., et al., Computational Modeling of Realistic Cell Membranes. Chem Rev, 2019. **119**(9): p. 6184-6226.

69. Petrov, E.P., R. Petrosyan, and P. Schwille, Translational and rotational diffusion of micrometer-sized solid domains in lipid membranes. Soft Matter, 2012. **8**(29): p. 7552-7555.

70. Camley, B.A., et al., Lipid Bilayer Domain Fluctuations as a Probe of Membrane Viscosity. Biophysical Journal, 2010. **99**(6): p. L44-L46.

71. Hormel, T.T., et al., Measuring Lipid Membrane Viscosity Using Rotational and Translational Probe Diffusion. Physical Review Letters, 2014. **112**(18): p. 188101.

72. Mika, Jacek T., et al., Measuring the Viscosity of the Escherichia coli Plasma Membrane Using Molecular Rotors. Biophysical Journal, 2016. **111**(7): p. 1528-1540.

73. Saffman, P.G. and M. Delbrück, Brownian motion in biological membranes. Proceedings of the National Academy of Sciences, 1975. **72**(8): p. 3111-3113.

74. B.D. Hughes, B.A.P.a.L.R.W., The translational and rotational drag on a cylinder moving in a membrane. J. Fluid Mech., 1981. **110**: p. 349-372.

75. Petrov, E.P. and P. Schwille, Translational Diffusion in Lipid Membranes beyond the Saffman-Delbrück Approximation(). Biophysical Journal, 2008. **94**(5): p. L41-L43.

76. Mueller, P., et al., Reconstitution of Cell Membrane Structure in vitro and its Transformation into an Excitable System. Nature, 1962. **194**(4832): p. 979-980.

77. Ries, R.S., et al., Black Lipid Membranes: Visualizing the Structure, Dynamics, and Substrate Dependence of Membranes. The Journal of Physical Chemistry B, 2004. **108**(41): p. 16040-16049.

78. Khan, M.S., N.S. Dosoky, and J.D. Williams, Engineering lipid bilayer membranes for protein studies. International Journal of Molecular Sciences, 2013. **14**(11): p. 21561-21597.

79. Hinman, S.S. and Q. Cheng, Bioinspired assemblies and plasmonic interfaces for electrochemical biosensing. Journal of Electroanalytical Chemistry, 2016. **781**: p. 136-146.

80. Montal, M. and P. Mueller, Formation of bimolecular membranes from lipid monolayers and a study of their electrical properties. Proceedings of the National Academy of Sciences of the United States of America, 1972. **69**(12): p. 3561-3566.

81. Walde, P., et al., Giant Vesicles: Preparations and Applications. ChemBioChem, 2010. **11**(7): p. 848-865.

82. Reece, J.B., Urry, L.A., Cain, M.L., et. al., Campbell Biology. 9 ed. 2011: Pearson.

83. Shi, Z. and T. Baumgart, Membrane tension and peripheral protein density mediate membrane shape transitions. Nature Communications, 2015. **6**: p. 5974.

84. Angelova, M.I. and D.S. Dimitrov, Liposome electroformation. Faraday Discussions of the Chemical Society, 1986. **81**(0): p. 303-311.

85. Pautot, S., B.J. Frisken, and D.A. Weitz, Production of Unilamellar Vesicles Using an Inverted Emulsion. Langmuir, 2003. **19**(7): p. 2870-2879.

86. Abkarian, M., E. Loiseau, and G. Massiera, Continuous droplet interface crossing encapsulation (cDICE) for high throughput monodisperse vesicle design. Soft Matter, 2011. **7**(10): p. 4610-4614.

87. Blosser, M.C., B.G. Horst, and S.L. Keller, cDICE method produces giant lipid vesicles under physiological conditions of charged lipids and ionic solutions. Soft Matter, 2016. **12**(35): p. 7364-7371.

88. Dürre, K. and A.R. Bausch, Formation of phase separated vesicles by double layer cDICE. Soft Matter, 2019. **15**(47): p. 9676-9681.

89. Baumgart, T., et al., Large-scale fluid/fluid phase separation of proteins and lipids in giant plasma membrane vesicles. Proceedings of the National Academy of Sciences, 2007. **104**(9): p. 3165-3170.

90. Levental, I., M. Grzybek, and K. Simons, Raft domains of variable properties and compositions in plasma membrane vesicles. Proceedings of the National Academy of Sciences, 2011. **108**(28): p. 11411-11416.

91. Levental, I., et al., Cholesterol-dependent phase separation in cell-derived giant plasma-membrane vesicles. Biochem J, 2009. **424**(2): p. 163-7.

92. Gray, E.M., G. Díaz-Vázquez, and S.L. Veatch, Growth Conditions and Cell Cycle Phase Modulate Phase Transition Temperatures in RBL-2H3 Derived Plasma Membrane Vesicles. PLoS One, 2015. **10**(9): p. e0137741.

93. Levental, K.R., et al., Polyunsaturated Lipids Regulate Membrane Domain Stability by Tuning Membrane Order. Biophys J, 2016. **110**(8): p. 1800-1810.

94. Beltramo, P.J., R. Van Hooghten, and J. Vermant, Millimeter-area, free standing, phospholipid bilayers. Soft Matter, 2016. **12**(19): p. 4324-4331.

95. Cascão Pereira, L.G., et al., A bike-wheel microcell for measurement of thin-film forces. Colloids and Surfaces A: Physicochemical and Engineering Aspects, 2001. **186**(1–2): p. 103-111.

96. Beltramo, P.J., L. Scheidegger, and J. Vermant, Toward Realistic Large-Area Cell Membrane Mimics: Excluding Oil, Controlling Composition, and Including Ion Channels. Langmuir, 2018. **34**(20): p. 5880-5888.

97. Schai, N., Interaction of Antimicrobial Peptides on an E. coli Lipid Bilayer. 2016, ETH Zurich.

98. Verkleij, A.J., et al., The asymmetric distribution of phospholipids in the human red cell membrane. A combined study using phospholipases and freeze-etch electron microscopy. Biochim Biophys Acta, 1973. **323**(2): p. 178-93.

99. Lu, L., J.W. Schertzer, and P.R. Chiarot, Continuous microfluidic fabrication of synthetic asymmetric vesicles. Lab on a Chip, 2015. **15**(17): p. 3591-3599.

100. Marquardt, D., B. Geier, and G. Pabst, Asymmetric lipid membranes: towards more realistic model systems. Membranes (Basel), 2015. **5**(2): p. 180-96.

101. Enoki, T.A. and G.W. Feigenson, Asymmetric Bilayers by Hemifusion: Method and Leaflet Behaviors. Biophysical Journal, 2019. **117**(6): p. 1037-1050.

102. Oropeza-Guzman, E. and J.C. Ruiz-Suárez, Dehydration/Rehydration Cycles for Mixing Phospholipids without the Use of Organic Solvents. Langmuir, 2018. **34**(23): p. 6869-6873.

103. Elson, E.L., et al., Phase separation in biological membranes: integration of theory and experiment. Annual Review of Biophysics, 2010. **39**: p. 207-226.

104. Benvegnu, D.J. and H.M. McConnell, Line tension between liquid domains in lipid monolayers. The Journal of Physical Chemistry, 1992. **96**(16): p. 6820-6824.

105. Benvegnu, D.J. and H.M. McConnell, Surface dipole densities in lipid monolayers. The Journal of Physical Chemistry, 1993. **97**(25): p. 6686-6691.

106. Rosetti, C.M., A. Mangiarotti, and N. Wilke, Sizes of lipid domains: What do we know from artificial lipid membranes? What are the possible shared features with membrane rafts in cells? Biochimica et Biophysica Acta (BBA) - Biomembranes, 2017. **1859**(5): p. 789-802.

107. Brewster, R. and S.A. Safran, Line Active Hybrid Lipids Determine Domain Size in Phase Separation of Saturated and Unsaturated Lipids. Biophysical Journal, 2010. **98**(6): p. L21-L23.

108. Heberle, F.A., et al., Bilayer Thickness Mismatch Controls Domain Size in Model Membranes. Journal of the American Chemical Society, 2013. **135**(18): p. 6853-6859.

109. Usery, R.D., et al., Line Tension Controls Liquid-Disordered + Liquid-Ordered Domain Size Transition in Lipid Bilayers. Biophysical Journal, 2017. **112**(7): p. 1431-1443.

110. García-Sáez, A.J., S. Chiantia, and P. Schwille, Effect of Line Tension on the Lateral Organization of Lipid Membranes. Journal of Biological Chemistry, 2007. **282**(46): p. 33537-33544.

111. Sriram, I. and D.K. Schwartz, Line tension between coexisting phases in monolayers and bilayers of amphiphilic molecules. Surface Science Reports, 2012. **67**(6): p. 143-159.

112. Kuzmin, P.I., et al., Line Tension and Interaction Energies of Membrane Rafts Calculated from Lipid Splay and Tilt. Biophysical Journal, 2005. **88**(2): p. 1120-1133.

113. Rosetti, C.M., G.G. Montich, and C. Pastorino, Molecular Insight into the Line Tension of Bilayer Membranes Containing Hybrid Polyunsaturated Lipids. The Journal of Physical Chemistry B, 2017. **121**(7): p. 1587-1600.

114. Brewster, R., P.A. Pincus, and S.A. Safran, Hybrid Lipids as a Biological Surface-Active Component. Biophysical Journal, 2009. **97**(4): p. 1087-1094.

115. Shimokawa, N., M. Nagata, and M. Takagi, Physical properties of the hybrid lipid POPC on micrometer-sized domains in mixed lipid membranes. Physical Chemistry Chemical Physics, 2015. **17**(32): p. 20882-20888.

116. Trabelsi, S., et al., Linactants: Surfactant Analogues in Two Dimensions. Physical Review Letters, 2008. **100**(3): p. 037802.

117. Himeno, H., et al., Charge-induced phase separation in lipid membranes. Soft Matter, 2014. **10**(40): p. 7959-7967.

118. Gao, Q. and J.M. Goodman, The lipid droplet-a well-connected organelle. Front Cell Dev Biol, 2015. **3**: p. 49.

119. Thiam, A.R., R.V. Farese Jr, and T.C. Walther, The biophysics and cell biology of lipid droplets. Nature Reviews Molecular Cell Biology, 2013. **14**(12): p. 775-786.

120. Bayley, H., et al., Droplet interface bilayers. Molecular bioSystems, 2008. **4**(12): p. 1191-1208.

121. Leptihn, S., et al., Constructing droplet interface bilayers from the contact of aqueous droplets in oil. Nat. Protocols, 2013. **8**(6): p. 1048-1057.

122. McIntosh, T.J., S.A. Simon, and R.C. MacDonald, The organization of n-alkanes in lipid bilayers. Biochimica et Biophysica Acta (BBA) - Biomembranes, 1980. **597**(3): p. 445-463.

123. McIntosh, T.J. and M.J. Costello, Effects of n-alkanes on the morphology of lipid bilayers A freeze-fracture and negative stain analysis. Biochimica et Biophysica Acta (BBA) - Biomembranes, 1981. **645**(2): p. 318-326.

124. Hishida, M., et al., Effect of n-alkanes on lipid bilayers depending on headgroups. Chemistry and Physics of Lipids, 2015. **188**: p. 61-67.

125. Richens, J.L., et al., The interactions of squalene, alkanes and other mineral oils with model membranes; effects on membrane heterogeneity and function. Journal of Colloid and Interface Science, 2015. **457**(Supplement C): p. 225-231.

126. Usuda, H., et al., Common Effects of Incorporated n-Alkane Derivatives on Molecular Packing and Phase Behavior of DPPC Bilayers. Chemistry Letters, 2018. **47**(12): p. 1512-1514.

127. White, S.H., G.I. King, and J.E. Cain, Location of hexane in lipid bilayers determined by neutron diffraction. Nature, 1981. **290**(5802): p. 161-163.

128. Pope, J. and D.W. Dubro, The interaction of n-alkanes and n-alcohols with lipid bilayer membranes: a 2H-NMR study. Biochimica et Biophysica Acta (BBA), 1986. **858**: p. 243-253.

129. Blanchette, C.D., et al., Galactosylceramide Domain Microstructure: Impact of Cholesterol and Nucleation/Growth Conditions. Biophysical Journal, 2006. **90**(12): p. 4466-4478.

130. Heberle, F.A. and G.W. Feigenson, Phase Separation in Lipid Membranes. Cold Spring Harbor Perspectives in Biology, 2011.

131. Frolov, V.A.J., et al., "Entropic traps" in the kinetics of phase separation in multicomponent membranes stabilize nanodomains. Biophysical Journal, 2006. **91**(1): p. 189-205.

132. White, S.H., et al., Formation of planar bilayer membranes from lipid monolayers. A critique. Biophys J, 1976. **16**(5): p. 481-9.

133. White, S.H., Formation of "solvent-free" black lipid bilayer membranes from glyceryl monooleate dispersed in squalene. Biophysical Journal, 1978. **23**(3): p. 337-347.

134. Blair, D. and E. Dufresne, *http://site.physics.georgetown.edu/matlab/index.html*.

135. Sternberg, S.R.J.C., Biomedical Image Processing. Computer, 1983. **16**: p. 22-34.

136. Zuiderveld, K., Contrast limited adaptive histogram equalization, in Graphics gems IV. 1994, Academic Press Professional, Inc. p. 474–485.

137. *https://imagej.net/Enhance_Local_Contrast_(CLAHE*).

138. Ramachandran, S., S. Komura, and G. Gompper, Effects of an embedding bulk fluid on phase separation dynamics in a thin liquid film. EPL (Europhysics Letters), 2010. **89**(5): p. 56001.

139. Bagatolli, L.A. and E. Gratton, A correlation between lipid domain shape and binary phospholipid mixture composition in free standing bilayers: A two-photon fluorescence microscopy study. Biophysical Journal, 2000. **79**(1): p. 434-447.

140. Tang, S., et al., Fractal Morphology and Breakage of DLCA and RLCA Aggregates. Journal of Colloid and Interface Science, 2000. **221**(1): p. 114-123.

141. Ardham, V.R., et al., Accurate Estimation of Membrane Capacitance from Atomistic Molecular Dynamics Simulations of Zwitterionic Lipid Bilayers. The Journal of Physical Chemistry B, 2020. **124**(38): p. 8278-8286.

142. White, S.H., The lipid bilayer as a 'solvent' for small hydrophobic molecules. Nature, 1976. **262**(5567): p. 421-422.

143. Tarun, O.B., M.Y. Eremchev, and S. Roke, Interaction of Oil and Lipids in Freestanding Lipid Bilayer Membranes Studied with Label-Free High-Throughput Wide-Field Second-Harmonic Microscopy. Langmuir, 2018. **34**(38): p. 11305-11310.

144. Gross, L.C.M., et al., Determining Membrane Capacitance by Dynamic Control of Droplet Interface Bilayer Area. Langmuir, 2011. **27**(23): p. 14335-14342.

145. White, S.H., How Electric Fields Modify Alkane Solubility in Lipid Bilayers. Science, 1980. **207**(4435): p. 1075-1077.

146. Heberle, F.A., et al., Hybrid and Nonhybrid Lipids Exert Common Effects on Membrane Raft Size and Morphology. Journal of the American Chemical Society, 2013. **135**(40): p. 14932-14935.

147. Palmieri, B., et al., Line active molecules promote inhomogeneous structures in membranes: Theory, simulations and experiments. Advances in Colloid and Interface Science, 2014. **208**: p. 58-65.

148. Israelachvili, J.N., 19 - Thermodynamic Principles of Self-Assembly, in Intermolecular and Surface Forces (Third Edition), J.N. Israelachvili, Editor. 2011, Academic Press: San Diego. p. 503-534.

149. Hu, Z., et al., Recent Advances in Ergosterol Biosynthesis and Regulation Mechanisms in Saccharomyces cerevisiae. Indian Journal of Microbiology, 2017. **57**(3): p. 270-277.

150. Simons, K. and E. Ikonen, How cells handle cholesterol. Science, 2000. **290**(5497): p. 1721-6.

151. Grunwald, C., Effects of free sterols, steryl ester, and steryl glycoside on membrane permeability. Plant Physiol, 1971. **48**(5): p. 653-5.

152. Hartmann, M.-A., Plant sterols and the membrane environment. Trends in Plant Science, 1998. **3**(5): p. 170-175.

153. Francavilla, M., et al., The red seaweed Gracilaria gracilis as a multi products source. Mar Drugs, 2013. **11**(10): p. 3754-76.

154. Karpova, N.V., et al., A search for microscopic fungi with directed hydroxylase activity for the synthesis of steroid drugs. Applied Biochemistry and Microbiology, 2016. **52**(3): p. 316-323.

155. Schrick, K., S. Debolt, and V. Bulone, Deciphering the molecular functions of sterols in cellulose biosynthesis. Front Plant Sci, 2012. **3**: p. 84.

156. Clouse, S.D., Arabidopsis mutants reveal multiple roles for sterols in plant development. Plant Cell, 2002. **14**(9): p. 1995-2000.

157. Aboobucker, S.I. and W.P. Suza, Why Do Plants Convert Sitosterol to Stigmasterol? Frontiers in Plant Science, 2019. **10**(354).

158. Tarkowská, D. and M. Strnad, Plant ecdysteroids: plant sterols with intriguing distributions, biological effects and relations to plant hormones. Planta, 2016. **244**(3): p. 545-55.

159. Olson, R.E., Discovery of the lipoproteins, their role in fat transport and their significance as risk factors. J Nutr, 1998. **128**(2 Suppl): p. 439s-443s.

160. Berger, S., et al., Dietary cholesterol and cardiovascular disease: a systematic review and meta-analysis. Am J Clin Nutr, 2015. **102**(2): p. 276-94.

161. Santos, F.L., et al., Systematic review and meta-analysis of clinical trials of the effects of low carbohydrate diets on cardiovascular risk factors. Obes Rev, 2012. **13**(11): p. 1048-66.

162. de Meyer, F. and B. Smit, Effect of cholesterol on the structure of a phospholipid bilayer. Proceedings of the National Academy of Sciences of the United States of America, 2009. **106**(10): p. 3654-3658.

163. Gunderson, R.S. and A.R. Honerkamp-Smith, Liquid-liquid phase transition temperatures increase when lipid bilayers are supported on glass. Biochimica et Biophysica Acta (BBA) - Biomembranes, 2018. **1860**(10): p. 1965-1971.

164. Huang, J., J.T. Buboltz, and G.W. Feigenson, Maximum solubility of cholesterol in phosphatidylcholine and phosphatidylethanolamine bilayers. Biochim Biophys Acta, 1999. **1417**(1): p. 89-100.

165. Ibarguren, M., et al., Quantitation of cholesterol incorporation into extruded lipid bilayers. Biochimica et Biophysica Acta (BBA) - Biomembranes, 2010. **1798**(9): p. 1735-1738.

166. Falck, E., et al., Lessons of Slicing Membranes: Interplay of Packing, Free Area, and Lateral Diffusion in Phospholipid/Cholesterol Bilayers. Biophysical Journal, 2004. **87**(2): p. 1076-1091.

167. Hung, W.C., et al., The condensing effect of cholesterol in lipid bilayers. Biophys J, 2007. **92**(11): p. 3960-7.

168. Kučerka, N., et al., The Effect of Cholesterol on Short- and Long-Chain Monounsaturated Lipid Bilayers as Determined by Molecular Dynamics Simulations and X-Ray Scattering. Biophysical Journal, 2008. **95**(6): p. 2792-2805.

169. Ayee, M.A. and I. Levitan, Paradoxical impact of cholesterol on lipid packing and cell stiffness. Front Biosci (Landmark Ed), 2016. **21**: p. 1245-59.

170. Róg, T., et al., Ordering effects of cholesterol and its analogues. Biochim Biophys Acta, 2009. **1788**(1): p. 97-121.

171. Boughter, C.T., et al., Influence of Cholesterol on Phospholipid Bilayer Structure and Dynamics. The Journal of Physical Chemistry B, 2016. **120**(45): p. 11761-11772.

172. Filippov, A., G. Orädd, and G. Lindblom, The effect of cholesterol on the lateral diffusion of phospholipids in oriented bilayers. Biophys J, 2003. **84**(5): p. 3079-86.

173. Nipper, M.E., et al., Characterization of changes in the viscosity of lipid membranes with the molecular rotor FCVJ. Biochimica et Biophysica Acta (BBA) - Biomembranes, 2008. **1778**(4): p. 1148-1153.

174. Tierney, K.J., D.E. Block, and M.L. Longo, Elasticity and Phase Behavior of DPPC Membrane Modulated by Cholesterol, Ergosterol, and Ethanol. Biophysical Journal, 2005. **89**(4): p. 2481-2493.

175. Needham, D., T.J. McIntosh, and E. Evans, Thermomechanical and transition properties of dimyristoylphosphatidylcholine/cholesterol bilayers. Biochemistry, 1988. **27**(13): p. 4668-4673.

176. Gracia, R.S., et al., Effect of cholesterol on the rigidity of saturated and unsaturated membranes: fluctuation and electrodeformation analysis of giant vesicles. Soft Matter, 2010. **6**(7): p. 1472-1482.

177. Pan, J., et al., Cholesterol perturbs lipid bilayers nonuniversally. Physical Review Letters, 2008. **100**(19): p. 198103-198103.

178. Pan, J., S. Tristram-Nagle, and J.F. Nagle, Effect of cholesterol on structural and mechanical properties of membranes depends on lipid chain saturation. Physical Review E, 2009. **80**(2): p. 021931.

179. Byfield, F.J., et al., Cholesterol depletion increases membrane stiffness of aortic endothelial cells. Biophys J, 2004. **87**(5): p. 3336-43.

180. Hissa, B., et al., Membrane Cholesterol Removal Changes Mechanical Properties of Cells and Induces Secretion of a Specific Pool of Lysosomes. PLoS ONE, 2013. **8**(12): p. e82988.

181. Needham, D. and R.S. Nunn, Elastic deformation and failure of lipid bilayer membranes containing cholesterol. Biophys J, 1990. **58**(4): p. 997-1009.

182. Levental, I. and S.L. Veatch, The Continuing Mystery of Lipid Rafts. Journal of Molecular Biology, 2016. **428**(24, Part A): p. 4749-4764.

183. Miller, E.J., et al., Divide and conquer: How phase separation contributes to lateral transport and organization of membrane proteins and lipids. Chemistry and Physics of Lipids, 2020. **233**: p. 104985.

184. Quinn, P.J. and C. Wolf, The liquid-ordered phase in membranes. Biochimica et Biophysica Acta (BBA) - Biomembranes, 2009. **1788**(1): p. 33-46.

185. Engberg, O., et al., The Affinity of Cholesterol for Different Phospholipids Affects Lateral Segregation in Bilayers. Biophys J, 2016. **111**(3): p. 546-556.

186. Wang, C., Y. Yu, and S.L. Regen, Lipid Raft Formation: Key Role of Polyunsaturated Phospholipids. Angewandte Chemie International Edition, 2017. **56**(6): p. 1639-1642.

187. Wang, C., M.R. Krause, and S.L. Regen, Push and Pull Forces in Lipid Raft Formation: The Push Can Be as Important as the Pull. Journal of the American Chemical Society, 2015. **137**(2): p. 664-666.

188. Krause, M.R. and S.L. Regen, The Structural Role of Cholesterol in Cell Membranes: From Condensed Bilayers to Lipid Rafts. Accounts of Chemical Research, 2014. **47**(12): p. 3512-3521.

189. Cerqueira, N.M.F.S.A., et al., Cholesterol Biosynthesis: A Mechanistic Overview. Biochemistry, 2016. **55**(39): p. 5483-5506.

190. Bloch, K.E., Speculations on the evolution of sterol structure and function. CRC Crit Rev Biochem, 1979. **7**(1): p. 1-5.

191. Vainio, S., et al., Significance of sterol structural specificity. Desmosterol cannot replace cholesterol in lipid rafts. J Biol Chem, 2006. **281**(1): p. 348-55.

192. Bui, T.T., et al., Melting-Temperature-Dependent Interactions of Ergosterol with Unsaturated and Saturated Lipids in Model Membranes. Langmuir, 2019. **35**(32): p. 10640-10647.

193. Dufourc, E.J., Sterols and membrane dynamics. Journal of Chemical Biology, 2008. **1**(1-4): p. 63-77.

194. Yeagle, P., The Roles of Cholesterol in the Biology of Cells. 2004.

195. Beck, J.G., et al., Plant sterols in “rafts”: a better way to regulate membrane thermal shocks. The FASEB Journal, 2007. **21**(8): p. 1714-1723.

196. Marquardt, D., et al., Cholesterol's location in lipid bilayers. Chemistry and Physics of Lipids, 2016. **199**: p. 17-25.

197. Marquardt, D., et al., Lipid bilayer thickness determines cholesterol's location in model membranes. Soft Matter, 2016. **12**(47): p. 9417-9428.

198. Kučerka, N., et al., Cholesterol in Bilayers with PUFA Chains: Doping with DMPC or POPC Results in Sterol Reorientation and Membrane-Domain Formation. Biochemistry, 2010. **49**(35): p. 7485-7493.

199. McConnell, H.M. and A. Radhakrishnan, Condensed complexes of cholesterol and phospholipids. Biochimica et Biophysica Acta (BBA) - Biomembranes, 2003. **1610**(2): p. 159-173.

200. Chong, P.L.-G., W. Zhu, and B. Venegas, On the lateral structure of model membranes containing cholesterol. Biochimica et Biophysica Acta (BBA) - Biomembranes, 2009. **1788**(1): p. 2-11.

201. Ikonen, E., Cellular cholesterol trafficking and compartmentalization. Nat Rev Mol Cell Biol, 2008. **9**(2): p. 125-138.

202. Somerharju, P., et al., The superlattice model of lateral organization of membranes and its implications on membrane lipid homeostasis. Biochimica et Biophysica Acta (BBA) - Biomembranes, 2009. **1788**(1): p. 12-23.

203. Ali, M.R., K.H. Cheng, and J. Huang, Assess the nature of cholesterol–lipid interactions through the chemical potential of cholesterol in phosphatidylcholine bilayers. Proceedings of the National Academy of Sciences, 2007. **104**(13): p. 5372-5377.

204. Radhakrishnan, A., T.G. Anderson, and H.M. McConnell, Condensed complexes, rafts, and the chemical activity of cholesterol in membranes. Proceedings of the National Academy of Sciences, 2000. **97**(23): p. 12422-12427.

205. Giri, R.P., A. Chakrabarti, and M.K. Mukhopadhyay, Cholesterol-Induced Structural Changes in Saturated Phospholipid Model Membranes Revealed through X-ray Scattering Technique. The Journal of Physical Chemistry B, 2017. **121**(16): p. 4081-4090.

206. Esposito, C., et al., Flicker Spectroscopy of Thermal Lipid Bilayer Domain Boundary Fluctuations. Biophysical Journal, 2007. **93**(9): p. 3169-3181.

207. Wintersmith, J.R., et al., Determination of interphase line tension in Langmuir films. Phys Rev E Stat Nonlin Soft Matter Phys, 2007. **75**(6 Pt 1): p. 061605.

208. Karamdad, K., et al., Engineering thermoresponsive phase separated vesicles formed via emulsion phase transfer as a content-release platform. Chemical Science, 2018. **9**(21): p. 4851-4858.

209. Tsai, W.-C. and G.W. Feigenson, Lowering line tension with high cholesterol content induces a transition from macroscopic to nanoscopic phase domains in model biomembranes. Biochimica et Biophysica Acta (BBA) - Biomembranes, 2019. **1861**(2): p. 478-485.

210. Tian, A., et al., Line Tension at Fluid Membrane Domain Boundaries Measured by Micropipette Aspiration. Physical Review Letters, 2007. **98**(20): p. 208102.

211. Suryabrahmam, B., A. Agrawal, and V.A. Raghunathan, Fluid–fluid coexistence in phospholipid membranes induced by decanol. Soft Matter, 2020. **16**(39): p. 9002-9005.

212. Kopeć, W., J. Telenius, and H. Khandelia, Molecular dynamics simulations of the interactions of medicinal plant extracts and drugs with lipid bilayer membranes. FEBS J, 2013. **280**(12): p. 2785-805.

213. Centi, A., et al., Inserting Small Molecules across Membrane Mixtures: Insight from the Potential of Mean Force. Biophysical Journal, 2020. **118**(6): p. 1321-1332.

214. Saenger, W., Cyclodextrin Inclusion Compounds in Research and Industry. Angewandte Chemie International Edition, 1980. **19**(5): p. 344-362.

215. Crini, G., Review: A History of Cyclodextrins. Chemical Reviews, 2014. **114**(21): p. 10940-10975.

216. Li, Z., et al., γ-Cyclodextrin: a review on enzymatic production and applications. Applied Microbiology and Biotechnology, 2007. **77**(2): p. 245-255.

217. Ohtani, Y., et al., Differential effects of α-, β- and γ-cyclodextrins on human erythrocytes. European Journal of Biochemistry, 1989. **186**(1-2): p. 17-22.

218. Christian, A.E., et al., Use of cyclodextrins for manipulating cellular cholesterol content. Journal of Lipid Research, 1997. **38**(11): p. 2264-72.

219. Melzak, K., et al., Cholesterol Organization in Phosphatidylcholine Liposomes: A Surface Plasmon Resonance Study. Materials, 2012. **5**(11): p. 2306.

220. Klein, U., G. Gimpl, and F. Fahrenholz, Alteration of the Myometrial Plasma Membrane Cholesterol Content with .beta.-Cyclodextrin Modulates the Binding Affinity of the Oxytocin Receptor. Biochemistry, 1995. **34**(42): p. 13784-13793.

221. Litz, Jonathan P., et al., Depletion with Cyclodextrin Reveals Two Populations of Cholesterol in Model Lipid Membranes. Biophysical Journal, 2016. **110**(3): p. 635-645.

222. Hao, M., S. Mukherjee, and F.R. Maxfield, Cholesterol depletion induces large scale domain segregation in living cell membranes. Proceedings of the National Academy of Sciences, 2001. **98**(23): p. 13072-13077.

223. Rahimi, M., et al., Shape Transformations of Lipid Bilayers Following Rapid Cholesterol Uptake. Biophysical Journal, 2016. **111**(12): p. 2651-2657.

224. Puglisi, G., M. Fresta, and C.A. Ventura, Interaction of Natural and Modified β-Cyclodextrins with a Biological Membrane Model of Dipalmitoylphosphatidylcholine. Journal of Colloid and Interface Science, 1996. **180**(2): p. 542-547.

225. Anderson, T.G., et al., Calorimetric Measurement of Phospholipid Interaction with Methyl-β-Cyclodextrin. Biochemistry, 2004. **43**(8): p. 2251-2261.

226. Huang, Z. and E. London, Effect of Cyclodextrin and Membrane Lipid Structure upon Cyclodextrin–Lipid Interaction. Langmuir, 2013. **29**(47): p. 14631-14638.

227. Reynaert, S., P. Moldenaers, and J. Vermant, Control over Colloidal Aggregation in Monolayers of Latex Particles at the Oil−Water Interface. Langmuir, 2006. **22**(11): p. 4936-4945.

228. Zhang, A., H. Bai, and L. Li, Breath Figure: A Nature-Inspired Preparation Method for Ordered Porous Films. Chemical Reviews, 2015. **115**(18): p. 9801-9868.

229. Böker, A., et al., Hierarchical nanoparticle assemblies formed by decorating breath figures. Nature Materials, 2004. **3**(5): p. 302-306.

230. Family, F. and P. Meakin, Scaling of the Droplet-Size Distribution in Vapor-Deposited Thin Films. Physical Review Letters, 1988. **61**(4): p. 428-431.

231. Family, F. and P. Meakin, Kinetics of droplet growth processes: Simulations, theory, and experiments. Physical Review A, 1989. **40**(7): p. 3836-3854.

List of Figures

Curriculum Vitae

Omitted in the electronic version

Scientific contributions

Publications

- P. J. Beltramo, **L. Scheidegger**, J. Vermant, *Toward Realistic Large-Area Cell Membrane Mimics: Excluding Oil, Controlling Composition, and Including Ion Channels*, Langmuir 34 (20), 5880-5888

- **L. Scheidegger**, L. Stricker, P. J. Beltramo, J. Vermant, *Domain size regulation in phospholipid model membranes using linactant and oil molecules*. Manuscript in preparation.

Conferences

- **Scheidegger, L.**, Beltramo, P.J., Vermant, J., *Large model biomembranes – a new setup to study membrane function*, MaP Graduate Symposium, ETH Zurich, 26 June 2018

- Beltramo, P.J., **Scheidegger, L.**, Vermant, J., *Large model biomembranes – a new setup to study membrane function*, Materials Day, ETH Zurich, 18 October 2017